Studies on Structural, Mechanical and Electrical Characterization of Polyaniline/Gelatin Composite and its Water Sorption Behavior

A SUMMARY OF THE THESIS

Submitted for the award of the degree of

Doctor of Philosophy

in

Physics

by

Ajay Singh Utiye
(Enrollment No. 13/06-079)

Supervisor
Dr. Bharat Mishra
Department of Physical Sciences
MGCGV Chitrakoot, Satna

Co-Supervisor
Dr. Sanjay Kumar Awasthi
Department of Physics
Govt. Science College Jabalpur

Co-Supervisor
Prof. Sunil Kumar Bajpai
Department of Chemistry
Govt. Science College Jabalpur

FACULTY OF SCIENCE & ENVIRONMENT
MAHATMA GANDHI CHITRAKOOT GRAMODAYA VISHWAVIDYALAYA
CHITRAKOOT SATNA (M.P.) 485 334, INDIA
October-2019

Dedication

* * *

I dedicated this thesis
my beloved brother and mentor,
Bhagat Singh Utiye

Thanks for being a person who always stands beside me.

* * *

DECLARATION BY CANDIDATE

I declare that the thesis entitled **“Studies on Structural, Mechanical and Electrical Characterization of Polyaniline/Gelatin Composite and its Water Sorption Behavior”** is my own work conducted under the supervision of **Dr. Bharat Mishra** at Department of Physical Sciences, Faculty of Science & Environment, Mahatma Gandhi Chitrakoot Gramodaya Vishwavidyalaya Chitrakoot, Satna, Co-supervision of **Dr. Sanjay Kumar Awasthi** at Department of Physics and **Prof. Sunil Kumar Bajpai** at Department of Chemistry, Govt. Science College, Jabalpur and approved by Research Degree Committee. I have put in more than 200 days of attendance with the supervisors at the approved centre.

I further declare that to the best of my knowledge, the thesis does not contain any part of any work which has been submitted for the award of any degree either in this University or in any other University/Deemed University without proper citation.

(Ajay Singh Utiye)
Research Scholar

Dr. Bharat Mishra
Supervisor

Dr. Sanjay Kumar Awasthi
Co-Supervisor

Prof. Sunil Kumar Bajpai
Co-Supervisor

Dr. Ajay Kumar
Head
Deptt. of Physical Sciences

Prof. I. P. Tripathi
Dean
Faculty of Science and Environment

CERTIFICATE

This is to certify that the work entitled **"Studies on Structural, Mechanical and Electrical Characterization of Polyaniline/Gelatin Composite and its Water Sorption Behavior"** is a piece of research work done by **Ajay Singh Utiye** under my guidance and supervision for the degree of Doctor of Philosophy in Physics at Mahatma Gandhi Chitrakoot Gramodaya Vishwavidyalaya, Chitrakoot, Satna (M.P.) India. The candidate has put in an attendance of more than 200 days with us.

To the best of my knowledge and belief the thesis:

(1) Embodies the work of the candidate himself;

(2) Has duly been completed;

(3) Fulfills the requirements of the Ordinance relating to the Ph.D. degree of the University; and

(4) Is upto standard both in respect of contents and language for being referred to the examiner.

Dr. Bharat Mishra
Supervisor

Forwarded

Dr. Ajay Kumar
Head
Deptt. of Physical Sciences

Prof. I. P. Tripathi
Dean
Faculty of Science and Environment

Examined and approved

CERTIFICATE

This is to certify that the work entitled **“Studies on Structural, Mechanical and Electrical Characterization of Polyaniline/Gelatin Composite and its Water Sorption Behavior”** is a piece of research work done by **Mr. Ajay Singh Utiye** under my guidance and Co-supervision for the degree of Doctor of Philosophy in Physics, Mahatma Gandhi Chitrakoot Gramodaya Vishwavidyalaya, Chitrakoot, Satna (M.P.) India. The candidate has put in an attendance of more than 200 days with us.

To the best of my knowledge and belief the thesis:

(1) Embodies the work of the candidate himself;

(2) Has duly been completed;

(3) Fulfills the requirements of the Ordinance relating to the Ph.D. degree of the University; and

(4) Is upto standard both in respect of contents and language for being referred to the examiner.

Dr. Sanjay Kumar Awasthi
Co-Supervisor

CERTIFICATE

This is to certify that the work entitled **“Studies on Structural, Mechanical and Electrical Characterization of Polyaniline/Gelatin Composite and its Water Sorption Behavior”** is a piece of research work done by **Mr. Ajay Singh Utiye** under my guidance and Co-supervision for the degree of Doctor of Philosophy in Physics, Mahatma Gandhi Chitrakoot Gramodaya Vishwavidyalaya, Chitrakoot, Satna (M.P.) India. The candidate has put in an attendance of more than 200 days with us.

To the best of my knowledge and belief the thesis:

(1) Embodies the work of the candidate himself;

(2) Has duly been completed;

(3) Fulfills the requirements of the Ordinance relating to the Ph.D. degree of the University; and

(4) Is upto standard both in respect of contents and language for being referred to the examiner.

Prof. Sunil Kumar Bajpai
Co-Supervisor

ACKNOWLEDGEMENT

With limitless humility, I bow my head to Almighty, Merciful Compassionate and Supreme power 'God' who showered his mercy on me and blessed me with the favorable circumstances to go through his gigantic task.

It is a matter of great pleasure for a student to work with an intellectual who has investigative spirit, academic enthusiasm, scientific outlook, tremendous patience and special sense of devotion to his field of specialization and I am enough lucky to get Dr. Bharat Mishra (Supervisor), Associate Professor and Dr. Sanjay Kumar Awasthi (Co-Supervisor), Associate Professor and Prof. Sunil Kumar Bajpai (Co-Supervisor), Professor for their noble guidance, determined direction, creative suggestions, constructive criticism and keen interest throughout my endeavor in carrying out the experimentation successfully. I am extremely indebted to him for being meticulous, throughout the course of investigation & preparation of this document.

I wish to extend my sincere thanks to Professor N. C. Gautam, Hon'ble Vice-Chancellor for providing all the facilities and inspiration for carrying the present investigation.

Words can never express the indebtedness, but I dare to take this opportunity to pay my deepest sense of gratitude with profound obeisance and heartfelt thanks to Prof. I. P. Tripathi, Professor & Dean, Faculty of Science and Environment, Dr. Ajay Kumar, Head, Department of Physical Sciences for their helpful and illuminating guidance, constructive criticism, constant encouragement and kind help throughout the thesis.

Words can never express the indebtedness, but I dare to take this opportunity to pay my deepest sense of gratitude with profound obeisance and heartfelt thanks to Dr. Sanjay Kumar Awasthi, Associate Professor, Department of physics Govt. Science College Jabalpur for their helpful and illuminating guidance, constructive criticism, constant encouragement and kind help throughout the thesis.

I wish to deepest thanks to the departments of Physics and Chemistry, Govt. Science College Jabalpur, and the Department of Physical Sciences, MGCGV Chitrakoot for their valuable suggestions during the course of data analysis and interpretations.

I express my sincere thanks to our Principal, Dr. A. L. Mahobia for his constant support and encouragement. I am indebted to Dr. Ravi Katare Head of the Department of Physics, Govt. Science College Jabalpur for providing facilities.

It's my great privilege to pay sincere thanks to Prof. S. K. Shrivastava, Dr. S. K. Panday, Dr. R.C. Tripathi, Dr. S. K. Tripathi, Dr. S. S. Gautam, and Dr. Veerendra Upadhyaya for extending their valuable suggestions during course of investigation.

I am highly indebted to Prof. M. K. Roy, Department of Physics, IIITDM Jabalpur, for providing lab facilities for this study and boost up throughout my research work.

All the words in lexicon will be futile and meaningless if, I fail to express the obligation of my Father Late Shri Dhoukal Singh Utiye, Mother Smt. Balo Bai Utiye, and my elder brother Mr. Sewa Ram Utiye, Mr. Bhagat Singh Utiye and for their love blessing, inspirations and support during the odd and difficult period, otherwise the present study would not be possible.

I express my foremost ineptness and gratitude to my beloved and venerable younger brother, Mr. Bhagat Singh Utiye.

My pen has no power to express my heartiest acknowledgement to my friends Mr. Raj Kumar Rajak, Dr. Mahendra Kumar Mishra, Dr. Sonam Ahuja, Dr. Abhishek Agrawal, Dr. Sweta Soni, Dr. Pradeep Daheriya, Dr. Satrudhan Jhariya, Dr. Farhan Shah, Mr. Abhishek Dubey, Dr. Gauri Shanker Kushwaha, Dr. Dev Ras Pandey, Dr. Virendra Rajak and *Dr. Dheerendra Mauraya who always stood with me for unmatched help and encouragement during the investigation as well as study period.*

I am also thankful to RGNF Fellowship UGC, for their financial support and help during my Research work.

Place**: **Chitrakoot *(Ajay Singh Utiye)*

Date: 15 October, 2019

INDEX

Chapter ***Contents*** ***Pages No.***

v *Dedication……………………………………………………………........................* *ii*
v *Declaration………………………………………………………………………….* *iii*
v *Certificate…………………………………………………………………………...* *iv*
v *Acknowledgement ………………………………………………..........................* *v*
v *Index……………...……………………………………………...........................* *vii*
v *List of tables……………...………………………………………………………….* *x*
v *List of figures………………...……………………………………………………….* *xii*
v *Abbreviations……………………………………………….................................* *xiii*

CHAPTER-1: INTRODUCTION

1.1 Definitions and classification of polymer……………….………………… **1**
1.1.1 Natural polymer based…..………………………………………………… 3
1.1.2 Semi synthetic based……………………………………………………. 3
1.1.3 Synthetic polymer based……………………..………………………… 4
1.1.4 Linear polymer………………………..…………...…………………... 4
1.1.5 Branched chain polymer…………………………………...…………… 4
1.1.6 Cross linked or network polymers..……………………………………... 4
1.1.7 Addition polymers……………………………………………………… 4
1.1.8 Condensation polymers………………………………………………… 5
1.1.9 Elastomers……………………………………………………………. 6
1.1.10 Fibers………………………………………………………………….. 6
1.1.11 Thermoplastic polymers………………………………………………. 6
1.1.12 Thermosetting polymers………………………………………………. 7
1.2 Polymer composite…………………….………………………………………. **7**
1.2.1 Classification of composites films……….……………………………... 8
1.2.1.1 Metal matrix composites…………..……………………………….. 8
1.2.1.2 Ceramic matrix composites………..……………………….……….. 8
1.2.1.3 Polymer matrix composites……………………………………….. 9
1.3 Characterization of polymeric materials………………………………….. **9**
1.3.1 Molecular weight and its distribution………………………………... 9
1.3.2 Crystallization………………………………………………………….. 11
1.3.3 Glass transition temperature…………………………………………… 12
1.3.4 Mechanical properties of polymer……………………………………… 13
1.3.4.1 Micro hardness of a polymer ………………………………….. 15
1.3.4.2 Mechanical properties of a thin film polymer ………………… 16
1.3.5 Electrical properties of polymer……………………………….………. 16
1.3.5.1 Dielectric polarization………………………………………… 17
1.3.5.2 Dielectric strength……………………………………………… 17
1.3.5.3 Electrical conductivity……………………………….……… 17
1.3.5.4 Dielectric constant (or permittivity)……………………………. 18
1.3.5.5 Dissipation factor………………………………..……………… 18

Chapter	*Contents*	*Pages No.*
	1.3.5.6 Dielectric loss……………………………………………….……..	18
	1.3.5.7 Volume resistance………………………………………………….	18
	1.3.5.8 Surface resistance……………………………………………..	19
	1.3.6 Water absorption properties of polymer…..……………………………	19
	1.4 Conducting polymers and their composite materials…………………..…..	**19**
	1.4.1 Polypyrrole………………………………………………………………..	20
	1.4.2 Polyaniline…………………………………………………………………	21
	1.5 Objectives of the thesis……………………..…………………………..	**22**
	1.6 Organization of the thesis…….……..…………..……………………….	**22**
CHAPTER-2: **REVIEW OF LITERATURE**		
	2.1 Review of Literature………………………………………………………	**24**
CHAPTER-3: **MATERIALS AND METHODS**		
	3.1 Materials………..………………………………………………………	**39**
	3.2 Methods……………………………………………………………………	**40**
	3.2.1 Preparation of glyoxal (Glox) crosslinked Glox-X-Gel films………….	40
	3.2.2 Determination of percent cross-linking (PC)……………...………..….	42
	3.2.3 Preparation of Glox-crosslinked Glox-X- Gel/PANI composite films….	42
	3.3 Characterization of Glox-X-Gel/PANI films……………………………….	**44**
	3.3.1 Fourier-transform infrared spectroscopy (FTIR)……………………….	44
	3.3.2 X –ray diffraction (XRD) Study……………………………………...	46
	3.3.3 Thermogravimetric Analysis (TGA)……………………………………	46
	3.3.4 Atomic Force Microscopy (AFM)………………………………………	48
	3.3.5 Tensile testing………………………………….……………………..	50
	3.3.6 Impedance analyzer……………………………………….….…..….	52
	3.3.7 Ultraviolet-visible spectrophotometer………………….…….……...	54
	3.3.8 Swelling study……………………………………………………......	55
	3.3.8.1 Water absorption behavior of composite films………………….	55
	3.3.8.2 Network parameters……………………………………………..	55
	3.3.8.3 Analysis of water uptake……………………………….……..	56
	3.3.8.4 Diffusion coefficients……………………………………………	56
	3.3.9 Determination of Moisture Sorption Isotherm……………….…….	57
	3.3.10 Sorption isotherm models…………………………………………...	58
	3.3.10.1 GAB isotherm model………………………………………....	58
	3.3.11 Blood compatibility…………………………………………………	59
	3.3.11.1 Thrombus formation test……………………………………..	59
	3.3.11.2 Heamolysis test…………………………………………….	60
CHAPTER–4: **RESULT AND DISCUSSION**		
	4.1 Experimental……………………………………………………………	**62**
	4.1.1 Formation of Glox-X-Gel film……………………………………….	62
	4.1.2 Formation of Glox-X-Gel/PANI film …………………………………..	62
	4.1.3 Percent of crosslinking (PC)………………………………………….	64
	4.2 Characterization of Glox-X-Gel and Glox-X-Gel/PANI Films…….……..	**64**
	4.2.1 Fourier-transform infrared spectroscopy (FTIR) analysis………………	64
	4.2.2 Thermogravimetric analysis (TGA)……………………………………	66
	4.2.3 Atomic force microscopy (AFM) analysis……………….…………….	67
	4.2.4 X–ray diffraction (XRD) analysis study films…………….…………	68
	4.2.5 Water uptake behavior of hydrogel………………….…………………	69

Chapter ***Contents*** ***Pages No.***

4.2.6 Effect of PANI on the swelling of Glox-X-Gel films……………............ 72
4.2.7 Modeling of water uptake data………………….……………………… 73
    4.2.7.1 Power function model……………………………………….……. 73
    4.2.7.2 Schott kinetic model……………………………………….………… 76
4.2.8 Evaluation of diffusion coefficients………………..………………….. 80
    4.2.8.1 Diffusion coefficient…………….…..……………….……………….. 80
4.2.9 Moisture sorption behavior …………...……...…………………………. 83
    4.2.9.1 GAB Model……………………………………………………………... 85
    4.2.9.2 Effect of temperature on moisture uptake……………….………….. 87
    4.2.9.3 Evaluation of thermodynamic parameters……….……….............. 90
    4.2.9.4 Entropy-enthalpy compensation theory………………………… 95
4.2.10 Blood compatibility……….………...…………………...…………. 97
    4.2.10.1 Thrombus formation test……………………………..………… 97
    4.2.10.2 Hemolysis test…………………………………….……………. 97
4.2.11 Mechanical properties of film…..…………...……………….……….. 97
    4.2.11.1 Tensile testing……………………………………................... 97
4.2.12 Electrical properties of film…………………………………………… 99

CHAPTER-5: **CONCLUSIONS AND FUTURE PROSPECTS**

5.1 Conclusion……………………………………..……..……..……….. **103**
5.2 Future prospects…………………………………….…………………… **109**

REFERENCES………..……………………………………..………………………….. **112**

- ***List of Publication and Seminar……………….………..………..……..............*** **126**
- ***Ph. D. Course Work Certificate…………………………..……………………….*** **131**
- ***Ph. D. Pre-Presentation Certificate………………………………………………*** **132**
- ***Plagiarism Verification……………………………………..…………………..*** **133**
- ***Plagiarism Report………………………………………………..……………...*** **134**

LIST OF TABLES

Table No.	*Caption*	*Page. No.*
3.1	The water activities (a_w) of saturated salt solutions 30^oC	40
3.2	Composition of gelatin and glyoxal	41
4.1	Data showing swelling ratio of various cross-linkers Glox-X-Gel samples (gH_2O/g gel) for the film samples A, B, C and D	68
4.2	Data showing dynamic water uptake for the film samples E, F, and G	70
4.3	Data showing the water absorption behavior of Glox-X-Gel and Glox-X-Gel/PANI films PF of pH 7.4	71
4.4	Data showing the value of ‘n’ and ‘k’ for the film samples B, C, D	73
4.5	Data showing the value of ‘n’ and ‘k’ for the film samples E, F, and G	74
4.6	Data showing the various parameters for power model	75
4.7	Data showing the value of t/ M_t Vs t for the film samples A, B, C and D	76
4.8	Data showing the value of t/ M_t Vs t for the film samples E, F, and G	77
4.9	The value of various parameters for Schott model	78
4.10	Data showing the value of ln (1-F) versus t plots for the water uptake data of film samples A, B, C, and D	79
4.11	Data showing value ln (1-F) versus t plots for the water uptake data of film samples E, F, and G	81
4.12	The value of the various types of diffusion coefficients the samples	82
4.13	The value of water activity (a_w) on moisture uptake (M_c) at 30^0C	82
4.14	Data showing the values of a_w and a_w/M_c of GAB isotherm for moisture uptake of Glox-X-Gel and Glox-X-Gel/PANI based film	85
4.15	Data showing the related parameters for GAB model	86
4.16	The value of temperature on moisture uptake of Glox-X-Gel films	87
4.17	The value of temperature on moisture uptake of Glox-X-Gel/PANI films.	88
4.18	Data showing the effect of 1/T and ln (aw) for the film Glox-X-Gel	89
4.19	Data showing the effect of 1/T and ln (aw) for the Film Glox-X-Gel/PANI	90
4.20	Data showing the effect of q_{st} with M_c for the film Glox-X-Gel	91
4.21	Data showing the effect of q_{st} with M_c for the Glox-X-Gel/PANI films	92
4.22	Data showing effect of M_c with $s_d$for the film Glox-X-Gel	93
4.23	Data showing effect of M_c with s_d for the Glox-X-Gel/PANI films	94
4.24	Data showing the value s_d versus q_{st} plot for Glox-X-Gel film	95
4.25	Data showing the value in s_d with q_{st} for Glox-X-Gel/PANI film	96

LIST OF FIGURES

Fig. No.	*Caption*	*Page No.*
1.1	Linear polymer…………………………………………………...................	4
1.2	Branched chain polymer…………………………………………………	4
1.3	Cross linked or network polymer……………………………………...	4
1.4	Schematic representation of the weight average and number average molecular weight distribution as a function of the degree of polymerization…………………………………………………………	11
1.5	Generalized tensile stress-strain curve for some polymeric materials…...	14
1.6	Tensile stress-strain curves for four types of polymeric material………	15
3.1	The overall scheme of formation of Glox-crosslinked Glox-X-Gel films.	41
3.2	The resulting Glox-crosslinked Glox-X-Gel films……….………………	42
3.3	The overall scheme of formation of Glox-X-Gel/PANI films…………...	43
3.4	The resulting Glox-crosslinked PANI composite films……….…………	44
3.5	The phase difference between current and voltage waveforms…..……	53
3.6	Static method apparatus set up for moisture sorption isotherm………..	57
4.1	Scheme showing crosslinking of gelatin chains by glyoxal…..…………	61
4.2	The optical images of Glox-X-Gel and Glox-X-Gel/PANI films…..……	62
4.3	The FTIR spectra obtained from the Glox-X-Gel film…………………	63
4.4	The FTIR spectra obtained from the Glox-X-Gel/PANI films……….…	64
4.5	The TGA pattern of Glox-X-Gel/PANI composite film…………………	65
4.6	The AFM images of Glox-X-Gel and Glox-X-Gel/PANI films……….	56
4.7	The XRD pattern of Glox-X-Gel films……….…………………………	67
4.8	The XRD pattern of Glox-X-Gel/PANI composite films……….………	67
4.9	Dynamic water uptake for the film samples A, B, C and D……………..	69
4.10	Dynamic water uptake for the film samples E, F and G ………….…….	70
4.11	Water absorption behavior of Glox-X-Gel and Glox-X-Gel/PANI films..	71
4.12	The value of ‘n’ and ‘k’ for the film samples B, C and D……………….	73
4.13	The value of ‘n’ and ‘k’ for the film samples E, F and G………………	74
4.14	The value t/M_t versus t plots to the film samples A, B, C, and D...........	77
4.15	The value t/M_t versus t plots to the film samples E, F and G………..	78
4.16	The value ln (1-F) versus t plots for the film samples A, B, C and D........	80
4.17	The value ln (1-F) versus t plots for the film samples E, F and G..…..…	81
4.18	Moisture sorption isotherms for Glox-X-Gel and Glox-X-Gel/PANI films at 30^o C ……………………………………………………..........	83
4.19	Polynomial curve obtained between a_w/M_c and a_w for Glox-X-Gel and Glox-X-Gel/PANI at 30^0C………………………………………........	85

Fig. No.	***Caption***	***Page. No.***
4.20	The effect of temperature on moisture uptake of Glox-X-Gel film...……	87
4.21	The effect of temperature on moisture uptake of Glox-X-Gel/PANI films…………………………………………………………………………	88
4.22	Variation in M_c with 1/T for the Glox-X-Gel film……………………..…	90
4.23	Variation in M_c with 1/T for the Glox-X-Gel /PANI film………………	90
4.24	Variation in q_{st} with M_c for theGlox-X-Gel film……………………….	91
4.25	Variation in q_{st} with M_c for the Glox-X-Gel/PANI film………………	92
4.26	Variation in s_d with M_c for the Glox-X-Gel film………………………	93
4.27	Variation in s_d with M_c for the Glox-X-Gel/PANI film……………..……	94
4.28	Variation q_{st}versus S_d plot for Glox-X-Gel film…………………………	95
4.29	Variation q_{st}versus S_d plot for Glox-X-Gel/PANI film………..…………	96
4.30	Plot of tensile strength V/S concentration of aniline in composite films..	97
4.31	Plot of elongation V/S concentration of aniline in composite films…….	98
4.32	Plot of elongation versus load for varying composition of aniline...........	98
4.33	The plot of capacitance of aniline doped Glox-X-Gel/PANI Films….....	99
4.34	The plot of conductivity of aniline doped Glox-X-Gel/PANI Films.........	100
4.35	The plot of Impedance of aniline doped Glox-X-Gel/PANI Films……...	100
4.36	The plot of inductance of aniline doped Glox-X-Gel/PANI Films………	101
4.37	Data showing Phase angle of aniline doped Glox-X-Gel/PANI Films…..	101

LIST OF ABBREVIATION

µm	Micron
Å	Angstrom
AC	Alternet current
ACD	Acid citrate dextrose
AFM	Atomic force microscopy
APS	Ammonium persulphate
BHJ	Banded hematite jasper
BPE	Bipolar electrode
C	GAB Guggenheim constant
CA	Contact angle
cm	Centimeter
CMC	Ceramic matrix composites
CP	Conducting polymer
CS	Chitosan
D	Diffusion coefficient
$\mathbf{D_{ave}}$	The average diffusion coefficient
$\mathbf{D_L}$	Late-time diffusion coefficient
DNA	Deoxyribonucleic acid
DW	Distilled water
ECoG	Electrocorticography
ECP	Electrical conducting copolymers
EDOT	Ethylenedioxythiophene
EMC	Equilibrium moisture content
ESR	Equilibrium swelling ratio
ExG	Exfoliated graphite
FET	Field-effect transistor
FTIR	Fourier transform infrared
g	Gram
g/g	Gram per gram
GAB	Guggenheim-Anderson-de Boer
Gel	Gelatin
Glox	Glyoxal
GOx	Glucose oxidase
HRP	Horseradish peroxidase
I	Current
ISMs	Ions selective membranes
k	Constant of interaction
Kg	Kilogram
kJ	Kilo/Joule
KPFM	Kelvin probe force microscopy
kV	Kilo-volt
LbL	Layer by layer

LEDs	Light emitting diode
m	Meter
mA	Mile impere
MA	Methacrylate
MHz	Megahertz
M_c	Moisture content at equilibrium
M_t	Composite's moisture content at time t
MW	Molecular mass
MWD	Molecular mass distribution
NIR	Near infrared
nm	Nanometer
OD	Optical densities
OGH	Oriented graphene hydrogel
OLED	Organic light emitting diode
P	Polarization
PANI	Polyaniline
PBD	Poly(2-butalene terephthalate)
PC	Percentage
PE	Percentage elongation
PEDOT	Poly(3,4-ethylenedioxythiophene)
PET	Polyethylene teraphthelene
P_{ext}	External polarization
pH	Potential for hydrogen
PI	Polyimides
P_{int}	Internal polarization
PMCs	Polymer matrix composites
PMPSA	Poly(2-acrylamido-2-methyl-1-propene
Poly(Ani)	Polyaniline
PPV	Poly (p-phenylene vinylene)
PPy	Polypyrrole
PSS	Poly styrenesulphpnate
PVC	Poly vinyl chloride
R	Universal gas constant
RADAR	Radio identification and running
R_{diff}	Relative rates of diffusion
RH	Relative humidity
rpm	Revolutions per minute
R_{relax}	Polymer relaxation
SC	Supercapacitor
SCISES	Solid contact ions selective electrodes
SEM	Scanning electron microscope
SR	Swelling ratio
STM	Scanning tunneling microscopy
TEM	Transmission electron microscopy

TFT	Thin film transistors
Tg	Glass transition
TGA	Thermo gravimetric analyzer
TS	tensile strength
UV	Ultraviolet-visible
V	Volt
V_s	Molar volume of the solvent
WS	Water solubility
WUR	Water uptake ratio
WVP	Water vapour permeability
WVUR	Water vapor uptake ratios
XRD	X-ray diffraction
ΔU	Activation energy
χ	Flory-Huggins interaction parameter
Φ	Volume fraction

LIST OF TABLES

Table No.	Caption	Page. No.
3.1	The water activities (a_w) of saturated salt solutions 30^oC..........................	41
3.2	Composition of gelatin and glyoxal..…………………………………	42
4.1	SR of various cross-linkers Glox-X-Gel samples A, B, C and D...............	69
4.2	Data showing dynamic water uptake for the film samples E, F, and G..	71
4.3	Data showing the water absorption behavior of Glox-X-Gel and Glox-X-Gel/PANI films PF of pH 7.4...	72
4.4	Data showing the value of ‘n’ and ‘k’ for the film samples B, C, D……...	74
4.5	Data showing the value of ‘n’ and ‘k’ for the film samples E, F, and G…	75
4.6	Data showing the various parameters for power model…….……………	76
4.7	Data showing the value of t/ M_t Vs t for the film samples A, B, C and D	77
4.8	Data showing the value of t/ M_t Vs t for the film samples E, F, and G….	78
4.9	The value of various parameters for Schott model ………….....................	79
4.10	Data showing the value of ln (1-F) versus t for the film samples A, B, C, and D…………………………………………………………………	81
4.11	Data showing value ln (1-F) versus t plots for the water uptake data of film samples E, F, and G…………………………………………………	82
4.12	The value of the various types of diffusion coefficients the samples....	83
4.13	The value of water activity (a_w) on moisture uptake (M_c) at 30^0C………	84
4.14	The values of a_w and a_w/M_c of GAB of Glox-X-Gel and Glox-X-Gel/PANI based films…………………………………………………..	86
4.15	Data showing the related parameters for GAB model……………………	87
4.16	The value of temperature on moisture uptake of Glox-X-Gel films……..	88
4.17	The value of temperature on moisture uptake of Glox-X-Gel/PANI films.	89
4.18	Data showing the effect of 1/T and ln (aw) for the film Glox-X-Gel.……	91
4.19	Data showing the effect of 1/T and ln (aw) for the Film Glox-X-Gel/PANI…………………………………………………………….	92
4.20	Data showing the effect of q_{st} with M_c for the film Glox-X-Gel…	93
4.21	Data showing the effect of q_{st} with M_c for the Glox-X-Gel/PANI films…	94
4.22	Data showing effect of M_c with $s_d$for the film Glox-X-Gel.……...........	95
4.23	Data showing effect of M_c with s_d for the Glox-X-Gel/PANI films……...	96
4.24	Data showing the value s_d versus q_{st} plot for Glox-X-Gel film…………	97
4.25	Data showing the value in s_d with q_{st} for Glox-X-Gel/PANI film………..	98

LIST OF FIGURES

Fig. No.	*Caption*	*Page No.*
1.1	Linear polymer	4
1.2	Branched chain polymer	4
1.3	Cross linked or network polymer	4
1.4	Degree of polymerization curve of the weight avg and number avg molecular weight distribution	11
1.5	Generalized tensile stress-strain curve for some polymeric materials	14
1.6	Tensile stress-strain curves for four types of polymeric material	15
3.1	The overall scheme of formation of Glox-crosslinked Glox-X-Gel films.	42
3.2	The resulting Glox-crosslinked Glox-X-Gel films	43
3.3	The overall scheme of formation of Glox-X-Gel/PANI films	44
3.4	The resulting Glox-crosslinked PANI composite films	45
3.5	The phase difference between current and voltage waveforms	54
3.6	Static method apparatus set up for moisture sorption isotherm	58
4.1	Scheme showing crosslinking of gelatin chains by glyoxal	62
4.2	The optical images of Glox-X-Gel and Glox-X-Gel/PANI films	63
4.3	The FTIR spectra obtained from the Glox-X-Gel film	64
4.4	The FTIR spectra obtained from the Glox-X-Gel/PANI films	65
4.5	The TGA pattern of Glox-X-Gel/PANI composite film	66
4.6	The AFM images of Glox-X-Gel and Glox-X-Gel/PANI films	67
4.7	The XRD pattern of Glox-X-Gel films	68
4.8	The XRD pattern of Glox-X-Gel/PANI composite films	68
4.9	Dynamic water uptake for the film samples A, B, C and D	70
4.10	Dynamic water uptake for the film samples E, F and G	71
4.11	Water absorption behavior of Glox-X-Gel and Glox-X-Gel/PANI films	72
4.12	The value of ‘n’ and ‘k’ for the film samples B, C and D	74
4.13	The value of ‘n’ and ‘k’ for the film samples E, F and G	75
4.14	The value t/M_t versus t plots to the film samples A, B, C, and D	78
4.15	The value t/M_t versus t plots to the film samples E, F and G	79
4.16	The value ln (1-F) versus t plots for the film samples A, B, C and D	81
4.17	The value ln (1-F) versus t plots for the film samples E, F and G	82
4.18	Polynomial curve obtained between a_w/M_c and a_w for Glox-X-Gel and Glox-X-Gel/PANI film	84
4.19	The effect of temperature on moisture uptake of Glox-X-Gel film	86
4.20	The effect of temperature on moisture uptake of Glox-X-Gel/PANI film	88
4.21	Variation in M_c with 1/T for the Glox-X-Gel film	89

Fig. No. ***Caption*** ***Page. No.***

4.22 Variation in M_c with 1/T for the Glox-X-Gel /PANI film……………… 91
4.23 Variation in q_{st} with M_c for theGlox-X-Gel film………………………. 92
4.24 Variation in q_{st} with M_c for the Glox-X-Gel/PANI film……………… 93
4.25 Variation in s_d with M_c for the Glox-X-Gel film……………………… 94
4.26 Variation in s_d with M_c for the Glox-X-Gel/PANI film……………..…… 95
4.27 Variation q_{st}versus S_d plot for Glox-X-Gel film………………………… 96
4.28 Variation q_{st}versus S_d plot for Glox-X-Gel/PANI film………..………… 97
4.29 Plot of tensile strength V/S concentration of aniline in composite films.. 98
4.30 Plot of elongation V/S concentration of aniline in composite films…… 100
4.31 Plot of elongation versus load for varying composition of aniline.......... 101
4.32 The plot of capacitance of aniline doped Glox-X-Gel/PANI Films…...... 102
4.33 The plot of conductivity of aniline doped Glox-X-Gel/PANI Films......... 103
4.34 The plot of Impedance of aniline doped Glox-X-Gel/PANI Films……... 103
4.35 The plot of inductance of aniline doped Glox-X-Gel/PANI Films……… 104

LIST OF ABBREVIATION

µm	Micron
Å	Angstrom
AC	Alternet current
ACD	Acid citrate dextrose
AFM	Atomic force microscopy
APS	Ammonium persulphate
BHJ	Banded hematite jasper
BPE	Bipolar electrode
C	GAB Guggenheim constant
CA	Contact angle
cm	Centimeter
CMC	Ceramic matrix composites
CP	Conducting polymer
CS	Chitosan
D	Diffusion coefficient
D_{ave}	The average diffusion coefficient
D_L	Late-time diffusion coefficient
DNA	Deoxyribonucleic acid
DW	Distilled water
ECoG	Electrocorticography
ECP	Electrical conducting copolymers
EDOT	Ethylenedioxythiophene
EMC	Equilibrium moisture content
ESR	Equilibrium swelling ratio
ExG	Exfoliated graphite
FET	Field-effect transistor
FTIR	Fourier transform infrared
g	Gram
g/g	Gram per gram
GAB	Guggenheim-Anderson-de Boer
Gel	Gelatin
Glox	Glyoxal
GOx	Glucose oxidase
HRP	Horseradish peroxidase
I	Current
ISMs	Ions selective membranes
k	Constant of interaction
Kg	Kilogram
kJ	Kilo/Joule
KPFM	Kelvin probe force microscopy
kV	Kilo-volt
LbL	Layer by layer

LEDs	Light emitting diode
m	Meter
mA	Mile impere
MA	Methacrylate
MHz	Megahertz
M_c	Moisture content at equilibrium
M_t	Composite’s moisture content at time t
MW	Molecular mass
MWD	Molecular mass distribution
NIR	Near infrared
nm	Nanometer
OD	Optical densities
OGH	Oriented graphene hydrogel
OLED	Organic light emitting diode
P	Polarization
PANI	Polyaniline
PBD	Poly(2-butalene terephthalate)
PC	Percentage
PE	Percentage elongation
PEDOT	Poly(3,4-ethylenedioxythiophene)
PET	Polyethylene teraphthelene
P_{ext}	External polarization
pH	Potential for hydrogen
PI	Polyimides
P_{int}	Internal polarization
PMCs	Polymer matrix composites
PMPSA	Poly(2-acrylamido-2-methyl-1-propene
Poly(Ani)	Polyaniline
PPV	Poly (p-phenylene vinylene)
PPy	Polypyrrole
PSS	Poly styrenesulphpnate
PVC	Poly vinyl chloride
R	Universal gas constant
RADAR	Radio identification and running
R_{diff}	Relative rates of diffusion
RH	Relative humidity
rpm	Revolutions per minute
R_{relax}	Polymer relaxation
SC	Supercapacitor
SCISES	Solid contact ions selective electrodes
SEM	Scanning electron microscope
SR	Swelling ratio
STM	Scanning tunneling microscopy
TEM	Transmission electron microscopy

TFT	Thin film transistors
Tg	Glass transition
TGA	Thermo gravimetric analyzer
TS	tensile strength
UV	Ultraviolet-visible
V	Volt
V_s	Molar volume of the solvent
WS	Water solubility
WUR	Water uptake ratio
WVP	Water vapour permeability
WVUR	Water vapor uptake ratios
XRD	X-ray diffraction
ΔU	Activation energy
χ	Flory-Huggins interaction parameter
Φ	Volume fraction

CHAPTER – 1
INTRODUCTION

CHAPTER- 1

POLYMER AN INTRODUCTION

Polymers are now finding their application in each and every aspect which behaves like a significant factor in overall growth of civilization. Without polymers, at present, it is difficult to imagine modern life. The use of these advanced materials is such an extent that, one can found them in everything of need along with in all the necessities of daily life. The polymers became more common in different areas like traditional sciences, medical sciences, different modern and traditional technologies and every industry from basic needs to biopolymers polymers. Because of this, polymer physics is rather important for understanding many scientific and practical problems associated with applications of polymers in modern engineering. Due to this not only chemists, technologists and structural engineer but also physicist are interested in numerous problems of macromolecular physics. The modern polymer physics is peculiar combination of the basic concepts, ideas and methods of molecular physics. The main significant of physics of polymer is to understand the relationship between physical and chemical structural properties of polymer.

1.1. Definitions and classification

As stated in the IUPAC definition, "a polymer is a material, made up of molecules that contain many different kinds of atoms or atoms, characteristics of different distinct groups of atoms, which are self-sufficient in providing a certain set of properties some constitutional units, are not quite different with adding or removing ".

In correspond to same elemental “composition”, it can be have many different polymeric materials, which differ constitution and/or in configuration and hence in properties. In relation to molecule, by “constitution” we mean atoms in molecule which are bound to each other with different types of bonds, while “configuration” specifies the spatial depositions of the bonds, for a given constitution without using into account the multiplicity of spatial dispositions that may arise through moving around single bonds. The spatial dispositions arising from the specifications of the angles of rotation around single bond represent possible “conformations”.

A regular polymer is that whose molecule in a single linear shape can be specifically represented by only one species of constituent unit. For example, in polyethylene, constitutional repeating unit is: --CH_2-- for the polymers of propylene group.

$$—\,—\,CH_2\,—\,—\,CH_2\,—\,— \qquad \dots (1.1)$$

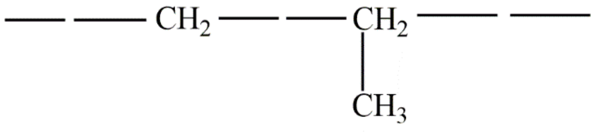

$$—\,—\,CH_2\,—\,—\,\underset{\displaystyle CH_3}{\underset{|}{CH_2}}\,—\,—$$

… (1.2)

Two regular macromolecules C_nH_{2n} with the above structure and same and large “n” would be “constitutional”; in fact, the two molecules would have the same composition and molecular mass but different constitution.

In real cases, even for a polymer which is substantially regular, such as polyethylene, any given macromolecule is not necessarily completely linear, and “branches” may be present. For example, in low density polyethylene; short branches with a magnitude of a few percent may be present. While long branches are present in fever number in each macromolecule, but their higher or lower concentration may have important effect on the polymers rheological charactistics.

From the constitutional view point, the graft block and crosslinked polymers are more complex. A block is part of a polymeric-molecule consisting of many constitutional units, each having at least one constitutional/configuration feature not exist in adjacent portions. A “block polymer” consists of blocks of monomers connected linearly. The blocks are connected directly or through a constitutional unit that is not part of blocks. A “graft polymer” has a main backbone of polymer with side chains of some other chemical species (i.e. monomers). These side chains encompass essential units comprise the main chain related to absolute of junction points. For example, if A and B are:

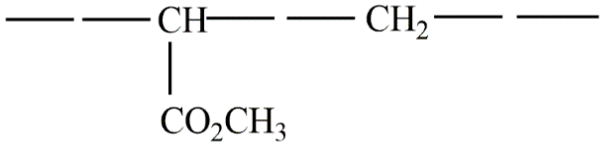

$$—\,—\,\underset{\displaystyle CO_2CH_3}{\underset{|}{CH}}\,—\,—\,CH_2\,—\,—$$

… (1.3)

and

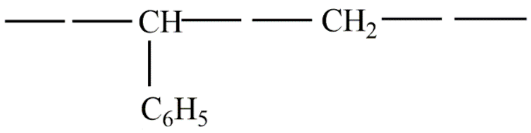

$$—\,—\,\underset{\displaystyle C_6H_5}{\underset{|}{CH}}\,—\,—\,CH_2\,—\,—$$

… (1.4)

A molecule of block polymer could be:

A——— ———B——— ———A——— ———B … (1.5)

While, a molecule of graft polymer could be:

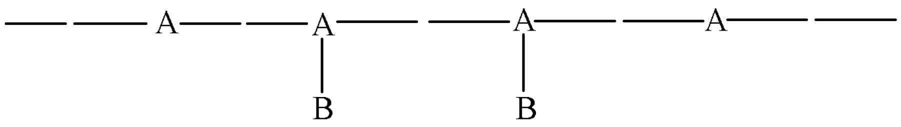

$$—— —— A—— ——\underset{B}{\underset{|}{A}}—— ——\underset{B}{\underset{|}{A}}—— ——A—— ——$$

… (1.6)

A “homopolymer” is made up of a species of monomer, while in “copolymer” more than one species of monomer are present. In an "alternating copolymer", monomeric units of two different species are alternately distributed in the order of the molecules. However, if the distribution is statistical in nature, the product should be terms as “statistical copolymer”, but is often referred to as “random copolymer”, there are number of ways in which polymers can be classified.

1.1.1. Natural polymer

The polymers that occur in nature are known as natural polymer conjointly referred to as biopolymers. Samples of such as natural rubber, natural cellulose, silk, proteins, starch, etc. Proteins are actually naturally found polymers of amino acids. They have long chains of amino acids, folded into three dimensional molecules; this structure makes proteins to establish their activity in nature, and their important roles in body of animals. Nearly whole of body of animals is constituted from proteins; almost all the vital organs like eyes, heart, lungs, and stomach are made of protein. Protein also consists of muscles, intestines, Veins and skin, arteries, fingernails, bones, hair, and stomach lining. Gelatin, define as hydrolyzed collagen, peptides collagen, collagen hydrolysate, gelatin hydrolysate and hydrolyzed gelatin. It is basically used as a gelling, gelatin food, vitamin capsules, photographic, films and papers, drug, medications and cosmetics. Due to wider range of physical properties which is a necessity of accommodating wide spectrum of functional requirements of living organisms, proteins always attracted materials scientists to synthesize wonder composite material having required properties.

1.1.2. Semi synthetic polymer

These polymers are artificially altered natural polymers, for example, proteins, hydrogenated natural rubber, starch, cellulose etc.

1.1.3. Synthetic polymer

These polymers which is synthesized in the laboratories is called synthetic polymer. They are also called manmade polymers. For example, polymers like PVA, polyethylene, polystyrene, polysulfone are synthesized in laboratory.

1.1.4. Linear polymer

These polymers comprise long linear chains of monomer. The examples of linear polymers are high density PVA, polythene. These are shown in Fig.1.1.

Fig.1.1: Linear polymers.

1.1.5. Branched chain polymer

These polymers have linear chains of monomer with some branches (Fig.1.2).

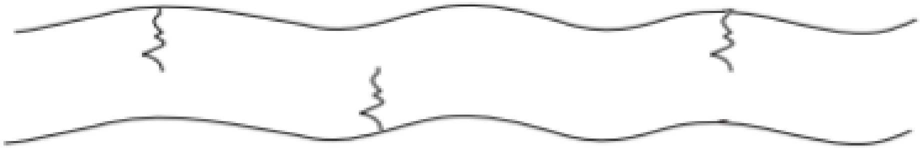

Fig.1.2: Crosslinked polymers.

1.1.6. Cross linked polymers

These are generally made up of bi-functional and tri-functional monomers and have solid covalent bonds between different chains of polymer, e.g. bakelite, melamine. Crosslinked polymers have a three dimensional space network formed by means of chemical bond (Fig.1.3).

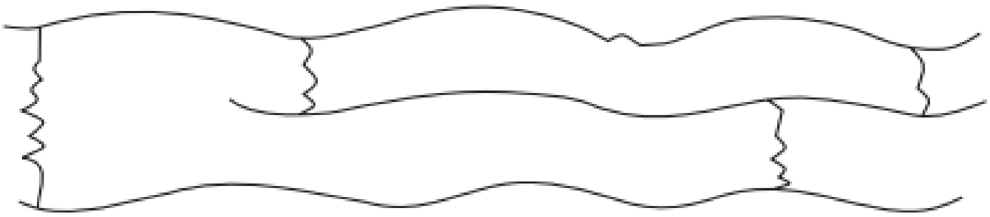

Fig.1.3: Crosslinked polymers.

1.1.7. Addition polymers

The addition polymers are synthesized by adding monomer molecules holds on double or triple bonds, repeatedly for example the synthesis of polythene from ethylene and polypropylene from propylene. However, the resulting from polymerization of a single monomer is known as homopolymers, e.g., polythene.

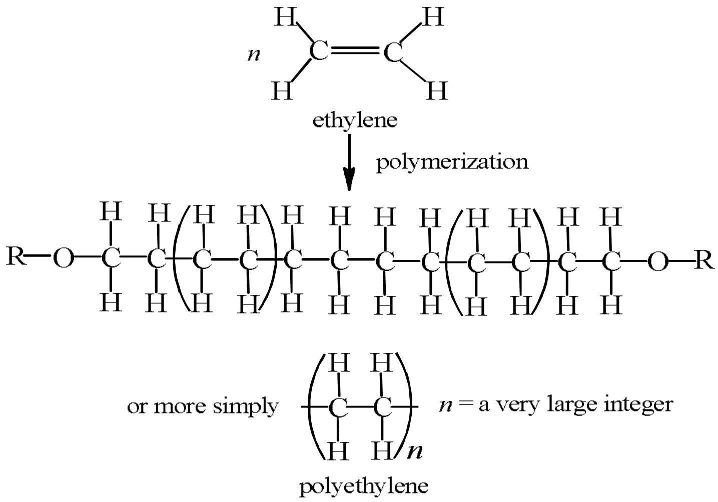

… (1.7)

The polymers prepared by addition polymerization such as Buna-S.

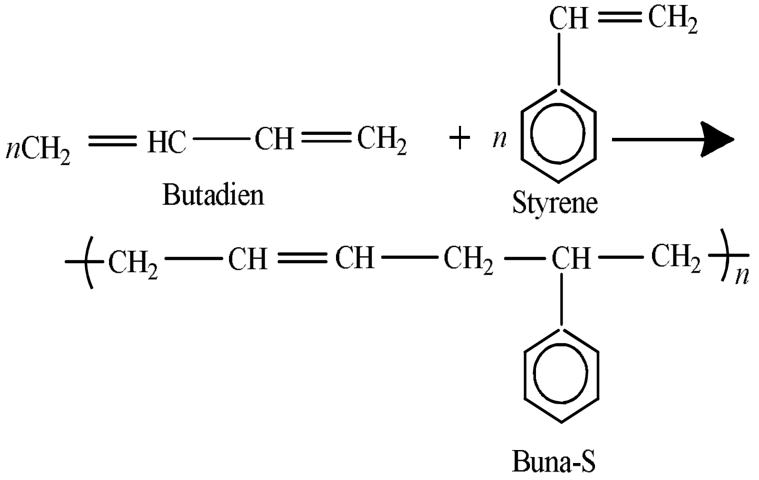

… (1.8)

1.1.8. Condensation polymers

This method can be taken as growing polymer in steps. In this type of polymerization, smaller molecules interact with every different to form large structural units, releasing smaller molecules as by product. Repeated condensation reaction occurs between two distinct monomeric bi-functional or tri-functional units and smaller molecules like water, hydrogen chloride, alcohol are eliminated. Examples: Terylene, nylon66 or 6, 6-Nylon, Nylon6, etc. For example, nylon66 is synthesized by hexamethylenediamine with adipic acid.

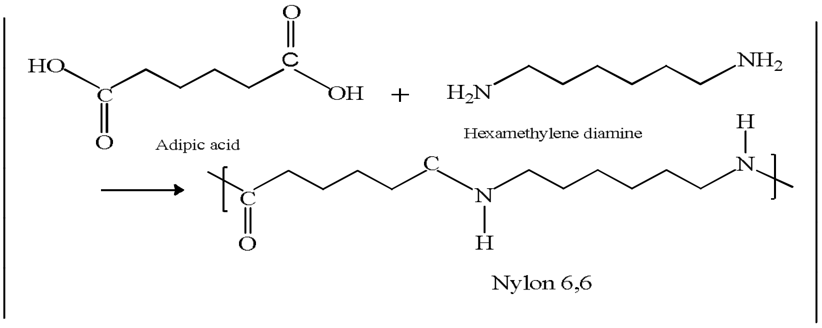

… (1.9)

1.1.9 Elastomers

Elastomers are rubber a like solid polymers having elastic properties. The polymers chains are placed with the weakest inter molecular forces allowing the polymer to be stretched. Many ‘crosslinks’ which are introduced in between the chains of polymers facilitate them to gain their original position when the deforming force is removed similar to the case of processed rubber.

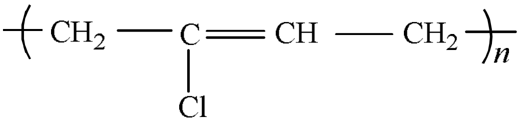

$$\left(CH_2 - \underset{\displaystyle Cl}{\underset{|}{C}} = CH - CH_2 \right)_n$$

Neoprene

… (1.10)

1.1.10 Fibers

The classes of polymers which are thread like in nature and can be woven easily. The strong intermolecular forces among the polymeric chains provide them with high tensile strength and modulus. The intermolecular forces existing between the macromolecular are hydrogen bonds/dipole-dipole interaction. The fibres have high and sharp melting points. Examples: polyamides (nylon 66), polyesters (Terylene).

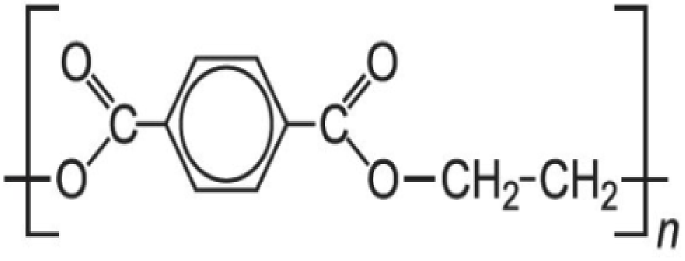

… (1.11)

1.1.11 Thermoplastic polymers

They are long chain polymers, in which the intermolecular forces viz. Van der Waal’s forces hold the chains together. They can be softened by heating or hardened (plasticized) by cooling. They don’t have any crosslinks so they can easily be shaped. Examples: Linear Polyesters, Nylons, PVC, Polyolefins, Polyethers, sealing wax etc.

1.1.12 Thermosetting polymers:

These are polymers have low molecular mass and by nature, they are semi-fluid. They undergo certain remarkable chemical changes while heating, they start cross-linking between polymer chairs, hence become hard and infusible. The curing or setting process further leads to growth of crosslinks which results giant three-dimensional structure. This reaction is irreversible in nature. The examples of this class are Bakelite, Epoxy Resins, Phenolic Resins, Urea-Formaldehyde, Diene Rubbers, etc.

1.2 Polymer composites

In the history of civilization, the most important creation of human race apart after the creation of dominant fireplace and discovery of the roll is the spinning of continuous yarns which made them survive outside the tropical climate zones and unfold mysteries across the surface of the planet. Plant-derived vegetable fibers are versatile materials, which are product of regionally grownup and spun fibers such as cotton; flax and jute were a giant success compared to animal skins. With growth of civilization, more and more additional fundamental assets were used, leading to the primary composites used in straw-reinforced walls, and chariots made from attached coatings of wood, bone and horn. These antique composites are replaced by more and more sturdy materials like wood and metal, with advancement of civilization.

Initiating since primary agronomic cultures and being nearly forgotten for centuries, a real revival of composite materials started with uses of light-weight composite structures for several technical solutions throughout the last half of the 20th century. In the get up of its electromagnetic assets (insulators and radar-arenas), composites are extensively utilized in aviation industries and military applications. Composite material well tailored and chosen can not only enhances the properties of radar, military and domestic aircrafts but also enhances execution of space shuttle and military flying machine. Previously cost of having enhanced material was not matter of concern for material scientists, but later with expanding costs, but the most recent developments in technology of composites; is the utilization of composites to secure a man against flame and life threatening impacts and an inclination towards more earth cordial outline, increasing to the reestablishment of primary fibers in the composite technology.

1.2.1 Classification of composite films

The classification of composites is either matrix phase based or reinforcement. On the basis of former classification, metal matrix composites, and polymer matrix composites, fall in to the following classes: ceramic matrix composites (CMCs), MMCs, and PMCs. The classifications as defined reinforcement phase is fibrous (composed of fibers), particulate (composed of particles), and laminate composites. Fibrous composites can also divide into natural/biofiber or synthetic fiber. Composites having bio-fibers are referred as biofiber composites. They are again divided on the nature of matrix as, unbiodegradable matrix and biodegradable matrix. Bio-based composites are made from natural/biofiber and biodegradable matrix composites are also called green composites. They can be further sub divided into hybrid and textile composites. However for simplicity, composites will be classified into classes based on the nature of the each type of matrix *(Thomas et al., 2012)*. Methods of fabrication also vary in line with physical and chemical assets of the matrices.

1.2.1.1 Metal matrix composites (MMCs)

Metal matrix composites, consists of matrix of a metal. Mostly used matrices are those of aluminum, magnesium and titanium. The fibers used include carbon and silicon carbide. Reinforcement of metal is done as per requirement. The elastic toughness and power of metals can be increased while thermal expansion and electrical conductivities of metals can be reduced by adding of fiber like silicon carbide.

1.2.1.2 Ceramic matrix composites (CMCs)

CMCs have ceramic matrix like alumina, calcium, alumino salt reinforced by silicon carbide. The benefits of CMCs include hardness, high mechanical strength, high service temperature, chemical inertness and lower density. Naturally resistant to high temperature, ceramic materials have a tendency to turn into stiff and to crack. Composites with ceramic matrices are reinforced with silicon carbide fibers are successfully made. These composites offer an equivalent extra temperature forbearance of super amalgams however without such high density. The ceramics are brittle in nature which makes their composite fabrication tough. Typically, most CMCs production procedures involve beginning materials in powder kind. There are four categories of ceramics matrices: glass (easy to fabricate due to low softening temperatures, embrace salt and aluminosilicates), standard ceramics (silicon nitride, silicon carbide, aluminumoxide and oxide are absolutely crystalline), concreted carbon components and cement.

1.2.1.3 Polymer matrix composites (PMCs)

The popular and common but advance composites are PMCs. These composites are generally polymer thermo plastic or thermosetting armored by fiber. These composites can be changed into a large range of shapes and sizes. They have an excellent toughness and strength along with appreciable resistance to corrosion. These are now very common because of their high strength, low cost and easy producing principles. Due to low density of the most commercially produced PMC's use a polymer as a basic matrix material which is often called as a resin solution.

To have a polymer matrix material, one can choose from several more various polymers depending upon the availability on initial raw ingredients. Several broad categories of polymers, each having numerous variations is available. The most common of these are polypropylene, polyether ether ketone, polyester, polyimide, like epoxy, phenolic, vinyl ester, polyamide and others. The choice of reinforcement materials is in most case is of fibers but other common ground minerals can also be used.

1.3 Properties of polymeric materials

To have required set of valuable properties, polymers differing from one another by their chemical structural properties are usually combined together to get new polymeric material having some properties identical to both polymers initially mixed. There are three ways of doing this, they are; copolymerization, blending and making composite materials. Synthesis of any organic compound, composites, and biocomposites without a detailed and deep characterization of its various properties is of no use. Properties of material synthesized in laboratory are very importance in materials science. We are describing important aspects related to properties in following section.

1.3.1 Molecular weight and its distribution

The knowledge and understanding of polymer's molecular weight is importance for the scientific and systematic study of polymer synthesis and application. The molecular weight of substance is 1/12th of an atom of ^{12}C as a ratio of average mass per formula unit. Molecular weight determines several physical properties of polymers. Molecular weight (M_W) is the average weight of the molecules within the mixer of different size molecules that constitutes the polymer. It is a parameter which relates directly to the size of constituent molecules. Molecular weight may be of two types, i.e.

either a number average (M_n) based on the number fractions of the weight of each of the constituent species or size of molecule present as a weight average (M_W) based on weight fraction of each of the constituent species or size of the polymer molecules. These are expressed as:-

$$M_n = \frac{\sum N_i M_i}{\sum N_i} \quad \ldots (1.12)$$

$$M_W = \frac{\sum (N_i M_i) M_i}{\sum N_i M_i} \quad \ldots (1.13)$$

Where N_i is the number of molecules, M_i is sum of the molecular weight and $\sum$ denotes summations over all M_i molecular weight.

The N_i can be better obtained from the number n_i of macromolecules for each degree of polymerization p_i. By taking for each degree of polymerization the product of the number of polymer molecules and their degree of polymerization $n_i p_i$ and dividing the total of these products by the total no. of monomers:

$$\bar{M}_n = \frac{\sum_{i=1}^{\infty} n_i p_i}{N_0} \quad \ldots (1.14)$$

The avg molecular weight $\bar{M}_w$ can be obtained in an identical fashion from mass m_i for each degree of polymerization p_i according to the equation:

$$\bar{M}_w = \frac{\sum_{i=1}^{\infty} m_i p_i}{M_0} \quad \ldots (1.15)$$

It plays significant to control the overall properties like tensile strength, adherence, toughness and environmental resistance (*Nunes et al., 1982)* of a polymer. This means high molecular weight has tougher and more chemically resistant polymer while low molecular weight polymers are weaker and more weaker.

By molecular weight distribution we mean the relative proportions of molecules of different weight. It gives us fundamental concept of the lowest and the highest molecular weight in polymer under study along with the distribution pattern of the species in it, according to molecular weight. When the molar mass distribution is very narrow, the number average and $\bar{M}_w$ are essentially equal. When the distribution is broad, the weight average molar mass is considerably greater than the number average molar mass and the gap between them is large (see Fig. 1.4). Tensile strengths increase with molecular weight. The melt viscosity of the polymer, however, shows a diverse trend. At very high molecular weights, the melt viscosity rises more sharply than for lower molecular weights. Molar mass distribution affects overall properties and performance for various applications of polymers. We must have good knowledge of average molar mass and its dispersion pattern to understand all polymer materials.

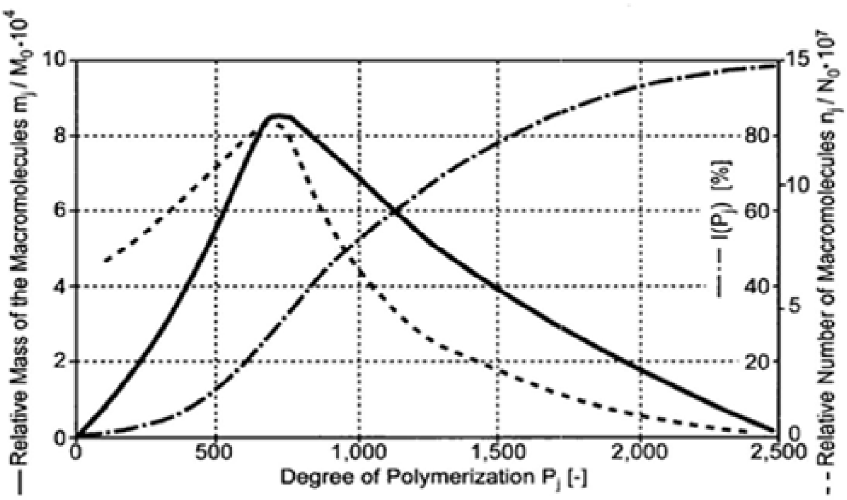

Fig.1.4: Schematic representation of the weight average and number average molecular weight distribution as a function of the degree of polymerization.

1.3.2 Crystallization

Materials having smaller molecules have three states viz. solid, liquid and gas and their behavior can easily be understood but polymers are very large molecules having strong intermolecular forces and having very complex twisted chains. Polymers are having vapor state because their decomposition starts before the temperature required to form vapor is reached. Crystallization is easier while for polymer having very long molecules; thus, in solid phase the polymers can be better understood in two phases viz. amorphous and crystalline. Polymer is defined as exists in three phases viz. melt, amorphous and crystalline. Studying crystallization in polymers attracted scientists both academically and also in quest of smart materials. Crystallization is an interesting property which is linked to phase transition that determines final properties of many technologically and academically exciting systems *(Pious and Thomas, 2016; Günter and Jens, 2003)*.

In crystallization process the molecular chains in polymers partially align. These molecular chains fold together to form ordered region called lamellae. These lamellae together form spherical semi-crystalline regions within polymer. Crystallization process starts with nucleation. This is the first stage of crystallization and time taken for nucleation to begin, depends upon temperature gradient, crystallization method and impurities present in polymer or polymer mix. Once the seeding (formation of nucleus) of crystallization i.e. nucleation is achieved further growth of crystals is dependent upon number of factors. The basic kinetics of nucleation is very complicated to analyze and to obtain as the rate of heterogeneous nucleation at impurities, defects and surfaces is quite faster than the homogeneous rate of nucleation inside the melt. After formation of nucleus, the kinetics of crystal growth decides the final rate of the phase transformation. For kinetics related to growth from liquid or solid solutions, the rate limiting phase is often mass diffusion. The crystal growth from a melt, for large molecules and polymers, the kinetics at microscopic level for linking a large molecule or polymer segment to the growing crystal is to be thoroughly studied for understanding the crystallization in polymers *(Mittal, 2010)*.

As discussed earlier the crystalline also the amorphous states coexist in polymer and the rate of crystallization greatly influences polymer properties. As polymers are semi-crystalline, crystallinity of a sample polymer may be termed as a portion of the sample which is crystalline i.e. fraction of ordered molecules in polymer. The highest crystallinity is achieved with polymers having smaller molecules, such polymeric materials have a simple unit cell structure and a relatively high degree of molecular order but they are brittle. A partially crystalline polymeric material's the final property (Q) may be define as a sum of its two components:

$$Q = Q_c + Q_a \qquad \dots (1.16)$$

Where Q_c and Q_a are respective contributions of the crystalline and the amorphous components of the sample. All the methods used for calculating the degree of crystallinity assumes a material as a mixture of two phases viz. totally disordered phase and perfect crystalline; while these phase are associated with transition of one phase to another a large amount percentage of expected. The methods to estimate degree of crystallinity are: X-ray diffraction, polarized light microscopy, infrared-absorption spectroscopy, differential thermal analysis, etc. Accurate and undisputed measurement of the volume crystallinity in a sample cannot be easily done because each of the method of measurement is concerned with a different physical nature of material. Nevertheless, the great practical consequences of crystallinity and its effects on mechanical properties leads researchers to observe at least relative changes in these factors by any applicable of polymeric material mean available, and correlate these finding with changes in processing and fabrication methods and with end-use behavior of prepared final product *(Takashi, 2005)*.

1.3.3 Glass transition temperature (Tg)

For scientific systematic study of polymers and polymeric materials and their applications, the concept of glass transition temperature must be thoroughly understood.

The materials having highest degree of crystallinity, have sharp melting point, at which transition from solid to liquid phase occur. However, glass transition temperature should not be distorted form the melting point. The polymers which are basically amorphous, have a temperature called glass transition temperature, transition from heating polymers above this temperature causes in which polymer changes from hard and brittle glassy state to soft and flexible rubbery state. When polymer is cooled below glass transition temperature, it becomes brittle and hard materials which added to polymers increases their glass transition temperature are called plasticizer. Polymers which are purely amorphous doesn’t have true melting point. The glass transition temperature is a characteristic of amorphous phase while crystalline phase shows distinct melting point. Since polymers are not 100% crystalline, both non crystalline and crystalline portions are present, the amorphous portion shows glass transition temperature while crystalline part exhibit distinct melting *(Scheirs, 2000; Nicholson, 2012; Feughelman, 1997).*

1.3.4 Mechanical properties of polymer

Polymers are now finding applications almost every field such as construction, communication, medical science, textile, transport, space and technology. Materials scientists for every part of world are studying polymeric materials and doing their characterization to find application specific material. Scientists are interested in bulk mechanical properties that are mostly an end-use interest. These charactistics in which determine how the polymeric material will actually behave on a macroscopic scale. Some of the important mechanical properties with regard to their application as a building material are hardness, tensile strength, compressive and flexural strength, creep, fatigue resistance and impact resistance. It depends upon various factors like method of their synthesis, temperature, heat treatment, radiation treatment etc. Polymers can express itself as glassy, brittle solid or an elastic rubber, or that of a viscous liquid, depending on the temperature and experimental time scale of measurement.

The studies are based on, applying some form of mechanical stress either continuous or in a periodic manner, on them, at varying rate. Toughness can be termed as the ability to absorb mechanical energy and to deform like plastics without fracturing. While tensile strength of polymer reflects it capable to resist breaking in tensile stress. Tensile strength falls into the most important and widely measured properties of materials used in structural material. Material becomes plastic beyond elastic limit. After elastic border, plastic deformation occurs. In the plastic area, the tensile strength of the composite material increases because the material starts getting worse i.e., a little stress requires more stress. This phenomenon is called strain hardening. Engineering applications of polymers are mainly governed by strain hardening considerations. The persons using polymeric materials as engineering material must, therefore, understand their mechanical behavior with respect to strain by knowing maximum permissible strain they can avoid failure of material. Similar to most building materials, stress-strain plots provides a compressive knowledge of mechanical behavior of specific polymer.

The stress-strain plot is usually obtained by increasing the specimen at constant rate until it breaks, on the contrary measuring the force established with a continuously increasing force. In Fig.1.5 represent the stress-strain behavior of any polymer and one can use this curve to define and derive several useful quantities that are mechanistic behavior of the polymer material under consideration.

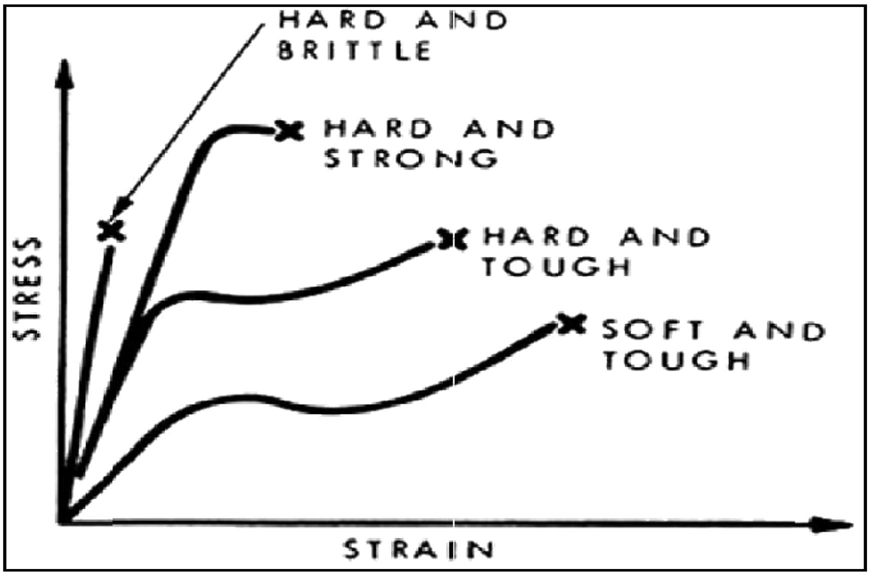

Fig.1.5: Tensile stress-strain curve for polymeric materials.

The starting part of slope provides a value for Young's modulus (or the modulus of elasticity) which is determine of stiffness. The curve also provides yield elongation, stress and strength at break. Strength of material expresses, amount of force which is required to break the sample, while toughness is related to amount of energy which is required to break the sample. Material may be strong but it is not required that it is also tough. A material which is not deformed appreciably before breaking are stronger but brittle, while a material which elongates or undergoes appreciable deformation before breaking is tougher. The materials showing longer elongation before breaking have larger area enclosed by stress-strain curve while stronger material have steep curve having smaller enclosed area.

There is usually has an initial slope which indicates a curve to moderate strength, very high modulus, low elongation at break, and low the stress-strain field (Fig.1.6). These materials are stronger but not very tough because they did not withstand much elongation before breaking. Polymeric materials showing brittle performance at room temperature or below are poly (methylmethacrylate), polystyrene and many phenol-formaldehyde resins.

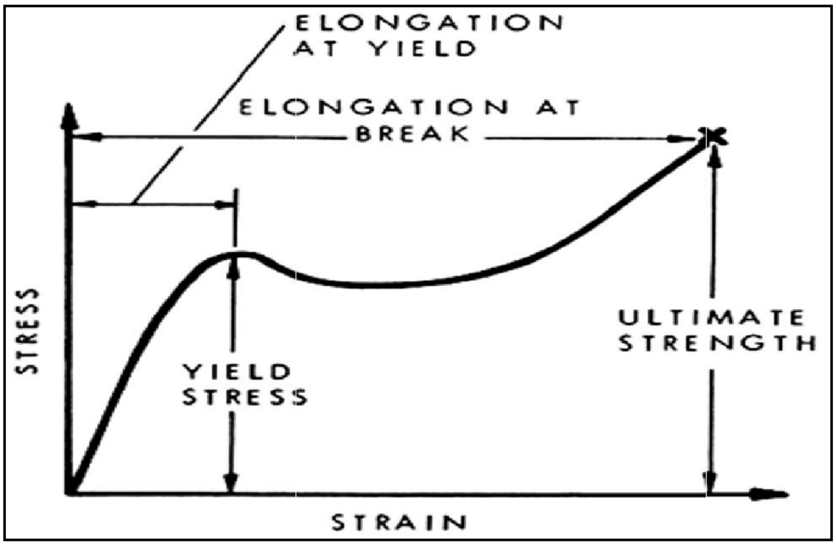

Fig 1.6: Tensile stress-strain curves for four types of polymeric material.

Polymers which are hard and strong possess high modulus of elasticity, high strength, and elongation at break of approximately 5%. The structure of the curve often suggests that the material has broken where a yield point might be expected. The two mechanical performances stress relaxation and creep is related to each other. Creep is stated as a phenomenon in which material deforms under load with time.

All plastics, creep to certain extent, in creep, elongation occur in the application of constant stress, and while in stress relaxation, a decrease in stress occurs when a specimen is held at constant essentially instantaneously induced strain. Repeated flexing of a sample (repetitive application of load) through a given elongation often causes deformation to accumulate and causes a sample to fail at a lower stress than it could for a single flexure *(Pious and Thomas, 2016).*

1.3.4.1 Micro hardness of a polymer

Hardness of the material is the most essential parameters for its mechanical characterization. It is very difficult to give exact definition of hardness, because measurement of this parameter involves diverse properties of material such as bulk modulus, Young’s modulus, dislocation contents and their configuration, etc. Hardness is well-defined as “a materials resistance to plastic deformation (which is permanent), usually by indentation”. It is a material estate by which a load can be applied to resist permanent deformation (bending, rupture, or shaping change). The material having greater hardness will have greater resistance towards deformation. Ash by *(Balta, 1985),* has given definition of hardness, which states that “hardness is the measure of resistance offered by a material to the permanent deformation/damage”. Micro hardness of material is measured at lower loads and is determined by applying a force via an exerting indenter like Vicker’s, Knoop or Wallace into the surface area of the material under 5g to 160g load. The prefix micro signifies very small vales of load and indentation. The indentation is such a small that it barely damages sample, therefore microhardness measurement is nondestructive technique. Usually the indentations made are such small that they can be only measured with the microscope *(Diego, 2007)*.

1.3.4.2 Mechanical properties of a thin film polymer

For polymeric materials, size of sample plays important role in deciding overall mechanical charactistics of the composite material in the study. Polymer blend, co-polymer and composite depend on its dimensional size weather it is thinner or thicker. The application of a polymeric material depends on its particular size. Thin film form of polymer most sorted form of polymers. Polymeric material in thin film form is fairly different from their counterpart in bulk. Today polymer are used widely in many applications in thin film form, like film coating, adherent epoxy under fills to localize the stress concentration during thermal expansion, in electronic packaging etc.

1.3.5 Electrical properties

Materials like ceramics, glass, polymers and bio-composites are mostly non-conducting materials. They obstruct passage of current through them. When these insulators are placed in an electric field, they bring changes in this field and they themselves pass through the appreciable changes within themselves, as a result they can store electrical charges. If we are interested in charges storage is to be main concern, the insulating materials are called dielectrics. For a material to be a dielectric, it must be an insulator. Being good insulators, polymers have excellent dielectric properties. Several authors have conveyed theoretical and experimental work related to these properties *(Scheirs, 2000)*. The common electrical properties of interest are discussed below:

1.3.5.1 Dielectric polarization

When applied to an electric field, polarization due to the shifting of charges inside the material, resulting in formation of dipoles, is known as internal polarization. Internal polarization includes electronic, orientational (dipolar), space charge or interfacial polarization. One can also charge dielectric by direct inject of charge carriers, on applying high electric field (10^5V/cm) between the electrodes which are close contact with dielectric material. Due to dielectric breakdown or corona discharge in the thin air gap between the electrode and the dielectric material, charges will get sprayed or deposited. If the injected charge is of opposite direction of the electrode in contact, it is called hetero-charge. The total polarization produced in dielectrics is the resultant of internal and external polarization.

$$P = P_{\text{int}} + P_{\text{ext}} \qquad \ldots (1.17)$$

Electrets are permanently charged materials which can hold charge for long time. Polymers do have dielectric properties and they are known to store charge quasi-permanently when subjected to field temperature treatment; due to this they are good candidates to work as an electret.

1.3.5.2 Dielectric strength

These are measures of the maximum electric field that a polymer can occur before it remains insulated. It is expressed as the proportion of the voltage in the thickness (volts/m) just before the breakdown. It depends upon temperature, thickness, conditioning of the sample, rate of rise in voltage, test duration and contamination etc.

1.3.5.3 Electrical conductivity

Polymers are recognized as insulators since long time. However, there are number of polymers which show conducting behavior. The polymers can have conductivity like metals or they have similarity with intrinsic or extrinsic semiconductors. The polymer electrical conductivity x, is the presence of free electrons not bounded chemically with the macromolecules. It also depends on low molecular weight impurities that can be a carrier source. The chemical constitution of polymer under study has only an indirect effect on the carrier's mobility.

Polymer's conductivity in glassy state is approximately 10^{13} to 10^{19} ohm^1. With increase in temperature, the conductivity of polymer also increases exponentially as follows:

$$X = Ae^{-\Delta U/RT} \quad \dots (1.18)$$

Where, coefficient A, mainly dependent upon temperature while R is a Universal Gas Constant, and ΔU is the Activation energy.

1.3.5.4 Dielectric constant (or permittivity)

The dielectric constant is a quantity measuring the ability of a material to store electric energy in an electric field. It represents the portion of the capacitance of an electric capacitor that is the capacitance of a dielectric material and a uniform capacitor with a vacuum between its plates, at a fixed external electric field frequency. This dimensionless number which is very important, have different values for polar and nonpolar plastics. It is very important parameter to keep in consideration for greater frequency uses and it varies with temperature, moisture, frequency and thickness.

1.3.5.5 Dissipation factor

Dissipation factor is quantity of inclination of dielectric material to captivate definite of the energy, when alternating power is applied to them. When AC is applied to dielectric, rapid polarization reversals takes place according to frequency of applied alternating current, due to these reversals some of the energy is lost within the dielectric material. The dissipation factor expresses this loss of energy.

It can be described as a ratio of lost energy transmitted at specific frequency in the form of heat current. It is usually measured at 1MHz. The dissipation factor is required to be very low when polymers are utilized as insulators in high-frequency applications such as radar and microwave equipments.

1.3.5.6 Dielectric loss

Dielectric loss is a loss of the energy which gets wasted when a dielectric material is heated in a varying electric field. It is the intemperance of energy due to charge transfer in a discontinuous electromagnetic field as polarization changes direction with alternating field. Dielectric loss in polymeric materials is due to the movement of chain sections consisting of large number of monomer units, when alternating electric field is applied.

1.3.5.7 Volume resistivity

Volume resistivity of a material is measure of resistance to the current when direct current distributes through the body of resistive material. It is measured as ohm per unit area of the electrode specimen thickness and is expressed in ohm-cm. Materials measuring volume resistance above 108 ohm-cm are insulators.

1.3.5.8 Surface resistivity

Surface resistivity is measure of resistance of the surface of resistive material to direct current, it shows how well current flows over the apparent of an object between electrodes situated on the related side of a specimen.

1.3.6 Water absorption properties of polymer

Most of the polymers absorb water, but this absorbed water induces changes only in very unique types of polymers. Water in a polymer matrix, is considered to be present in the free quantities and it is only active when hydrogen bonds is connected to polymer chain. Similarly, all polymer materials absorb moisture when are in contact with humid environment or when they are immerged in water. Water absorption affects mechanical as well as electrical properties of polymer composites. The polymer-matrix interface in composite will degrade due to absorption of moisture which in turn will reduce stress transfer efficiency, resulting in poor mechanical and dimensional properties. When the polymer absorbs moisture, Polymer erosion of a matrix interface area is the consequence of bad mechanical and dimensional characteristics that create bad stress transfer capability *(Dhakal et al., 2006)*. Water absorption poses a threat during the processing of polymers. Despite having water absorption as low as 0.2%, polymer melt can be distinguished from hydrolytic degradation during processing, results in a major loss of mechanical and physical properties. Mechanical, physical, chemical, and dimensional properties may be unfavorable due to the absorption of water/moisture of the polymer *(H'ng et al., 2011)*. In the presence of water, some polymers become swollen and soften, while some may dissolve in water such as polyvinyl pyrrolidone and PVA *(Mardas et al., 2002)*. In case of soft and inflammation, molecular mobility will increase through water absorption. Due to the accumulation of solvent molecules, polymer structures will open and solvent swelling, resulting in differences between polymer molecules increased. It leads to reducing secondary affinity and due to lack of inter-molecular friction, leads to a lower resistance to stress applied, which allows for easy translational motion *(White, 2006)*

1.4 Polymers with conducting properties and their composites

Polymeric materials are finding their use in all fields due to their exciting properties like: flexibility, strength, stability, elasticity, easy processing and ease of handling, mouldability, etc. Because of their high resistivity, polymeric materials are better suited as insulators in various electronic as well as electrical industries. For metals, their mining, processing and shipping is costly affair, therefore conducting polymers are most attractive and cheaper alternative for metals because of their exciting properties discussed earlier. The industrial requirement of electrically conducting polymers with polymer matriculation has been met by using a high mixture of gold, silver and graphite (sometimes very high, the content of conductors is as high as 80%) *(Mattan et al., 1988)*. But there are many disadvantages in this approach such as high processing costs and other physical-chemical properties degradation. Intrinsically conducting organic polymers like PANI, PPy and polythiophene etc. were studied extensively, because of having easy processibility and flexibility with other benefit of conductivity *(Talaie et al., 2000)*. Conducting polymers have many applications such as they are used for electronic circuits used as an antistatic coating material to prevent the risk of electrical discharge on photographic emulsions, it is used as an organic compound in OLEDs. The electrodes of the emitting electroluminescent layer can be employed as injection holes. Able to emit light in response to an electric current, can be used in mobile telephones in electroluminescent displays, as an emitting layer of high definition video matrix displays, etc. Materials scientists are interested in finding environmentally friendly ways to process and synthesize conducting polymers. The important conducting polymers are described in brief below:

1.4.1 Polypyrrole (PPy)

Apart from all known polymers, PPy have attracted special interest due to their remarkable mechanical, electronic and electrical properties. They possess high conductivity. Their ease of preparation and high flexibility and their environmental good mechanical and stability properties have developed great interest *(Rowley and Mortimer, 2012; Mishra, 2018)*. It is referred for its outstanding electrical, mechanical, thermal, and chemical characteristics, as a stable conducting polymer. *(Adeloju et al., 1993; Sakthivel and Boopathi, 2015)*. PPy is known for their potential applications in electronic and electrochromic devices *(Sukeerthi and Contractor, 1994; Teasdale et al., 1991; Mermilliod and Tanguy, 1986)*, as counter electrode in electrolytic capacitors (Jing et al., 2007), as sensors *(Khalid and Mohammad, 2007; Ragunathan*et al., 1998), use for chromatography *(Sanjai et al., 1998)*, use in manufacturing light-weight batteries *(Han et al., 2002)*, membrane based separation etc. PPy has a nodular surface morphology similar to cauliflowers the roughness of the surface always depends on the electrochemical synthetic conditions *(Tchmutin et al., 2003)*. PPy is conjugated polymer having backbone chain of alternate single and double bond. In the ground state the PPy has a non-degenerate conduction band with polarons and dipoles as the prevalent charge carriers. Several models in the mechanism of conduction in PPy were recommended, but no conclusive evidence was established due to structural defects present in PPy *(Srinivasan et al., 1999)*. The most widely accepted model to describe conductivity of PPy is hopping model which describes charge transport along the polymer chains, through hopping of carriers *(Ahmad and Mohammad, 2006; Yam et al., 2000)* (holes, bipolarons, etc.). ECP are like intrinsic semiconductors having a filled valence band and an empty conduction band. These bands are immersed by an energy gap. The doping of these polymers creates a new level in the energy difference, allowing electrons to go to these new levels and increase the conductivity of materials *(Hsu et al., 1991)*. The effective combination of conventional polymers with conductive polymers as filler may allow us to create new polymer materials with unique electrical properties. Composites of PPy with polypolefinshes discovered new applications, for example, electromagnetic shielding by blending with antistatic plastic films or PPy, polythiophene, PANI, or other conducting polymers.

1.4.2 Polyaniline (PANI)

PANI is a circulating polymer that is a center of attraction for polymer chemists as well as physical scientists. It related to the semi-flexible rod polymer family. Although it was discovered back in 1834, only in the 1960s PANI has attracted the attention of the scientific community due to its discovery of high electrical conductivity. Nowadays it is increasingly used in conductive coating of intellectual and multifunctional yarns in many applications in antistatic coating and electromagnetic shielding applications, as fibrous sensors, connection devices in smart coating and potentially as chemical sensors in electronic devices to growing rapidly *(Gould et al., 2000; Tian et al., 1991)*. The PANI is very special type of conducting polymer because its synthesis is easy; also, it has environmental stability and simple doping/de-doping chemistry *(Yakuphanoglu et al., 2006)*. Although the methods used to produce PANI are simple, but its polymerization mechanism and the true nature of its oxidation chemistry are very complex. Because of rich chemistry involved, PANI has been unique studied and investigated in the past 20 years. Like PPy, PANI is conjugated polymer, having single and double bond. The conjugated polymers exhibit conducting or semiconducting properties. Semiconducting polymers are at the centre of attraction for researchers in materials science field because they prove to be promising materials for the development of optoelectronic devices such as light emitting diodes, photovoltaic cells, and nonlinear optical systems *(Willander et al., 1993)* as well as used such as diodes, transistors, field effect transistor (FETs) etc. *(Lei et al., 1992)*. PANI behaves like a p-type semiconductor *(Mishra and Chandra, 1994)*. PANI which is simply synthesized by polymerization of cheap monomer aniline has good controllable electrical conductivity (depending upon the level of doping), good optical properties, and good stability in air and shows interesting behavior in redox reaction *(Gutman and Luons, 1967; Singh et al., 2001; Assadi et al., 1992; Chen et al., 1993).* These charactistics make it helpful for applications in optoelectronic, electrical, biochemical and other fields. It has three basic forms which are different by the unit of oxidation i.e. emerald (half oxidized), pernigraniline (fully oxidized) and leucoemeraldine (fully reduced), Emeraldine base is characterized by high durability at room temperature and because of the fact that it may be driven by doping as the PANIs emerald salt. The conductivity depends on the doping level of the proton i.e. the boundary of the proton *(Meikap, et al., 1993; Bredas, 1985)*. The maximum conductivity for PANI is obtained by 50% doping of protons. For doping levels above 50%, some amine sites are protonated, and at levels lower than 50% doping, some amine sites do not turn protonated. In both the eases, delocalization of the charge carriers over the backbone of the polymer get disrupted, which will result reduction in overall conductivity of polymer.

The present work as described *in-situ* polymerization of aniline (Ani) in the gelatin crosslinked hydrogel film was done so that a uniformly distributed array of PANI could be obtained within the Gel film matrix.

1.5 Objectives of the thesis

The major objectives of the proposed work are as below:

(i) To synthesize polyaniline /gelatin composite films.

(ii) Study of water sorption behavior of these composite films.

(iii) Electrical, mechanical and chemical characterization of polyaniline/gelatin composite films.

(iv) To investigate the results obtained to study the viability of composite films in modern applications.

1.6 Organization of the thesis

The whole study consists of following five chapters as mentioned below:

Chapter-1: It deals with the general introduction to science of polymers with physics and chemistry involved. It covers relevant topics based on definitions, classifications, structure, morphology and physico-chemical properties of polymers with special emphasis on composite materials. It presents a general introduction of polymer hydrogel films. The main highlight of this chapter is the various strategies that have been put forward to prepare PANI and glyoxal (Glox)-crosslinked gelatin (Gel) films and thereafter how the loading of aniline molecules was done and then final step of *in-situ* oxidative polymerization, resulting Glox-X-Gel/PANI composite films.

Chapter-2: It includes literature survey of various researches in the field which closely relates to present investigation. This survey was made on different system which provided an idea about the present research work.

Chapter-3: Describes 'Material and Methods': The materials and methods used in this investigation are discussed in this chapter in following order:

Firstly the chemical used and their procurement was described, then the preparation method of crosslinked gelatin film and loading of aniline and *in-situ* oxidative polymerization of PANI into the Glox-crosslinked Glox-X-Gel films to yield Glox-X-Gel/PANI composite films, have been described. This chapter also describes interpretation of various kinetic models that have been put forward to explain the kinetic uptake data. This chapter also discusses evaluation of various types of diffusion coefficients.

After this description of the characterization of films so prepared with XRD, tensile testing and conductivity measurements, follows. It is also discussed that how the variation in aniline concentration alters the deviation in mechanical and electrical characterization of Glox-X-Gel/PANI composite films. Finally the moisture sorption and physico-chemical properties of Glox-X-Gel/PANI films were described. The moisture sorption property of the plain Glox-X-Gel and Glox-X-Gel/PANI films has been described under various RH at various temperatures. The interpretation of data with GAB model is also described. The altered of thermodynamic parameters like q_{st} and s_d using Clasius-Clapeyron equation, have also been described.

Chapter-4: This chapter consists of results and discussion as well as describes results obtained in all the experiments and they were discussed and correlated with available literature.

Chapter-5: This chapter discusses a conclusion of research work with future prospects.

CHAPTER – 2
REVIEW OF LITERATURE

CHAPTER-2

REVIEW OF LITERATURE

Polymer Science is promising branches of modern science, because of widespread applications of polymers all around the world in nearly all fields such as construction, communication, medical science, textile, transport, space and technology etc. Various classes of synthetic polymers were studied for not only understanding the relationship between physicochemical structure of polymers but also to develop new material as per need. To have necessary set of valuable properties as per application, polymers having different chemical, mechanical and electrical properties were mixed together to form polymer blends. We have polymer composite having levels of properties or unique combinations by combining a polymer with different tactically selected material, like a another polymer, glass, carbon, or other bio materials

Awasthi et al. (2012) were studying polymer blends and composite in which various constituents and combinations gave the mixer thermal pretreatments including blending of polymers viz. polyethylmethacrylate and polyethylene oxide and then studied effect of on the mechanical properties of the synthesized blend under investigation. They have also studied microhardness, compatibility and thermal stability of polyethylene oxide (PEO) and polyethylmethacrylate (PEMA) polyblends. Hydrogel is a hydrophilic three dimensional polymer network sometimes they are seen like colloidal gel (which requires a liquid, in which solid is dispersed) and the role of dispersion medium is played by water. Hydrogels are highly absorbent; they can contain more than 99% of water. They possess a high degree of flexibility which is an identical to natural tissue, because these hydrogels have significant water content. Water absorbed by hydrogel is estimated hardly using some pressure.

Bajpai et al. (2012) was done a unique approach to make Poly (acrylamide-co-itaconic acid)/Graphite composite polymer and investigate the same for electrical conducting properties. They were also examined swelling behavior of dextran hydrogels cross-linked with epichlorohydrin (Ech) and preliminary Gliclazide release behavior. In another study *(Bajpai et al., 2016)* have determined release of gentamicin sulfate from alginate dialdehyde crosslinked casein films to antimicrobial applications.

Bajpai et al. (2018) have synthesized and characterized amoxicillin loaded poly (vinyl alcohol)-g-poly (acrylamide) (PVA-g-PAM) hydrogels and studied their swelling triggered release of antibiotic drug.

Bajpai et al. (2014*)* have prepared cellulose nano-whiskers (CNWs) doped poly (sodium acrylate) films and the obtained CNWs/poly (SA) films were reinvestigated for their property of absorbency of water in the physiological fluid. The water vapor permeation experiments were also done. Water vapor transmission rates (WVTR) were reported as very low film samples. The variation in parameters which defines mechanical characterization of films like tensile strength and % elongation (PE) was observed with variation in CNWs content. All samples exhibit good folded endurance (FE) without cracks and able to fold more than 600 times. Thin polymer films and also in the sorption of low molecular entrants due to structural changes, have a high degree of importance in the number of areas of application.

Philipp et al. (2015) have recently worked in the area of applications for the sorption of lower-molecular penetrants by thin polymer films and the resulting structural changes. Swelling, permeation, diffusion and dissolution treatments are induced often within films by solvents or gases. Similarly, *(Vogt et al., 2004)* studied the measured thickness dependent swelling, moisture absorption like equilibrium absorption. Even there are more studies related to the water barrier properties (sorption, permeability and diffusion) of water borne emulsion polymer coatings, but not the comparative properties of secondary dispersion (SD) coatings, completely studied by researchers. Here, dynamic water vapor adsorption analysis was used to analyze the equilibrium of the same structure of monomers of two different structural phase styrene-acrylate copolymers. Polymer coatings were not sufficiently strong and capable to inhibiting moisture and also do not prevent drugs -related moisture deterioration.

Wesigwa et al. (2016) have recorded frequently used barrier coatings on solid oral dosages designed to avoid moisture loss in the core of the table, preventing premature moisture of the active ingredients. However, the capability coatings of moisture barrier remain suspicious and debatable since degradation can be effectively accelerated. This study aims to demonstrate the barrier capably of four coating systems, followed by their application on a low hygroscopic drug formulation including aspirin as a particular moisture sensitive drug. The efficiency of polymer coating acting as a barrier on low hygroscopic cores is verylimited and use of these coatings can, besides these boost drug degradation in solid dosage forms.

Alves et al. (2010) studied the improvement in the barrier properties for water vapour and other (CO_2 and O_2) gases of a polymeric matrix having composition of kappa-carrageenan and pectin (66.7% kappa-carrageenan), with incorporation of mica flakes. The impact mica content on the film was discovered to depend on the inter force of water vapour permeability.

Giannola et al. (1999) described the development of an innovative antibiotic drug delivery system appropriate suitable for injury. This system was developed to deliver epidermal cultured keratinocytes together with transplantation of stem cells. The antibiotic was trapped in a reservoir compartment that was quite efficient at discharging the drug at a previously controlled rate. The required delivery profile was deduced*in vitro* using a very familiar two-compartment linear time-invariant model. The suitable rate for a release of the antibiotic in sufficient amounts for a therapy of 5-6 days was determined using a combined mechanism based on diffusion through a membrane and reductionin drug movement properties in the vehicle.

Jong and Wang (2013) and co-workers, the multi component hydrogel films composed of agar, carrageenan, konjacglucomannan powder, and nanoclay (Cloisite® 30B) were made and their characterization that is determination of their mechanical and water barrier characterization like water solubility water vapor permeability and water vapor uptake ratio and were done.

Porter et al. (2007) reported that hydrogels may find application in sensing of different polymer materials such as individual polymers and other composite materials, where in the swelling/de-swelling of the material is first sensed in response to some applied stimuli and then converted via transducer to a measurable electrical signal. They analyzed various models for prediction of the swelling activities of hydrogels which may be further used in applications closely related to monitoring of hydration in humans.

Zhang et al. (2015) communicated synthesis of hydrogel films having PVA-COOH and chitosan in various concentrations, which were crosslinked by the formation of amide linkages. They further stated that both dry and swollen states with higher swelling ratios (SR) improved the mechanical characterization of cross-linked films. The analysis of water vapor and oxygen permeability noticed that hydrogel films that cross-linked over wound beds can hold a moist environment. The biocompatibility experiment has shown very positive results in the absence of cytotoxicity and hemolytic potential of crosslinked hydrogels.

About 40^{yrs} ago all polymers were considered rigidly as insulators. Polymers were also used as passive storage and insulating materials by the electronics area due to their insulating characteristics. But with the advent of new class of polymer known as intrinsically conducting polymer or electroactive polymer, researchers started to reveal facts about synthesis, characterization and applications of this new class of material. Conducting polymer comprises the charactistics of metals and organic compound. Their biggest advantage lies in their processability. Being plastics, they have added advantage of mechanical property (flexibility, toughness, malleability, elasticity etc). The understanding of conducting polymers has been developing quickly. Various methods of conducting polymer’s synthesis have been extensively developed and studied. Several attempt to focus on obtaining novel conducting composites by mixing carbon, conducting organic monomer to some polymers. These conducting polymer have usually in the solid state. The conducting polymer can be formed by incorporating hydrogels with satisfactory conductivity with the hydrogel/conducting polymer based on the conductivity of the PANI and the water absorption of super absorbent polymers. A conducting hydrogel can find applications in die sensitive solar cells, fuel cells, super capacitors, rechargeable batteries, electrodes as well as actuators or sensors and many other applications.

However, in the past decade, some reports are cited because of their significant contribution to this field, in the tremendous research work done on PANI and other biopolymer-based electroactive and stretchable degradable composites and their applications. Some reviews have been noted due to their extensive contribution to this field.

Bhadra and Sarkar (2010) have reviewed applications of PANI and its composites with other polymers. Similarly, *(Chan and Mooney, 2008)* have discussed electrically conductive materials as a class of new materials for tissue engineering, capable of gaining greater control over biological response, and of neural-tissue engineering For, and is of particular interest to responsive prosthetics.

Gangopadhyay et al. (2001) tried to synthesis of polyaniline in stable aqueous solution/dispersion mode, applying PVA as an efficient steric stabilizer. Resulting method of synthesis of composite leads to successful approach of having combination of desirable physical properties like mechanical strength, electrical conductivity as well as solution processibility of PVA and PANI components.

Mohamoud and Mohamoud (2013) studied an unexpected but significant improvement of the redox behavior of conducting PANI films by trapping intrinsically nonconducting PVA in the matrix the polymer acting as stiffening and/or cross-linking agents.

Khosrozadeh et al. (2016) have developed flexible PANI based film to enhance the electrochemical activity of electrode. A facile and cost beneficial mechanism for fabrication of a high intensity performance supercapacitor (SC) with superior cyclic stability that is, tunable power, durability and energy densities using PANI was reported. Fabrication of SC electrode containing a loading of very high mass of active materials in a flexible film of PANI, silver nano-particles, exfoliated graphite (ExG) and tissue wiper-based cellulose with promising and exciting applications in wearable electronics, was also reported. The minimum weight ratios of ExG/aniline and aniline/silver nitrate prepared in this research were approximated to be 0.18 and 0.65 (or higher) respectively. The result indicates that a maximum capacitance of (3.84 F/cm^2) (240.10 F/g) at 5 mA discharge rate that may be obtained. In addition, research indicates promising that with a reduction in power density, the weight ratio of ExG/aniline can be rise from 1531.3 to 3000 W/kg, taking the previous ratio of 0.65 to more than 0.65.

Yang et al. (2017) provided a novel Nano structuring methodfor PANI electrochemical homemade using a noble forced convection approach. It was reported that PANI films the structure and morphology of at the nanometer scale can be controlled by changing the rotation speed of the disc electrode at the time of the electro-polymerization process. The very capable electrical nature of electrochemically arranged nano-PANI film based electrodes was also demonstrated by the authors.

Zhou et al. (2017) have synthesized of PANI/MnO_2 hybrid electrochromic films *via* anodic electro-deposition through a pot consisting from an aqueous solution having aniline and MnO_2. It has been studied that the unique deposition mechanism results in appreciable distinct differences between the hybrid and pure PANI films in morphology, structures, electrochromic and electrochemical properties. The film with optimum MnO_2 contenting compared to neat PANI films depicts cycling stability, higher optical contrast and coloration efficiency has been further reported. This great and appreciable potential of film can be attributed is due to unique porous morphology of film other than the small nanoparticles and donor-acceptor interactions among PANI and MnO2.

Srinives et al. (2017) investigated in an efficient way to electro polymerize a PANI nano-thin film on prefabricated microelectrodes and then modified the film with potassium iodide (KI) resulting in remarkable sensing performance related to one-dimensional nanostructure occurred like PANI nanowires. This resulted in sensitized contact to detect ozone as an effective chemically coupled sensor.

Pengcheng et al. (2015) worked on PANI-modified focused graphene hydrogel (OGH) films which have used to flexible solid-state SCs with the free-standing electrode. Flexible solid-state SCs relying on OGH films modified by PANI have much potential as energy-storage devices as free-standing electrodes (a stationary electrode with nano building blocks). Similarly *(Baheiraei et al., 2016)* have studied films of electroactive polyurethane/siloxane, containing aniline tetramer synthesized viva the sol-gel reaction of tri-methoxysilane functional intermediate polyurethane prepolymers made from castor oil and poly (ethylene glycol), having physicochemical, electrical, and mechanical properties optimized for cardiac patch (tissue-engineered cardiac patch aims at regenerating an infracted heart by bettering cardiac function and giving strong mechanical support to the diseased myocardium) applications.

Jeon et al.(2013) has acknowledged of polyaniline: poly (2-acrylamido-2-methyl-1-propanesulfonic acid) (PANI:PAAMPSA) a complex of water-processed complexes that have been assisted by a polymerized model that is renamed for attaining elevated doping concentrations with a potential equal to 4.5 V versus Li/LI + in LbL electrodes. by means of poly-acrylamide-2, methyl-1-propanesulphonatedic acid (PANI:PAAMPSA). They added that PANI/PANI: PAAMPSA electrode shows the excellent performance with respect to capacity and cycle life. *(Bayer et al., 2010)* synthesized of PANI template with PANI-PAAMPSA; such template synthesized PANI can be implemented as a conductive and functional biomaterial successfully.

Juarez et al. (2016) studied implementation of active bio-hybrid system formed by cells adhering to films of PANI, a semiconductor polymer having memristive properties assembled with polyelectrolytes. They further investigated whether PANI devices could survive by supporting the adhesion and difference of many cell lines, including neuron as 'SHSY5Y' cells. Cell viability reported as the most important factor for designing and developing a reliable functional memristor-based bio-hybrid which could mimic plasticity and neuronal activity.

Shao et al. (2011) have proposed synthesis of a considered range of new aniline-based tetramers in one step, without the need of protecting groups using Buchwald-Hartwig cross-coupling reaction. They further explained that the central variation of the aromatic ring has open up the possibility of carefully tuning the optoelectronic characteristics in this series, thus allowing structure-activity relationship to be formed.

Yslas et al. (2015) have described an easy to organize conjugates backbone changes using l-cysteine. The method discussed is the synthesis of PANI films supported onto polyethylene terephthalate (PET) films, and altered using cysteine (PANI-Cys) for production of biocompatible substrate for cell culture. The ability of these PANI-Cys films to support cell attachment and growth has been reported, infecting their potential application as biosensitive surfaces and tissue engineering.

Farias et al. (2014) have proposed preparation of composites from PANI and the ceramic technology of titanium dioxide (TiO2). The antibacterial study of the PANI (TiO2)/CTAB films was studied and the final results advise their usage as antimicrobial coatings. Similarly, with the target to develop new inorganic-organic films for gas sensing *(Xu et al., 2013)* have reported the manufacturing of layered double hydroxide (LDH)/conductive polymer multilayer films by assembly of alternate layers of exfoliated (over-stacked thin layers) ZnAl-LDH Nano sheets and PANI on silicon wafer substrates using the LbL deposition technology. They further explained, that the high selectively response of $(LDH/PANI)_n$ multilayer films to ammonia at room temperature. Because of poor process capability, doped PANI thin films were difficult to fabricate.

Kim et al. (2007) have investigated fabrication of one-dimensional multiwalled carbon nanotube (MWNT) nanocomposite fibers having better electrical properties applying electrospinning. They used PANI and poly (ethylene oxide) (PEO) as a conducting and a nonconducting matrix, respectively, for hybrid nanofibers including MWNTs. These hybrid confluent nanofibers can be implicated to chemical and biosensors that require high sensitivity.

Shishkanova et al. (2008) report repeated deposition of PANI to include the thickness of polymer film deposited on the PVC membrane surface. Oxidation of aniline was performed in a dispersion mode; with the existence of poly (N-vinpyrrolidone) (PVP) was present. They used two types of PVCs for this goal: PANI deposition within non plasticized PVC trophyloctyl ether (NPOE) and for the investigation of plasticized PVC. They further studied that the ionic selectivity of TDDMACl-based membranes was not noticeable to any degree by the thickness of PANI film, but their existence enhanced potentiometric characteristics (sensitivity and linear response range) of correction and stabilization

Ishiguro et al. (2011) have shown that a novel approach for conducting polymer films successfully demonstrates the concept of bipolar electrochemistry. The implementation of local produced of anodic potential to poly (3, 4-ethylenedioxythiophene) (PEDOT) and poly (3-methylthiophene) (PMT) on a bipolar electrode depends on the local electrochemical doping and reaction relying on the dependent on the auxiliary salt used. They pointed out this is consistent with the potential applied to BPE. This array-type driving electrode system was capable of drawing complex patterns in a site-controlled manner.

Baek et al. (2014) have systematically analyzed the impact of coating platinum (Pt) electrodes with the conducting polymer PEDOT doped with a series of common an ions for sensing applications. They have been also using polymers for coating for metal electrodes, in order to promote intimate cell interactions by reducing mechanical disparity with neural tissue.

Vyas et al. (2010) have employed poly (p-phenylene vinylene) (PPV) conducting polymer which synthesis the LbL process of a steady thin film. They have been applied to characterize ionic conductivity of multilayer PPV films with electrochemical impedance spectroscopy and cyclic voltammetry. These films have been observed to possess ionic conductivity which is depends on the temperature of the polymerization. For analyzing conductivity of films, they are fitted to the transformed Randle's circuit. They performed circuit equivalent calculations to provide diffusion coefficient values. A well-defined DNA biocogenous surface was an important component in establishing efficient biosensor platforms for diagnosis of diseases and for their treatment. It can be found that the application differs from bio-degradable and electro-active polymers because of different diagnostics and medicine for different pathogens and viruses as well as new drugs, forensics for tissue engineering point-of-care and to invent food technology.

Travas et al. (2011) described a universal and fast technique to develop such surfaces based on functionalized conducting polymer thin films. Sensing characteristics were used in circulating polymers for their ability to signal transducers for the occurrence of bio-detection. They reported that biosensor designs based on conducting polymers demonstrates several important features of potential uses, such as alabel-free sensing, fast analysis, long-term stability and the capacityto be applicable for both electrochemical and fluorescent protocols for DNA detection.

Mengyan et al. (2006) used blended polyaniline mixed with gelatin, and co-electrospun, a natural protein in nano-fibers to create a conductive scaffold for the purposes of tissue engineering to investigate its future use. Electrospun gelatin fibers with PANI were characterized applying SEM, electrical conductivity, tensile testing and DSC. They reported that PANI-Gel blend nanofibers can provide an innovative conductive material well suitable for biocompatible applications.

Mishra et al. (2010) has given a methodology for their possible use of fields for uniform coating of polyaniline (PANI) on carbon fiber. B–Naphthalenesulphonic acid (β–NSA) was used to provide and dopant to provide uniform coating on carbon fiber coverage as surfactant. They prepared the PANI-carbon fiber composites route, which had a conductivity of 10.73-23.5S/cm. TEM analysis of composites shows thick and uniform coating of PANI on the surface of carbon fiber. SEM of PANI carbon fiber results in non-coating uses for selective inclusion of other types of carbon. PANI's morphology-carbon fiber demonstrated introductory carbon fiber in PANI matrix. They further explained that such strategically prepared polymer coated carbon fiber could be a suitable for the next generation of building materials in several applications.

Wu et al. (1957) prepared Poly (butylene terephthalate) (PBT) composites containing PANI using a melt-blending methods. The compatibility with PANI in the PBT matrix was enhanced using maleic anhydride-grafted (g-MA) and PANI. The synthesized PBT-*g*-MA/PANI composites show remarkably superior mechanical properties then PBT/PANI due to maximum compatibility with PANI added to matrix. The fundamental bacteria for deducing the antibacterial characteristics of composite materials are Escherichia coli. The amide bonds established by condensation of the anhydride carboxylic acid groups of PBT-g-MA in the amino acids of PANI showed much greater antibacterial and antistatic characteristics compared to PBT/PANI composites.

Liu et al. (2012) explored basics of employing Nano cellulose as matrix material in a composite system. They reported that electromagnetic interference in these tuned electrically arranged biocomposites has potential for future applications in anti-static, shielding, electrodes, sensors, and storing devices. The hydrolysis was used in combination with sulfuric acid (60 wt. percent) of nanocellulose bleached flax yarn 55% to 1 hr under a vigorous stirring period. Thin composite films of nanocellulose with inclusion of PANI at different loading of aniline molecules, were synthesized using in-situ polymerization; here aniline was polymerized in acidic medium (HCl) with APS as oxidant in aqueous nano-cellulose suspension. Composite thin films possess improved flexibility and conductivity, together. These films can be bent upto 180º without breaking.

They also examined depend upon the amount of polyaniline (PANI) (0, 10, 20, 30 percent wt. %), the conductivity of synthetic film. The significant rise in conductivity of film was observed, when PANI concentration is increased from 10 to 30%. They study having 30 wt.% reached 1.9 × 10-2 S/cm, which is higher than reported values and shows encouraging signs of having applications as paper-based sensors, flexible electrode and conducting adhesives.

For investigating hydrogels having inherently conductive properties evolved for tissue engineering applications and for the bioactive scaffolds for electrically stimulating cells and modulating their function, *(Wu et al., 2016)* have proposed interfacial polymerization of aniline monomers within the matrix of gelatin methacrylate (GelMA) to make a hybrid composite, conductive in nature. They demonstrated that in comparison to pure GelMA and GelMA-PANI composite has identical swelling properties and compressive modulus, almost identical cell adhesion and spreading responses, but have superior electrical properties. Furthermore, they exhibited that synthesized composite of gelatin methacrylate and PANI may be produced in complex manual geometries by using digital projection stereo-lithography, and can find application in developing next-generation bioelectric linter faces.

Humpolícek et al. (2015) purified and modified Xa PANI hydrochloride (which is naturally conducting), PANI base (non-conducting) and PANI with poly (2-acrylamido-2-methyl-1-propanesulfonic acid) (PAMPSA) and thin films were synthesized. They examined the certain parameters of their hemocompatibility. The modification in the films was brought out either by addition of PAMPSA in the modification to the films was either by PAMPSA being added to the synthesis composite or by PANI base reprotonation. They showed that PANI-HCl and PANI base does not affect blood clotting and platelet adhesion. In contrast, the PANI, reprotonated with PAMPSA totally blocks clotting to inter-action components Va, Xa and IIa. Admirably reduced platelets adhesion was also cut on its surface. Furthermore, the film remains conductive upto pH of 6 that is a far better result in comparison because standard PANI-HCl loses all of its conductivity at 4 pH. PANI film with PAMPSA inducted during preparation has an effect on platelet adhesion but not clotting. The combined promising features such as conductivity, anticoagulation activity, low platelet adhesion, and largely enhanced pH conductivity are opened up for successful applications of PAMPSA reprotonated polyaniline in catheters or blood vessel grafting systems.

Sun et al. (2011) studied the morphological, electric and dielectric characterization of water-based conjugated polymer blends, like PPy: PSS or PEDOT: PSS were influenced by the water content. These characterizations also affect the macroscopic potential when conjugated polymer blends were applied to a device. By coating thin films of PPy: PSS films on hydrophobic graphite substrates through drop by drop of solution of PPy: PSS films (which are called drop-coating). Hydrophilic PSS flows onto the substrate after increasing relative humidity, as the hydrophobic PPy remains almost unaffected. Inflammation and dewatering of PSS produce irreversible morphological changes in thin films, in addition to nanoscopic rearrangements on the surface area of PPy: PSS films also result. Nanoscopic rearrangements can only be identified by dielectric imaging. They further reported that the relative humidity has different effects on dissolved and thermally characterized PPy:PSS thin films.

Hardy et al. (2015) synthesized the preparation of thin conducting composite biomaterials based on multilayer films of poly (3.4-ethylenedioxythiophene) derivatives, chitosan and gelatin by LbL method. They further reported that prepared conducting polymer-based films enhance the arrangement of fibroblasts on their surface that is more significant property of many types of tissues.

Mindroiu et al. (2013) studied the dependence of the macrophage reaction of the surfactants, which was generally used in the pyrrole polymerization process. They suggested that the immune reply to biomaterials having coating of PPy films, might be controlled and regularized by the choosing matching surfactant molecules

He et al. (2017) reported in recent work that 'ECPs' were important members in a family of very popular materials that interacted with ion-selective membranes (ISMs) to obtain solid-contact ion-selective electrodes (SCISEs) with electron conducting substrate. For maximum ion to electron transduction and potential stability, P-doped ECPs with low oxidation potentials, such as PPy, require that they, generally, be in their circulating form, allowing them to combat aqueous layer formation.

Golabi et al. (2016) worked on the single step synthesis approach, which not require the buildup and synthesis of rapidly individualized functional monomers, and can be easily extended to electrochemical, and can also be chemical, novel functional. Built-in surfaces and interfaces not only with pre-defined chemical properties as well as pre-defined sensing properties. *(Xie et al., 2016)* studied that the flexible electrodes, gas sensors and surface-enhanced Raman scattering substrates. In a report from *(Özer and Çete, 2016)*, a novel amperometric biosensor was described a successful method of developing anionic dopant altered electrode using organized polymer for cholesterol detection. *(Shrestha et al., 2016)*, fabricated biosensor, which since an effective and very sensitive platform for glucose sensing and may open up door for new possibilities for clinical applications. *(Kurra et al., 2016)* investigated the frequency response of micro pseudo capacitors based on conducting polymer electrodes. *(Rickard et al., 2016)* has guided the way of effectively regulating the dimensions of the tailor-made architectures whichcan open a new path towards various submicron device applications in supercapacitors,photovoltaic, sensors, and electronic displays. *(Pal et al., 2016)* reported that the conductivity-based sensory application of C-dot nanocomposite is fundamental in traditional contrast fluorescence-based sensory approaches. *(Ayenimo et al., 2016)* described an amperometric glucose biosensor of reliance having appreciable sensitivity for rapid tracing of metal determination. They further reported that this biosensor was successfully implemented to detect of metals in blow water samples.

Marvizadeh et al. (2017) recently, explored a nano-packaging material to be used as a coating or edible film. The effects of nanofiller mixing on the physicochemical, mechanical, physicochemical and crystalline structures including the barrier characterization of bio-nanocomposite films were studied. They films can be effectively used in food, and pharmaceutical packaging. In recent work, *(Ogawa et al., 2017)* reported that the improvement of chitin-based materials with desirable mechanical characterization and bio-capability was an interesting and important research objective, due to widespread functional uses. The films developed were fit for requirements in biological applications, e.g., tissue engineering, medicines, and cosmetics.

Uz et al. (2017) examined the Gelatin based 3-D conduits for trans separation of mesenchymal stem cells into Schwann cell. This work exhibits the necessity of adjusting the 3-D microstructure to simplify issues relating to tissue engineering strategies and techniques including stem cells that may further applied as promising approaches for peripheral nerve regeneration. In a significant work, *(Dammak et al., 2017)* noted the nano-emulsions in gelatin systems can function as potential active packaging systems to boost shelf life of food products and thus showing a way to provide high-quality products which are fresh and safe. *(Oladzadabbasabadi et al., 2017)* studied that completely altered sago starch in group with κ-carrageenan has features very much identical to those of gelatin, thus recommended system can find uses in pharmaceutical capsules methods.

Janjarasskul and Krochta (2010) have studied that by tailoring the properties of gelatin film by the incorporation of various types of maize starch facilitate the potential to extend its edible for food packaging applications. *(Zhuang et al., 2016)* reported that this composite was safe, eco-friendly, stable and bio-refractory and that may be decomposed by the environment gelatin cellulose properties were found after the disposed. The incorporation of a cellulosic cross-linker to gelatin-based films was an ideal choice with respect to developing a packaging for the food industry. In an interesting work *(Mohajer et al., 2007)* have studied that conducting composite film with the objective of successful characterization of physico-chemical in fish gelatin (FGel) based films.

Qi et al. (2017) investigated the work contains potential for making optoelectronic devices based on reduced graphene oxide-gelatin (rGO-Gel) films, such as photo detectors, photo sensors, optical modulators, switches and continuous photonic memory devices in the Tera Hertz region. *(Davidenko et al., 2016)* studied effective ways of simplifying the combined impact of chemistry and dimensional features of a substrate, on the activity of cell of protein-derived materials. This would assist in modifying their biological properties for specific tissue engineering applications.

Bipolar polymers were found naturally or may be derived from biological origins and may have several biological and industrial applications. A usable biopolymer should be non-toxic, non-antigenic, non-irritant, non-carcinogenic, pasteurize able and must be easily available for their widespread applications. *(Ahmed and Ikram, 2016)* investigated biodegradable Chitin and Gel based films and found them potent serve as packing films. A report from *(Van et al., 2016)* showing the construction of the correct scaffold matrix whose physico-chemical properties can be identified in relation to tissue regeneration application. They have achieved definite fine-tuning of the physico-chemical characterization of hydrogels which make them promising for tissue engineering technique.

Ge et al. (2016) informed that Genipin was natural cross-linking agent for biomedical applications, which can provoke and undergo polymerization related to ring openings in the alkaline state. Polygenipin was excellent for performing short and long-range inter-molecular cross-linking between chains of proteins. In this research, polygenipin of varying degrees were successfully synthesized in a laboratory and were used to fix gelatin content. The composite films are ideal candidates for food and pharmaceutical packaging materials. In an interesting work by in vitro study *(Amadori et al., 2015)* has demonstrate that the films crosslinked with genipin don't show any cytotoxic response, whereas glutaraldehyde crosslinking initiate an acute and dose dependent cytotoxic effect.

Nur et al. (2014) presented a review on fabrication and probable application of biodegradable films for food packaging. They observed that biodegradable films for food application has increased interest of scientists as they can be alternatives to traditional food packaging due to their sustainable nature simply associated with their easy availability, wide and abundant range, environmentally, compostability friendly image, food application and compatibility with food stuffs. They further added that gelatin is one such material which is a unique and usually hydrocolloid by the food industry today. It provides many food industrial applications because of intrinsic features. Gelatin from different sources was different in a different sense because they have different amino acid content and was believed to be due to the changing characteristics used in food systems. Packaging films can be successfully produced from all gelatin sources and the behavior and characteristics of gelatin-based films can be varied by incorporating other food ingredients, which results, composite films possessing excellent physical and mechanical characterization. This review presents the current scenario regarding the use of gelatin as a packaging source material and the problems that are in the way of moving the production of gel-based films closer to commercial reality.

Schönwälder et al. (2014) considered that in the area of surgery and regenerative medicine, it was crucial to have knowledge of interactions of proteins with the biomaterials used as implants. Protein adsorption directly impacts in vivo relations between cells and materials and leads to cell adhesion control on both the cell surface. Therefore, the scientific studies on applicable and suitable analytical techniques combined with well-defined model systems to uses for the detection, quantification, and characterization of protein adsorbates were very essential. In this important study, a protocol was developed for the deposition of extremely stable, thin gelatin-based films on different substrates. Their approach opens up interesting opportunities for sensitive screening of blind biomaterials that could be used in the future for regenerative medicine.

Several groups are doing research in the field of synthesis and characterization of hydrogels as well as use of hydrogels in variety of fields such as chemical engineering, medicine and pharmaceuticals food processing or preparation and agriculture. Similarly conducting polymers are extensively studied all over the world. Conducting hydrogels were studied and their application in fuel cell, super computer, dye sensitive solar cell and rechargeable lithium batteries due to their better conducting property, colloid stability, and simple preparation were reported by various researchers. Polyaniline based composite received attention of researchers owing to their various applications. Synthesis of composite of hydrogel with aniline and influence of preparation conditions on conductivity of composite was also reported in literature. But the study related to synthesis and detailed characterization of biopolymer and aniline composite has not been studied much. In fact, it seems that this is the first time when somebody is proposing a detailed study in which synthesis and characterization of composite of polyaniline and gelatin is to be done.

CHAPTER – 3

MATERIALS AND METHODES

CHAPTER-3

MATERIALS AND METHODS

This chapter is describing research materials and methodology, also helps in presenting a comprehensive rationale for selection of methods and tools used in research work, choosing suitable methodology and making guidelines for material collection. Finding and finding important material for research is also very important so the research process is covered in terms of implementation of polymer films with an overview of qualitative and quantitative methods.

3.1. Materials

The materials used in this research work with its source of procurement are listed below:

(i) Aniline(Ani)

Aniline(Ani); (Hi Media Chemicals, Mumbai, India) with molecular weight-93.13.

(ii) Gelatin(Gel)

Gelatin(Gel); (Hi Media Chemicals, Mumbai, India) was GR grade and used as received.

(iii) Ammonium persulphate (APS)

The initiator ammonium persulphate (APS; Hi Media Chemicals, Mumbai, India) was used as analytical grade and received.

(iv) Glyoxal (Glox)

The crosslinker glyoxal (Glox) $C_2H_2O_2$; (Glox) (40% LR) of analytical grade were obtained from Research Laboratory, Pune India.

(v) Hydrochloric acid

Hydrochloric acid (HCL) was obtained from Mumbai, India and was of analytical grade.

(vi) Water

The CO_2 free water was used to prepare various solutions, and was prepared by double distillation of water, containing a little amount of alkaline $KMnO_4$ in Pyrex glass assembly.

In order to create desired relative humidity (RH) environments for the obtaining moisture sorption isotherm, various salts i.e. KOH, CH_3COOK, K_2CO_3, Mg $(NO_3)_2$, NaCl, KCl and K_2SO_4 were purchased from SRL. Mumbai, India. Water activities (a_w) of saturated salts solutions at 30 ° C were adopted from elsewhere *(Jania et al., 2012),* and are listed below in Table 3.1.

Table 3.1. The water activities (a_w) of saturated salt solutions 30°C.

Salt a_w	**at 30°C**
KOH	0.0738
CH_3COOK	0.2161
K_2CO_3	0.4317
$Mg(NO_3)_2$	0.5140
NaCl	0.7509
KCl	0.8362
K_2SO_4	0.9700

3.2. Methods

The experimental methods and techniques used in this work were described in this section. First part of this section describes the method of preparation and chemistry involved for making experimental samples. The second part describes experimental techniques for characterization of the prepared samples.

3.2.1. Preparation of glyoxal crosslinked gelatin films

Crosslinking of gelatin was done with Glox in aqueous medium as described elsewhere *(Jari and Ali, 2011).* A solution having concentration of 10 % (w/v) of gelatin was by adding fixed quantity of gelatin in distilled water (DW) and keeping it over -night for complete dissolution. Next day, gelatin solution was heated upto 40°C under normal agitation within one hour and then filtered with sieve to get almost transparent solution.

Through adding 20 mL of this resolution of gelatin, 0.5 mL of 40 % glyoxal used to be then delivered and the final volume of ensuing combo used to be made up to 25 mL by means of including extra water to the answer. The solution was then transferred to Petri plate (identification 75 mm) and was once saved in an electric oven made through Tempstar, India, kept at 60°C for an interval of 12h to ensure complete crosslinking.

The films were peeled off carefully, washed in distilled water for a period of 6 h to remove un-reacted chemicals and then dried in a vacuum chamber until constant weight. Such crosslinked samples of gelatin (Gel) were prepared in all samples. These samples, three differed in amount of glyoxal in the film forming solution and the remaining three differed in amount of gelatin, but the solutions contents the same polymer to cross-linker ratio. The compositions of various film samples, synthesized, are given in Table-3.2. The complete setup of formation of Glox-X-Gel film (see Fig.3.1). The resulting Glox-crosslinked Glox-x-Gel films are shown in Fig. 3.2.

Table 3.2. Composition of Gelatin and Glyoxal.

Sample	**Gelatin**	**Glyoxal**	**Ratio**
A	1.5g	----------	1.5:00
B	1.5g	3.4482mm	1.5:.003482
C	1.5g	17.241mm	1.5:.017241
D	1.5g	27.586mm	1.5:027586
E	2.0g	10.844mm	2.0:010844
F	2.8g	17.241mm	2.8:017241
G	3.6g	27.586mm	3.6:027586

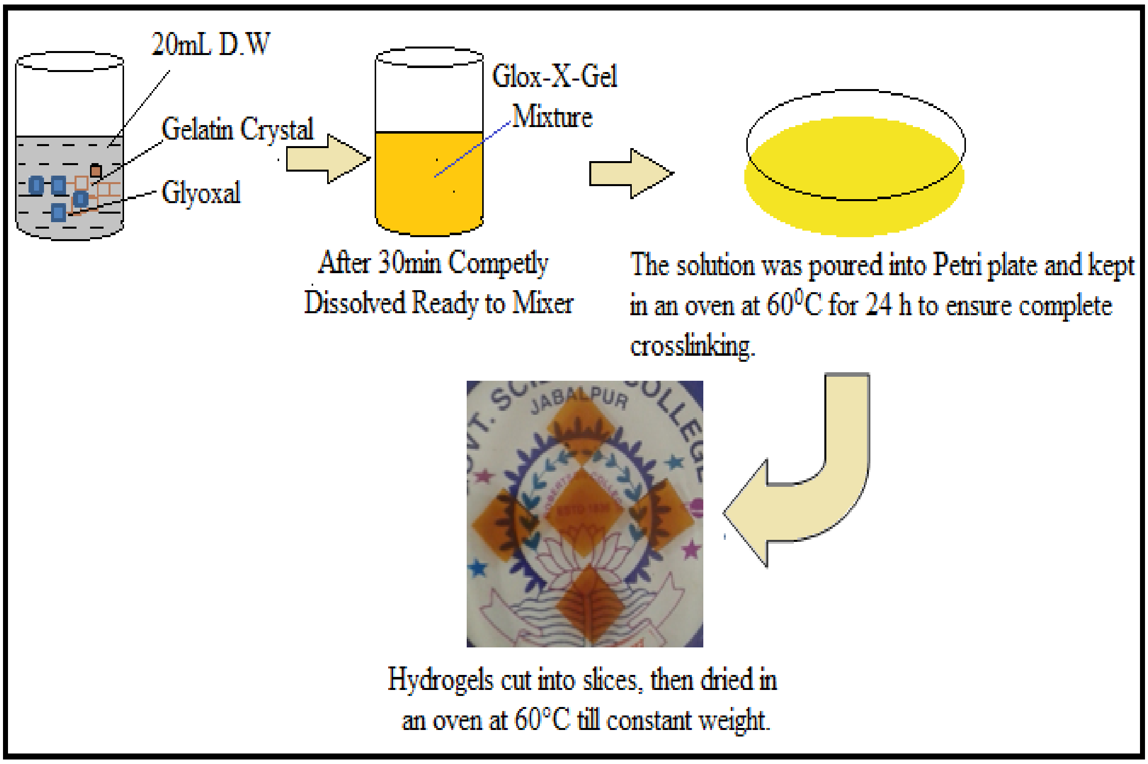

Fig.3.1: The overall scheme of formation of Glox-crosslinked Glox-X-Gel film.

Fig. 3.2: The resulting Glox-crosslinked Glox-X-Gel films.

3.2.2. Determination of percent cross-linking(PC)

To determine the amount of crosslinking, expressed as PC, ninhydrin method was described elsewhere (*Sungwoo et al., 2012*). The film samples (both crosslinked and un-crosslinked) were first weighed and then placed in 25 mL solution of ninhydrine having concentration of 1% (w/v) after which boiled for 15 minutes. The hot experimental mixture was cooled down. After cooling down the mixture was made 100 mL and then its absorbance was noted at 570 nm by using an ultraviolet-visible spectrophotometer. As an amino acid nitrogen standard, glycine was used.

The total number of free amino groups within the blend under investigation, before (A) and after (B) cross-linking is proportional to the optical absorbance of the solution. The *PC* was calculated using the following expression:

$$PC = \frac{(A-B)}{A} X100 \qquad \ldots (3.1)$$

Where, A and B are the mole fractions of free amino groups in the crosslinked and un-crosslinked gelatin (gel) films respectively.

3.2.3. Preparation of Glox-crosslinked Glox-X-Gel /PANI composite films

The composite film of Gel crosslinked with Glox and Aniline (Ani) used to be synthesized by using in-situ polymerization of Aniline within the matrix of gelatin. Briefly, 30 mL of aniline was taken right into 100 mL beaker (corning, India) and maintain within the ice bath at 5°C. Now, 20 mL of hydrochloric acid (HCl) (2 mL) was introduced drop-shrewd under smooth stirring so to ensure the complete disintegration of Aniline. Now, in other beaker, 1.0 g of APS was dissolved in 50 mL of distilled water (DW) and this solution was transferred into the resolution of aniline. First, a fixed measurement of Glox-X-Gel film was weighed and then this weighed crosslinked film used to be positioned in this solution of aniline and left for a period of 12h the reafter, the composite film that's the Glox-X-Gel/PANI film used to be taken out, washed with water after which allowed drying at 40°C till constant weight. The whole scheme of formation of Glox-X-Gel/PANI film is presented in Fig.3.3. In all five such samples were prepared, of which differed in quantity of aniline in the film forming solution and rest differed in amounts of aniline, but having same polymer to cross-linker ratio. The resulting Glox-crosslinked Glox-x-Gel/PANI composite films are obtained as displays in Fig. 3.4.

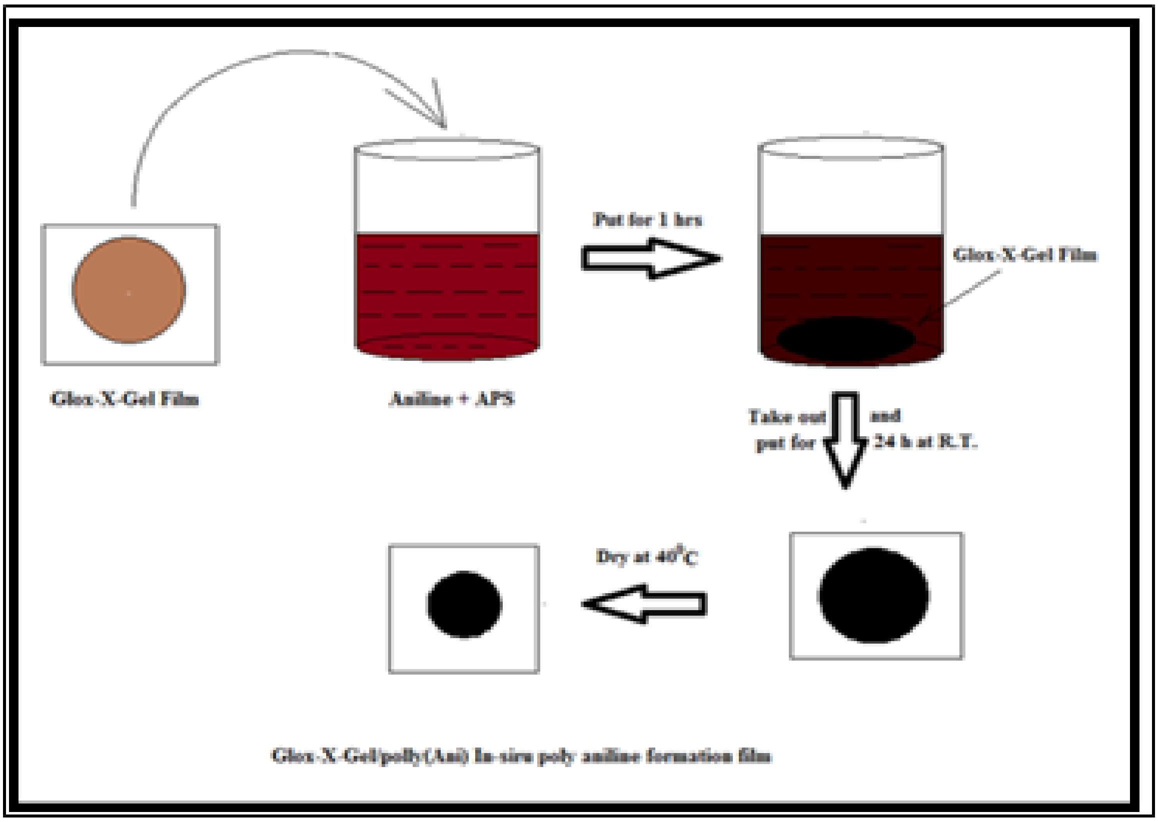

Fig. 3.3: The overall scheme of formation of Glox-X-Gel/PANI films.

Fig. 3.4: The resulting Glox-crosslinked PANI composite films.

3.3. Characterization of Glox-X-Gel/PANI films

3.3.1. Fourier transform infrared spectroscopy (FTIR) analysis

Fourier transform infrared spectroscopy which is also called as FTIR analysis is a scientific analytical technique of significance; always used to determine natural, polymeric, and in few cases used to identify inorganic materials also. The FTIR analyses are based on application of infrared light to appearance samples under test and observe their chemical properties.

The FTIR instrument exposes IR radiation of nearly 10,000 to 100 cm^{-1} through a sample. Some of this radiation is absorbed while some get passed through. The molecules of the film sample under investigation, converts absorbed radiation into rotational and/or vibrational energy. The resulting signal at the detector appears as a spectrum, typically from 4000 cm^{-1} to 400 cm^{-1}, representing a molecular fingerprint of the film sample. Each molecule or chemical structure will produce its unique spectral fingerprint; this makes FTIR analysis a magnificent apparatus for chemical identification.

FTIR spectroscopy has now becomes an effective tool and established method for quality control when evaluating industrially manufactured material. This technique often serves as 1st step in the analysis of material. A little variant in the sample characteristic the absorption band clearly affects the change in the composition of the material under investigation or the presence of infection within the established material. If problems with the product are trace by visual inspection, the origin of contamination present can be easily determined by FTIR microanalysis. This method is very helpful for the analysis larger areas such as small 10-50 μm of the chemical structure of smaller particles.

FTIR is used for analysis:

(i) Identification and characterization of unknown materials (in state: films, powders, or liquids, solids,)

(ii) Identification of contamination in a material (in state: particles, powders, or liquids, fibers,)

(iii) Identification of additives after extraction from polymer matrix

(iv) Identification of decomposition, or uncured monomers, oxidation, in failure analysis investigations.

As a quantitative device for measuring specifics functional groups, when their chemistry is well known and standard reference materials are available. The intensity of of the absorbance of radiation may be correlated to the extent the functionality present in the sample. FTIR is a completely capable and efficient tool with many applications in substances technology; however, data interpretation isn't always sincere. Naturally, the resulted overall spectrum of a sequence of absorbed strength reactions (consequently this method has Fourier Transform in the name). The bands showing absorption expressed within the spectrum are extremely discrete and degenerative. The particular “peak” of energy at a positive wavenumber can flow throughout and round a spectrum; this is based on diverse chemical and matrix factors (as well as at the manner of introducing incident strength). Therefore, we do not simply cross at a “research” desk to expect that a selected band of power within the ensuing spectrum will without a doubt belong to a few details. The spectrum has to be understood as an entire system and consequently, it probably needs positive know, which maximum experienced analysts do own. They have knowledge of all of the spectrographic strategies and that they have an understanding of applying them efficiently and characterizing the capability presented. In this work for samples during the study, the powder samples were mixed with KBR and obtained spectrum using FTIR spectrophotometer (Shimadzu, 8400, Japan). The recorded scans were averaged over 100 scans and the range of selected spectra falls between 400 and 4000 cm^{-1}.

3.3.2. X-ray diffraction (XRD) analysis

X-ray diffraction has been major tool for investigating the structure of relying on given that German physicist Max von Laue *(Panchbhai, 2015)* first advised in 1912 that X-ray can be diffracted through crystals. Within a quick time, the simple concept of XRD changed into developed and the technique changed into carried out to determine the shape of an ever-increasing variety of crystals.

In early 1920s Hermann Staudinger formulated a macromolecular principle of polymers. The use of XRD to determine the crystals structure, greatly equipped this theory to understand structure and properties of polymers *(Bragg et al., 1912)*. It is thrilling and perhaps tremendous of the problem of know-how polymer structure, that the early packages of XRD to decide the structure and morphology of polymers had been misinterpreted. Previously because of presumption that entire molecule must lie within a single unit cell, the XRD measurements on polymers interpreted that unit cell of polymer should not be longer than that of low molecular compounds *(Bragg et al., 1913)*, which concludes that the molecule of polymer having very large molecular weight must also be small. This presumption proved to be fallacious of course.

Since polymers are semi-crystalline there are arguments about the validity of a two phase model for describing the morphology of semi crystalline polymers and especially concerning the details of model incorporating chain folding. One of the limitations is that XRD analysis may not always yield a unique interpretation of the data. Often other techniques need to be used to complement the diffraction experiments. Nevertheless, XRD is still the single most effective technique for establishing the crystal structure and crystallinity of material.

XRD patterns have been recorded at IISER Bhopal. The XRD technique became implemented here to degree the crystalline nature of the Glox-X-Gel and Glox-X-Gel/PANI film. These measurements had been implemented on a Rikagu Diffractometer (Cu radiation = 0.1546 nm) operating at 40 kV and 40 mA. The diffractogram turned into decided in the range of 2 from 3 to at the speed rate of 2 degree/min.

3.3.3. Thermogravimetric analysis (TGA)

Thermogravimetry Analysis (TGA) was evolved around 1900 and the technique is based on totally the determination of decaying mass of aninvestigated specimen under regulated isothermal condition or under temperature varying linearly in aparticular given atmosphere. TGA is a technique, which is based on a fact that, on heating a material, there is rise or fall in its weight. Alternatively, TGA measures the weight loss of the sample when it is heated or cooled. TGA is an analytical method based on temperature where a thermobalance (a combination having a digital microbalance with a furnace equipped with the best appropriate temperature controller) measures changing sample mass. Commercially available thermobalances are thermo-gravimetric and chevenard recording thermobalances *(Nobert and Bikales, 1971)*. This method was used to investigate the material weight loss due to decomposition, oxidation, or loss of volatiles like moisture in a set temperature range. TGA gives a typical temperature (or time) versus mass (or mass %) plot. TGA is an important, effective and useful tool to infer about moisture, volatiles content, life expectancy, thermal stability and decomposition profile oxidative of sample. The approach of analysis on this method entails continuously tracking mass of a substance underneath have a look at as a characteristic of temperature or time whilst the sample specimen of a substance below study kept in a managed environment is subjected to controlled temperature software. Most TGA experiments use purging. Purging way the usage of an inert sample purge gas surroundings to keep away from combustion within a closed machine. A TGA meeting includes a pan having a pattern that's supported by way of the stability of tremendous precision. This pan sits inside of electric oven and is heated or cooled in the course of the scan. In most cases, sample weights are monitored within the test path. A pattern purge fuel controls the atmosphere in the course of the investigation and prevents burning. This fuel may be inert to combustion, which continuously flows over the sample and exits via an exhaust. The thermogravimetric statistics obtained from this controlled thermal reaction under constant surroundings is amassed and compiled through a graph with mass or percentage of preliminary mass on the y-axis versus either temperature or time at the x-axis via related laptop and required software.

This dimension gives facts approximately bodily phenomena, which include section transitions, absorption, and desorption; in addition to chemical phenomena consisting of chemisorption, thermal decomposition, and solid-fuel reactions. The TGA approach, like the DSC very famous and green method in polymer research, in particular, to take appear at the thermal stability of polymeric systems beneath given software situations. This is executed so the sample most effective reacts to temperature in the course of decomposition; we are able to say that its research pyrolysis of material. Such chemical decomposition of natural materials through heating the fabric without oxygen or other reagents can be described as pyrolysis that can induce burning i.e. inert environment. Pyrolysis is complex reaction during which various other reactions, both endothermic (bond rupture, volatilization, etc.) and exothermic (bond reforming) can happen simultaneously. Thermal degradation of polymers can be studied by TGA or derivative TGA. Derivative thermal DTG records derivative of TGA curve i.e.it records rate in alternating in weight of material upon heating against temperature. DTG simplifies closely placed thermogram peaks. Knowledge gained from study of thermal degradation may be useful in determining the thermal degradation of polymers. TGA technique provides valuable data which can be applied not only for selecting material for certain end-use applications but also to predict the performance of the product and vice versa to improve its quality. Thermo analyzers are available which can simultaneously record temperature and weight loss along with derivative TGA (rate of weight loss versus temperature or time) and differential thermal analysis plots *(Nobert and Bikales, 1971).*

A fixed range of grinded pattern used to be positioned in a ceramic crucible and then analyzed over the temperature variety of 30 to 800°C, on the heating expense of 10°C min^{-1} underneath the consistent flow of N_2 on the cost of 30 mL min^{-1}.

3.3.4. Atomic force microscopy (AFM) analysis

Atomic force microscopy or scanning force microscopy (SFM) is a high-resolution type of scanning probe microscopy (SPM), with resolution in order of fraction of a nanometer. This resolution is more than 1000 times better than the optical diffraction limit. AFM, measures surface topography, imaged areas can be from the nm scale to large as 100 µm x 100 µm. Height and depths of features on surface will also be measured and many surface roughness factors can be calculated. We can have 3-D images also for presenting data dramatically. The information about sample is gathered by "feeling" or "touching" the surface with a mechanical probe. Piezoelectric elements that expedite small but accurate and precise movements on electronic command enable precise scanning of sample.

In this process, roughness and the sizes of elements on the floor are determined through the mechanical motion of a diamond stylus over the sample. The trace of the surface is modified into digital data and is stored in a computer (PCs) for display on a CRT and can be outputted to a printer, for printing. The stylus drive can also be managed to protect delicate surfaces from injury. The Stylus Profilometer can do measurement laterally upto 1 μm and vertically upto 5 Å with the amazing magnification of 20-100,000X. It gives us a good two dimensional topographical data and it is a nondestructive system. The complete AFM technique includes three important abilities: imaging, force measurement and process. In force measurement, the force between the probe and the specimen was once measured as perform of their common separation. This will also be applied to perform force spectroscopy that is for measuring the parameters involving the mechanical properties of the sample, like young modulus and to access the toughness of the sample. In imaging technology, the probe response to the forces exerted by a sample on a probe is used to image the three-dimensional shape (topography) of the surface of specimen in high resolution. For making this image raster scanning is used. By raster scanning from one end of the sample to the other, there is continuous recording of the probe height at different positions of the specimen with respect to the tip, which corresponds to a continuous probe-sample interaction. The surface topography is usually displayed as a pseudo-color plot. Manipulation, precisely controlling the forces between tip and the sample, involves suing to isolate the characteristics of the specimen sample. Examples: locally atomic operation, scanning probe lithography, and stimulation of cells. The properties which can be measured are mechanical properties viz. adhesion strength or stiffness and electrical properties like surface potential or conductivity. In fact, the most of the SPM techniques are modification of AFM which use this methodology.

The principle difference between AFM and other equally competent technologies such as electron optical microscopy and microscopy is that the AFM does not employ lenses/beam irradiation. Therefore, AFM is not affected due to a limitation in spatial resolution due to diffraction and separation, and thus it was not necessary to prepare a location to direct the beam (by creating a vacuum) and to blur the sample.

There are several scanning microscopy including scanning probe microscopy which includes AFM, scanning tunneling microscopy (STM) and near-field scanning optical microscope (NSOM), simulated emission depletion microscopy (STED), and scanning electron microscopy (SEM) and electrochemical microscopy (ECM). Although SNOM and STED use visible, infrared or even terahertz light for illuminating the sample, under probe, however diffraction limit does not pose any threat on their resolution.

AFM has been successfully applied to many issues in a wide range of natural sciences, including solid state physics, molecular engineering, material science, molecular biology and cell biology. Applications in the area of solid state physics includes following:

(i) For the identification of atoms which are present at the surface of test sample,

(ii) For the evaluation of interactions between a particular atom and its surrounding atoms and

(iii) To study of changes in physical characterization as a resulting of changes in an atomic system due to atomic manipulation.

AFM patterns were recorded with the Hitachi S-4700 (New Jersey, USA) operating at an acceleration voltage of 15 kV. All samples were first dried in hot air oven at 37°C and then, gold coating was done before scanning. The imaging of surface morphologies was done at different magnifications.

3.3.5. Tensile testing

Tensile testing is a fundamental test in materials science and engineering in which a specimen is subjected to controlled stress until failure. One can directly measure ultimate tensile strength, maximum elongation, breaking strength, and area reduction from this test. From these measured physical quantities, one can determine other such as: Young's modulus, Poisson's ratio, yield strength, and strain-hardening characteristics. Modern tensile testing machines are designed for computer aided digital testing and determining the elongation and tensile strength of polymeric materials, textiles, yarn and many other products including fine aluminum, copper and steel wires, where bearing load remains in the maximum specified working range of material under study. The most generally used testing machine to obtain the mechanical properties of isotropic materials in tensile analysis is the universal testing machine. For testing with this machine, it is required to prepare standard specimen in a square or a circular section along the gauge length, depending on the applied standard. It is necessary that, specimen should have appreciable length both of its ends should have sufficient length and surface condition to hold the specimen between the crossheads of the machine during testing. There are two crossheads in this machine one for the adjustment of the sample length and another is induced to apply tension to the specimen being tested. These machines are basically dependent on constant rate of traverse (CRT) theory. The tensile strength is measured in such method that the test sample is held between two vertically arranged grips which is placed one after the other and then the tensile stress is applied slowly and continuously to the test specimen. Finally the process gradually becomes elongated. The elongation stops with braking of the sample. During this process, the elongation of the gauge section of the specimen is recorded against the applied force. The data is manipulated accordingly so that it does not depend exclusively on the geometry of the test specimen. Along with this elongation of the specimen, which is nothing but the expansion of the specimen placed between the grips during the tensile test is also determined. Elongation measurements are used to calculate engineering stress and other parameters. It is essential that the test specimen should have sufficient capacity for testing. There are four parameters of machine-demand capacity force capacity, speed, and accuracy. Force capacity is related to the basic fact that the machine must be able to generate enough force to break the sample. It is also necessary that the machine must be able to mimic both the conditions of naturally occurring conditions during real application, in the real world that isomerism force can be applied or sometimes it is applied slowly.

In this study UNILAB Digital Tensile Strength Tester was used. This machine is very well designed machine and is driven by electromechanical screw having precision and column construction also having variable speed drive. Mainly two option are available, which give machine accuracy and worth fullness, they are Acme threaded screw with DC Motor drive & ball lead screw with servo drive. The drive is driven by an electric AC motor torque by which the drive channel is moved through two intermediate phase pulleys. By selecting the "V" belt in the appropriate grooves, different transverse speeds can be set to 10 mm/min or as desired. In the lower and upper limit conditions of the drive, the motor stops automatically. The top frame of the machine holds the load cell assembly. Digital load indicators are provided with zero adjustment and maximum peak hold load buttons. This machine has digital load measuring, in order that both minimum and maximum loads can be read as accurately as possible. The extension experienced by test specimen during the tensile testing is obtained by evaluating changes in the distance between the two gripping arrangements. The monitor of the machine has capability of displaying elongation. This machine is equipped with gripping arrangement consisting of screw type finger tight grips, which allows convenient gripping and releasing flat specimens of up to 150 mm wide. The mechanical property of Glox-X-Gel/PANI composite films was studied using this tensile testing machine. Technical specifications of the machine are given below:

Technical data capacity of the tester: 0-2500N (250Kg) or 0-500kg / 0-5000N Sensitivity: 50 g and 100 g speed of the tester as required minimum grip separation can be

50, 100, 250 or 300 mm/min. 25mm maximum grip separation: 750mm Motor: ¼ hp, single phase 220v, 80rpm. The measurements were achieved at 25°C under a constant humidity of 50%. The tensile test samples were prepared by cutting strips, each with a width of 10 mm and length of 50 mm. Initially the flue separation and mechanical crosshead speed were precisely maintained at 25 mm and 100 mm per minute, respectively. The various formulae used are given below:

$$\text{Tensile strength } (\sigma) = \text{force or load } (F)/MA \qquad \ldots (3.2)$$

Where F applies max load and 'MA' is the minimum cross-sectional area of the experimental film specimen. Results obtained were converted to mega Pascal units (MPa).

$$\text{Young Modulus } (Y) = \text{Tensile strength}/\text{Tensile strain} \qquad \ldots (3.3)$$

$$Y = F \times L_0/MA \times (L_0 - L) \qquad \ldots (3.4)$$

$$\%\ \text{Elongation} = (L_0 - L)/L_0 \times 100 \qquad \ldots (3.5)$$

L_0 refers to initial length and L is the elongation when the film breaks *(Kumar et al. 2010).*

3.3.6. Impedance analyzer

Impedance may be very fundamental parameter. It is using various *AC* (alternating current) parameters of electronic accessories and circuits. Impedance can be described as the resistance of an *AC* of some frequency when it is allowed to pass through an electronic device or circuit. The methods often used for impedance measurement are: bridge method, resonance technique, RF *I-V* method, *I-V* method, auto balance bridge method and network analysis method.

Impedance, expressed by a symbol *Z*, expresses resistance to the flow of *AC* current. It can be calculated from the current *I* that flows through the element whose impedance is being measured and the voltage *V* in this element. Since the impedance is represented as a vector on the plane, LCR meter, which measures not only the ratio of the RMS values of current and voltage. Phase difference waves shown in Fig. 3.5.

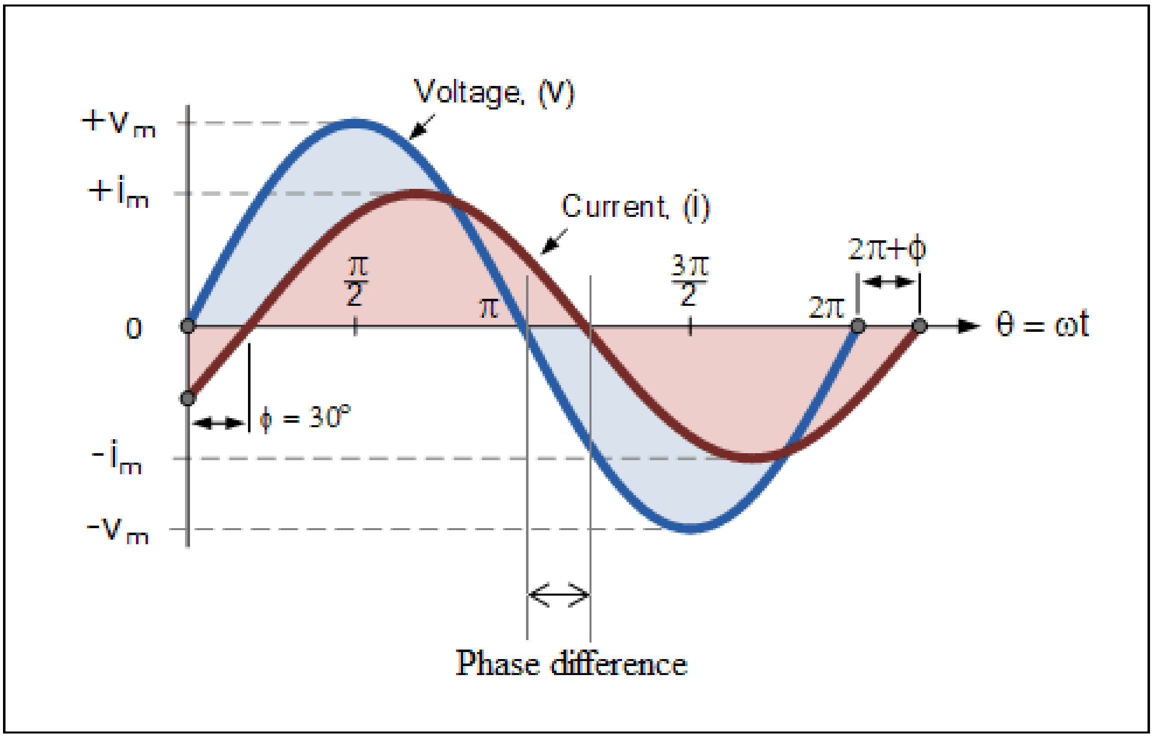

Fig. 3.5: Phase difference between current & voltage waveforms.

Impedance vector includes real part (resistance, *R*) and imaginary part (reactance, *X*).

$Z = R + jX$ (In rectangular form) … (3.6)

Z = |Z|Angle (θ) (In polar form) … (3.7)

Admittance $Y = 1/Z = G + j \times B$ … (3.8)

Where, *G* is conductance and *B* is susceptance Impedance is measured in Ohm while admittanceis measured in Siemen.

When real (*R*) and imaginary $(j \times X)$ components are connected in series

Impedance$(Z) = R + j \times X$ … (3.9)

When real and imaginary parts are connected in parallel,

Impedance$(Z) = \frac{R \times X}{R + j \times X}$ …(3.10)

OR $Y = G + j \times B$ … (3.11)

Here admittance is used for simplicity. Reactances are in two forms viz. inductive reactance *(X_L)* and capacitive reactance *(X_c)*.

$X_L = \omega L = 2\pi f L$ And$X_c = -(\omega C)^{-1} = -1(2\pi f C)^{-1}$ … (3.12)

Where in *f* is frequency, *L* is inductance and *C* refers to capacitance $W = (2\pi f)$ is known as angular frequency.

Impedance meter or LCR meters are measuring instruments that measures impedance.

$$\dot{Z} = \frac{\dot{V}}{\dot{I}} = \frac{|V|<\theta_V}{|I|<\theta_I} = \frac{|V|}{|I|} < (\theta_V - \theta_I) = |Z| < \theta \qquad \ldots (3.13)$$

In this study we have used impedance analyzer to measure impedance, admittance, conductance, capacitance, inductance, resistance, reactance susceptance, phase angle, quality factor and D-factor offered by composite sample in frequency range from 100 Hz to 50 MHz using parallel equal circuit at a temperature of 30°C keeping drive level of 1000 volts. These measurements are carried out at IIITDM, Jabalpur using Impedance Analyzer (Make, Wayne Kerr Electronics, UK).

3.3.7. Ultraviolet-visible spectrophotometer

Ultraviolet-visible spectroscopy (UV-V or UV/V) is a technique, which is based on absorption spectroscopy in the UV region of spectrum. This optical technique make use of light in the visible and nearby (near-UV and near-infrared (NIR) ranges. UV/V spectrophotometer is used to determine quantitatively, quantity of the absorber within the solutions of transition metallic ions and highly conjugated organic mixtures. Principle behind this method is Beer-Lambert law. The statement of this law is “The absorbance of a solution is directly proportional to amount of absorbing species in the test solution and the path length”. Thus, for a fixed length of path, UV/V spectroscopy can also be applied to obtain the amount of absorber in a solution. The absorbance of light varies with the amount of absorbent in the solution.

This instrument has certain unique features. It has over coating of quartz which protects the optics applied, from the surrounding environment and permits cleaning without damage to their reflective surface. Exposure to corrosive environment is protected through optics which is sealed. Double choppers make it correct sothat strike at the detector by the sample and reference beams occurs at the same point. This removes all possibilities of occurring errors, during experiment due to non-uniformly of the detector. The optimum control over data resolution is achieved through variable slits. One can set spectral bandwidth to as low as 0.2 nm. Possibility of occurrence of shifting and suppression of peaks at high scan speeds is nullified by a phase locked wavelength drive. The large sample compartment offers more flexibility in sample size. The UV-V is Spectrophotometer made by Shimadzu, Genesis 10-S placed in Chemistry department of Govt. Science College was used for this study.

3.3.8. Swelling study

3.3.8.1. Water absorption behavior of composite films.

Using an electronic the water absorption of Glox-X-Gel films was studied gravimetrically in this research work *(Bajpai et al., 2015)*. The swelling medium employed was distilled water with pH 6.6. A pre-weighed film sample was first placed in 150 mL of distilled water at 37°C and it was then taken out at regularly at different time intervals, cleaned and dried gently externally with tissue paper to remove loosely bound surface water and then weighed correctly with balance (Denber, Germany), and then the sample is again placed in the swelling medium. Finally, the swelling ratio (SR) was considered using the following expression:

$$SR(g/g) = \frac{(M_t - M_0)}{M_0} \ g/g \qquad \ldots(3.14)$$

Where M_0 and M_t are the initial weight and the final weight at different time intervals, respectively. To determine Equilibrium Swelling Ratio (ESR), M_t was replaced by M_e which is the weight of the swollen film at equilibrium.

3.3.8.2. Network parameters

The equilibrium water uptake of any polymer sample shows its swelling capacity and it is the network structure, hydrophilicity, the crosslinking ratio and the degree of ionization of functional groups *(Gan et al., 2001)*. One of the most significant parameters characterizes crosslinked hydrogels is (M_c) the average molar mass between the crosslinks which is directly linked to the crosslink density. The Flory-Rehner equation *(Flory and Rehner, 1943)* was used to calculate M_c can be given as:

$$M_c = -d_p V_s \Phi^{1/3} [1n(1 - \Phi) + \Phi + c\Phi^2]^{-1} \qquad \ldots (3.15)$$

Where volume fraction Φ of the swollen polymer is calculated using the equation:

$$\Phi = \left[1 + d_p/d_s(M_a/M_b) - d_p/d_s\right]^{-1} \qquad \ldots (3.16)$$

In the above equation, d_p and d_s represent the densities of polymer solvent respectively; M_b and M_a are mass of polymer before and after swelling; V_s is the molar volume of the solvent and χ refers the Flory-Huggins interaction parameter between solvent and the polymer which may be calculated by a method described *(Aithal et al., 1990)*.

The crosslink density q is given as:

$$q = M_o/M_c \qquad \ldots (3.17)$$

Here M_c is molecular weight between crosslinks and M_o is molar mass of the repeat unit. The crosslink density V_e may also be taken as the number of chains which are elastically effective and are totally inducted in a typical network for unit volume:

$$V_e = d_p N_A / M_c \qquad \ldots (3.18)$$

3.3.8.3. Analysis of water uptake

When a glossy polymer is dropped in a solvent, the solvent diffuses into the polymer matrix, which results, swelling of polymer.

In this diffusion process, migration of water to pre-existing or dynamically produced spaces occurs between macromolecular chains. Swelling of hydrogels involves large-scale segment motion that ultimately results in widening of the separation distance between macromolecular chains *(Saraydin et al., 1994)*.

The portion of water absorption curve, with a fractional water uptake M_t/M_∞ less than 0.60 was analyzed using Peppas equation *(Philip et al., 1987)*:

$$M_t / M_\infty = kt^n \qquad \ldots (3.19)$$

where M_t and M_∞ are the masses of water absorbed at time t and at equilibrium respectively, k is the gel characteristic constant and 'n' is the swelling exponent describing the mode of penetrates transport mechanism. One can evaluate these constants n and k with the help of slopes and intercepts of the plots of $ln\ (M_t/M_¥)$ versus lnt from the experimental data.

For a cylindrical gel, n = 0.45-0.50 corresponds to Fickian-type diffusion process while $0.50<n<1.0$ shows non-Fickian or anomalous transport, and n = 1 implies relaxation controlled transport.

3.3.8.4. Diffusion coefficients

Ficks 1st and 2nd laws of diffusion adequately describe the most diffusion processes. For film shape hydrogels, the integral diffusion over short times, the main result is

$$\frac{M_t}{M_\infty} = F = 4[(D_t/l^2)^{\frac{1}{2}}]/\pi^{1/2} \qquad \ldots (3.20)$$

where, F is the fractional water uptake (M_t/M_∞) and D is diffusion coefficient. In equation (3.20) the slope of the linear plots of $F\ (M_t/M_¥)$ versus $t½$ yielded initial diffusion coefficients D_i for the various hydrogel samples.

$$D_{ave} = 0.049 l^2 / t^{1/2} \qquad \ldots (3.21)$$

The avg diffusion coefficient D_{ave} may also be calculated for 50 present of the equilibrium swelling by putting $M_t/M_\infty = 0.5$ in the above expression, which finally yields where $t_{1/2}$ is the time required for 50% swelling. Diffusion coefficients were also deduced using the late time approximation as described by *(Brazeland Peppas, 1999)*.

$$M_t/M_\infty = 1 - [8/\pi^2\{exp(\pi^2 - D_t/4l^2)\}] \quad \text{… (3.22)}$$

Using the data for swelling, plots for *ln (1-M_t/M¥)* versus *t* are drawn and with the slope of the linear plots thus obtained; late-time diffusion coefficient D_L may be calculated using the following expression:

$$D_L = -(Slope\ X\ l^2/\pi^2) \quad \text{… (3.23)}$$

3.3.9. Determination of moisture sorption isotherm

The moisture adsorption isotherms of the plain and the aniline-loaded films that have been described in detail by the gravimetric static method elsewhere *(Bennaceur et al., 2015)*. Prior to the moisture adsorption experiments, the films were dried in oven made by Tempstar, India, at a temperature of 40°C for two days. We have taken completely saturated salt solutions of seven salts in sevenseparate jars. Crystalline salts were settle down at the bottom of jars at 30°C. A polypropylene chamber was placed in each jar (see fig.3.6)

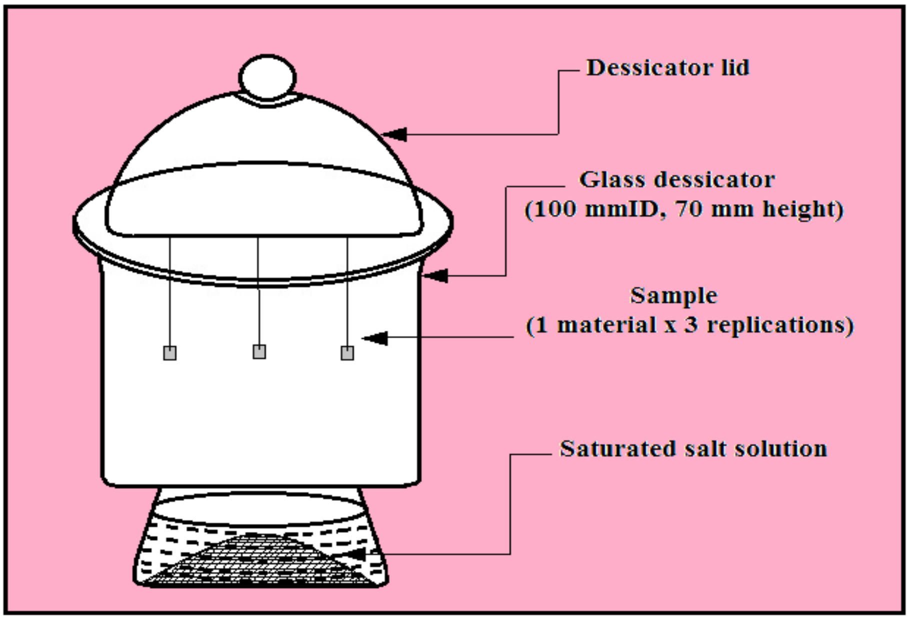

Fig.3.6: Static method apparatus set up for moisture sorption isotherm study.

The film samples are then weighed first in a small crucible of 1 gram and then aluminum foil, and then these crucibles are placed in a jar of polypropylene in the samples, which were then tightly closed. The jars were placed in a Sanyo MIR 152 incubator at 30°C for equilibration of the samples. It took about 3 days to reach equilibrium. The moisture of the balanced samples was obtained using the vacuum oven method *(Kaymak and Gedik, 2004)*. The equilibrium moisture contents of samples have been represented by way of unit viz. gg^{-1} dry solids. All of the experiments of moisture adsorption have been repeated three times in identical fashion. The percentage difference in the moisture contents at equilibrium, between triplicate samples was, on the average found to be less than 1% of the mean of the three values. The average values were then used for the moisture adsorption isotherms process.

The equilibrium moisture content (*EMC*) used to be determined using the following formulation *(Kong et al., 2014)*:

$$EMC = \frac{(\,Final\ weight - Initial\ weight\,)}{Initial\ weight}\, g/g \qquad \ldots (3.24)$$

3.3.10. Sorption isotherm models

The moisture sorption behavior of various film samples were usually carried out under different relative humidities to predict the affinity of films towards environment. The quantitative interpretation of moisture uptake data was made with the help of GAB isotherm model.

3.3.10.1. GAB isotherm model

Among the most capable equations for the prediction of the experimental data, the well-known GAB (Guggenheim-Anderson-de Boer) isotherm model *(Oliveira et al., 2009)* was used. The major advantage of the GAB model is its viable theoretical background, need for only three parameters and its capacity to describe the sorption of water vapor in wound up to water activity of 0.03 to 1.00. The GAB equation is expressed in the following method:

$$M_c = \frac{M_0 C K_{a_w}}{(1-K_{a_w})(1-K_{a_w}+CK_{a_w})} \qquad \ldots (3.25)$$

Where M_c is the equilibrium moisture content of the material on a dry basis (*g/g*), *C* is the Guggenheim constant related to heat of sorption, a_w is water activity, *K* is the constant related to properties of multilayer molecules and M_o is the moisture content of single layer in the BET theory. After transformation, GAB equation has an equivalent form similar the *(Hail and Horrob, 1946)* in equation.

$$\frac{a_w}{M_c} = (a.a_w^2 + \beta.a_w + \gamma) \qquad \ldots (3.26)$$

Then following relationship occur between the parameters of the above equation and those of the GAB model:

$$\alpha = \frac{K(1-C)}{M_0 C} \qquad \ldots (3.27)$$

$$\beta = \frac{C-2}{M_0 C} \qquad \ldots. (3.28)$$

$$\gamma = \frac{1}{M_0 C K} \qquad \ldots (3.29)$$

$$K = \frac{-\beta \pm \sqrt{\beta^2 - 4\alpha\beta}}{2\gamma} \qquad \ldots (3.30)$$

$$\mathrm{C} = \frac{2\left(\pm\sqrt{\beta^2 4\alpha\gamma}\right)}{-\beta \pm \sqrt{\beta^2 4\alpha\gamma}} \qquad \ldots (3.31)$$

$$M_0 = \frac{1}{\sqrt{\beta^2 4\alpha\gamma}} \qquad \ldots (3.32)$$

Finally, the above equation may be solved to yield parameters for GAB model.

From the parameter α, β and γ the values of constants K, C and M_o were calculated through following above relations (equation 3.30, 3.31 and 3.32).

3.3.11. Blood compatibility

The blood compatibility of Glox-X-Gel and Glox-X-Gel/PANI samples used to be decided in the terms of thrombogenicity, haemolytic potential and total protein adsorption following the standard ISO *(Achala et al., 2012)* method given. All tests were carried out at pH 7.4 9 *(Paul et al., 2006).*

3.3.11.1. Thrombus formation test

A gravimetric method was used for the evaluation of thrombus formation on the film samples. The film samples, with surface area of 1 sq. cm. were equilibrated in a solution of salt having 0.9% concentration, for 24 h at 37°C. Thereafter, the films were taken out and on the surface of the film, 0.05 mL and the solution of acid citrate dextrose (ACD), blood and 0.03 mL of 0.1M $CaCl_2$ were placed and the film, treated as described above was left for 10 min. After 45 min, the clotting method was stopped by addition of 4.0 mL of distilled water, followed by fixation of clots by using 2.0 mL of 36% formaldehyde solution.

The samples were now dried and finally weighed. Negative and positive controls were taking beakers without sample and blood, respectively *(Ferreira, et al., 2007)*. For comparison, a commercial paraffin gauge (G/1289 India) was also used. The thrombus percentage used to be calculated as follows:

$$\text{Thrombose}(\%) = \left[\frac{Weight\ of\ test\ sample - Weight\ of\ (-)control}{Weight\ of\ (+)\ control - Weight\ of\ (-)control}\right] \times 100\% \qquad \ldots(3.33)$$

3.3.11.2. Heamolysis test

The Heamolysis tests were performed as described in American Society for Testing and Materials (ASTM) ASTM F 756-00 (2000) *(Tamer et. al., 2000)*. The film samples having surface area of 1 cm^2) were dropped in 7mL of saline solution of concentration 0.9%, placed in test tubes. Afterward incubating the mixer of the sample at 37°C for 24 hours, the samples were taken out, and 0.05 mL of acid citrate dextrose (ACD) and blood was poured on the surface of films. After a wait of 15 min, 10ml of 0.9% salt solution was added and the films were again placed in the incubator at 37°C for 3 hr. Positive and negative controls were made by adding the equal amount of ACD and blood to 10 mL of distilled water (DW) and 0.9% saline solution, respectively. Each tube was gently inverted twice to make contact of the blood with the film. After incubation, each fluid was poured to a suitable tube and centrifuged at 100rpm for 15min. The hemoglobin released by Heamolysis was determined by the optical densities (OD) of the supernatants at 545 nm using a UV-visible spectrophotometer. The percentage of Heamolysis was calculated as follows *(Kamoun et al., 2015)*.

$$\text{Hemolysis}(\%) = \left[\frac{OD\ of\ test\ sample - OD\ of\ (-)control}{OD\ of\ (+)\ control - OD\ of\ (-)control}\right] \times 100\% \qquad \ldots (3.34)$$

According to ASTM F 756-00, classification of materials can be done in three separate categories according to their % heamolysis. Materials with >5% Heamolysis are called as haemolytic; while 2%-5% belongs to class of slightly haemolyticmaterials and <2% are taken as a non-haemolytic material.

CHAPTER – 4
RESULTS AND DISCUSSIONS

CHEPTER – 4

RESULTS AND DISCUSSION

In this work as previously described *in-situ* polymerization of aniline (Ani) in the gelatin crosslinked hydrogel film was done so that a uniformly distributed array of PANI could be obtained within the Gel film matrix. The results of various studies done on this composite are summarized below.

4.1. Experimental

4.1.1. Formation of Glox-X-Gel film

Glyoxal has been a popular cross-linker for number of proteins and polysaccharides which have amino groups within their structures *(Marquié, 2001)*. Gelatin is delivered fibrous insoluble protein collagen, through a controlled hydrolysis. Since gelatin is a protein; it consists of unique arrangement of amino acids. It is a characteristic of a gelatin, that it possesses a high amino acid content viz. proline, hydroxyl proline and glycine. More specifically visualizing structure of gelatin it consist of repeating sequences of glycine-α-β triplets, where *α* and *β* are mostly proline and hydroxyproline amino acids. The triple helical arrangement of gelatin and its capacity to form gels is due to these repeating sequences. Their action of gelatin with glyoxal results in crosslinking. For the formation of crosslinking, Schiff base reaction between unrestricted amino groups of lysine is present in proteins and an aldehyde group of glyoxal is responsible. The crosslinking formula is given in Fig.4.1.

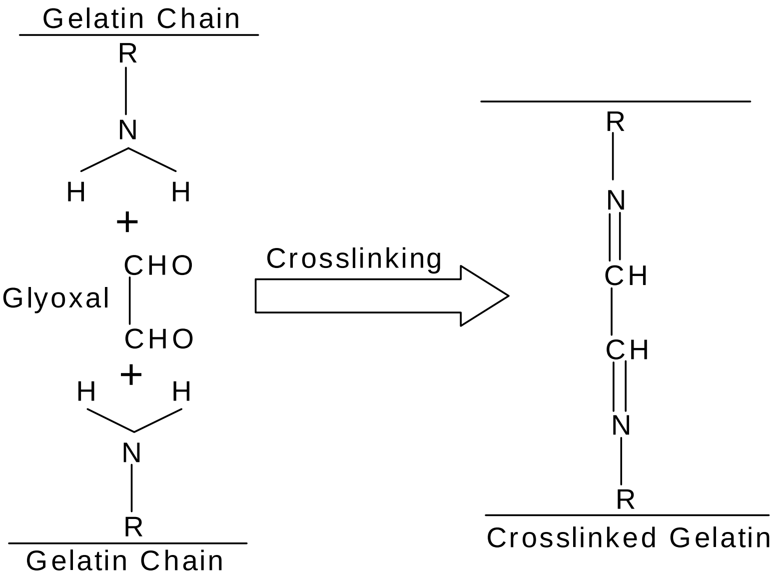

Fig. 4.1: Scheme showing crosslinking of gelatin chains by glyoxal.

4.1.2. Formation of Glox-X-Gel/PANI film

As started earlier, this work is unique in the sense that first time attempt was made to carry out *in-situ* polymerize aniline in the matrices of gelatin film. The polymerizing of aniline to result PANI is due to oxidative polymerization of aniline, within gelatin matrix *(Subrahmanyama et al., 2012)*. PANI synthesis comprises two interrelated procedures. The first of these two processes is occurrence of chain reaction for monomers which results, forming of regular macromolecules, the second process involve growth of chains which simultaneously get prepared into complex supramolecular arrangements. Because of these two processes, conducting polymer of aniline having stable supramolecular structures with numerous morphologies is shaped and the synthesis of PANI takes place inside the bulk of film further its surface.

Whenever Glox-X-Gel film sample is placed in aqueous solution of aniline (see section Experimental) plus APS, soluble Aniline molecules and persulphate ions pass towards in the matrix of gelatin along with penetrating water. The incoming Aniline molecules suffer from oxidative polymerization inside the gelatin, thus outcome in formation of PANI. The presence of dark brown-cum-black color shows formation of PANI within the Glox-X-Gel film. The optical images of Glox-X-Gel and Glox-X-Gel/PANI films are shows in Fig.4.2.(A) and (B).

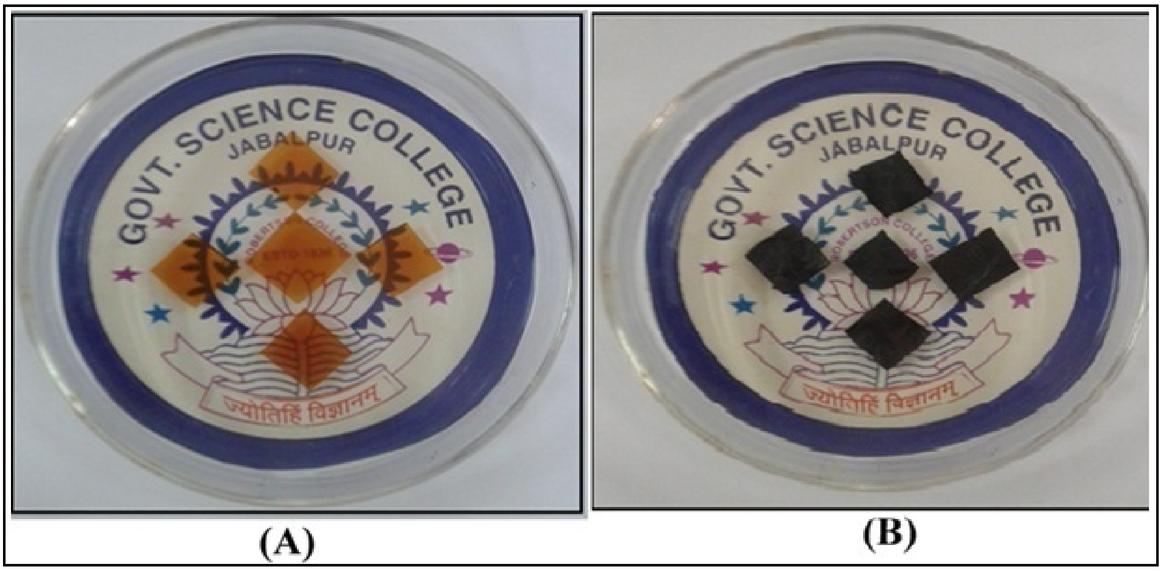

Fig. 4.2: The images of Glox-X-Gel (A) and Glox-X-Gel/PANI (B) films.

4.1.3. Percent of crosslinking (PC)

The results of method i.e. using the ninhydrine assay, used to determine percentage of crosslinking was observed to be 7.3, 9.4 and 9.8 for samples B, C and D respectively. It is essential to remember here that the ESR for the film samples B, C and D were 3.8, 2.6 and 2.1 g/g respectively. The almost nearer percentage crosslinking of samples C and D is very much clear by their ESR, i.e. 2.6 and 2.1 g/g respectively. The reason for this low value of ESR is that milimol of cross-linker glox may be almost sufficient to crosslink the film sample C to a saturation level and therefore after saturation is achieved; still using high brightness glox concentration does not increase the percentage of crosslinking of the sample.

4.2. Characterization of Glox-X-Gel and Glox-X-Gel/PANI Films.

4.2.1. Fourier-transform infrared spectroscopy (FTIR)

The FTIR spectra got from the Glox-X-Gel and Glox-X-Gel/PANI films samples (see: Fig.4.3 and Fig. 4.4.) respectively.

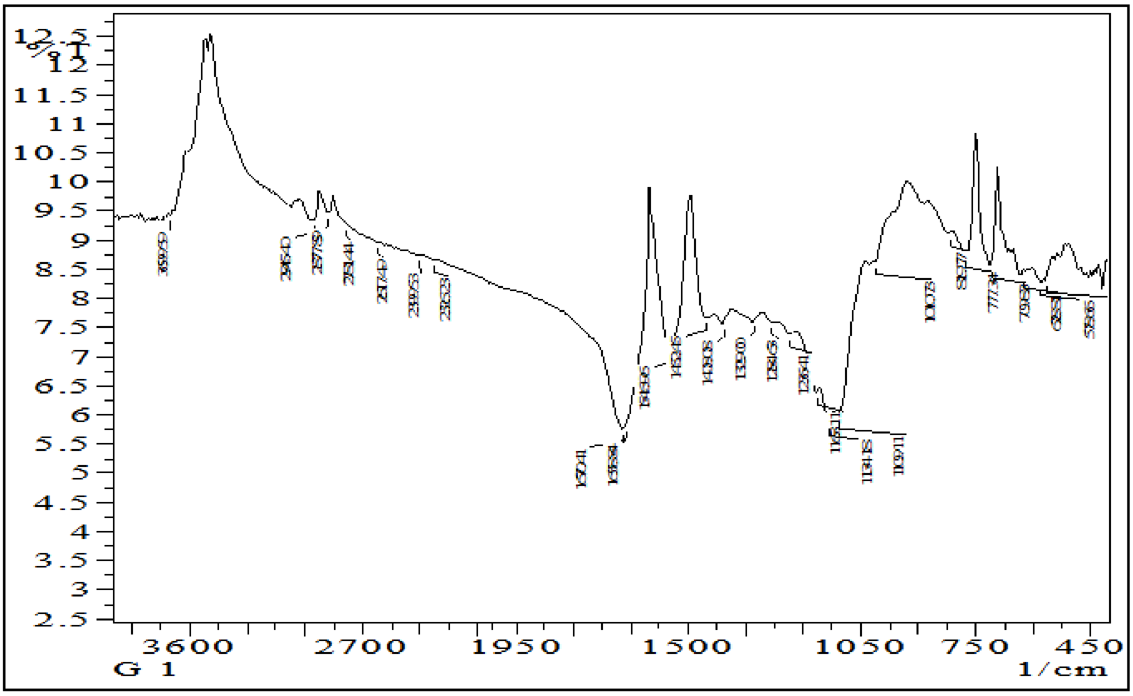

Fig. 4.3: The FTIR images obtained from the Glox-X-Gel films.

Fig. 4.4: The FTIR Pattern from the Glox-X-Gel/PANI films.

, The FTIR pattern centered at 1635 cm^{-1}, due to stronger band, C=N stretching vibration from Schiff bases, and C=O stretching from the mixture of amide I band and unreacted aldehyde groups in the Glox-X-Gel film. The Schiff bases were shaped inside amino groups of gelatin and carbonyl groups of the glyoxal *(Farris et al., 2010)*. The peak amide II band of 1540 cm^{-1} indicates that it becomes stronger after cross-linking. The pattern of Glox-X-Gel/PANI film, the peaks confirm at 1637.67 cm^{-1} are attributed to the stretching of C=C in the aromatic nuclei. Also, the band seen at 3433 cm^{-1} is owing to N-H stretching. The bands with maximum in 1574 and 1488 cm^{-1} are assigned to stretching vibrations of quinoid and benzenoid rings, respectively *(Izabela, 2010)*. The spectra of PANI-HCl have a low intensity band at 1373 cm^{-1}, due to the stretch of the C–N bonds closure of the quinoid ring (C – N = Q = N –C) *(Izabela, 2010)*.

4.2.2. Thermogravimetric analysis (TGA)

The curves obtained after TGA studies on Glox-X-Gel and Glox-X-Gel/PANI samples are represented in Fig. 4.5.

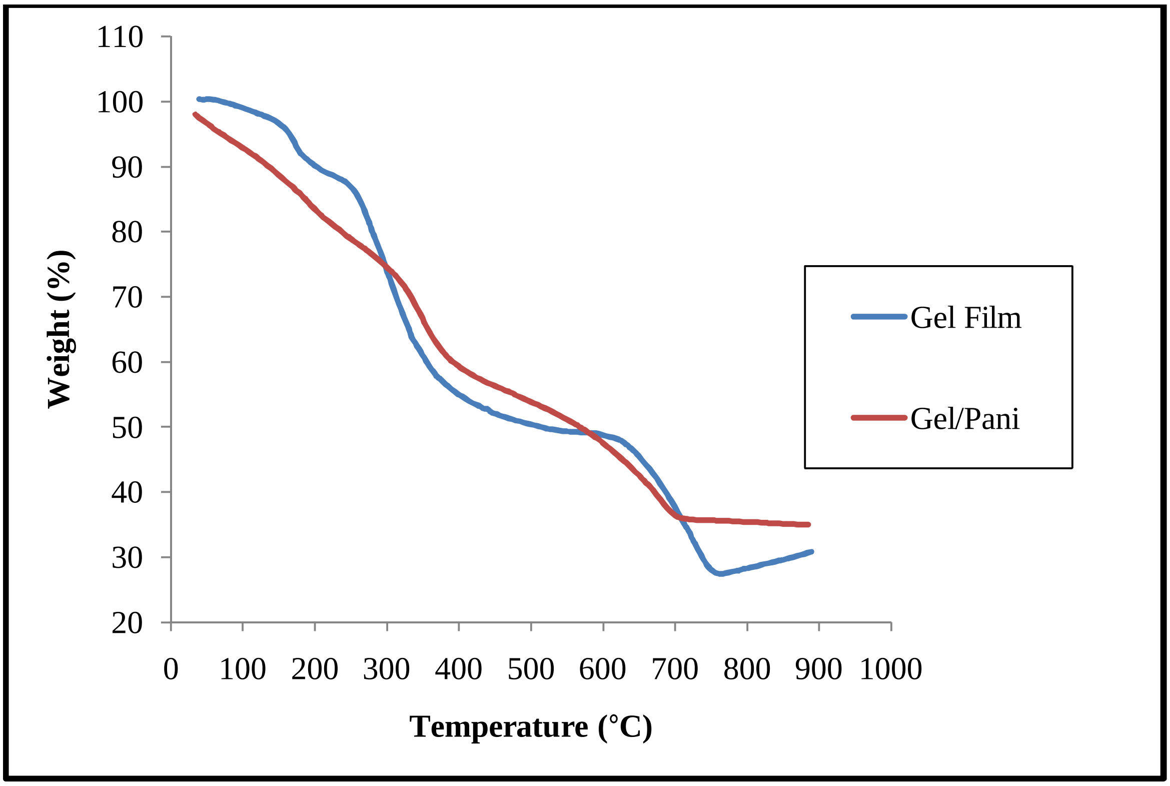

Fig. 4.5: The TGA pattern of Glox-X-Gel/PANI composite film.

A close inspection at the 2 weight-loss profiles unfolds a fact that up to 180°C the sample of Glox-X-Gel experience a loss of weight by almost 8% while in the same temperature range, the Glox-X-Gel/PANI sample demonstrates a loss of weight by nearly 16%. It seems that the water is bound more strongly tied in the Glox-X-Gel sample, with the polar active spaces different forms of amino acids, thus making it difficult for the water to eject as vapor. However, almost double weight loss of the sample Glox-X-Gel/PANI indicates greater moisture loss, probably because of the presence of PANI chains which binds to the water molecules relatively through weaker interactions and therefore this loosely bound water is volatilized in the given temperature range. More interestingly, the total weight loss, suffered by the two polymers up to 300°C is nearly 27%.Here, it is noteworthy that TGA of PANI, as studied by Gomes and Oliveira *(Zeng and Ko, 1998)*, also revealed that PANI suffered a loss of weight by nearly 28% up to 300°C.It means that Glox-X-Gel and PANI suffers the same weight loss up to 300°C and that may be the reason that composite film sample Glox-X-Gel/PANI also shows the similar results. Further, the weight loss experienced by the Glox-X-Gel and Glox-X-Gel/PANI samples between 300 to 700°C is about 22%, hence showing a total loss of weight by 50%. The degradation of the polymeric backbones of the two constituent partner polymers, viz. gelatin and PANI is responsible for this weight loss. This shows a 10% greater loss of weight than 800°C in the Glox X gel film sample, and a negligible loss in the mixed film. This results in a little more stability for the Glox-X-Gel/PANI sample.

4.2.3. Atomic force microscopy (AFM)

The AFM images of Glox-X-Gel and Glox-X-Gel/PANI$_{20}$ film samples are showing in Fig.4.6 (A) and (B), respectively. The area of the pure gelatin film clearly shows that gelatin particles are uniform distributed of in the film matrix. In addition, one can see that the surface has a little grooved texture throughout entire surface of the film. Contrary, the AFM of the Glox-X-Gel/PANI film, as depicted in Fig.4.6 (A) and (B), exhibits quite rough texture with unevenly shaped grooves over the entire matrix, which that PANI indicating the presence of particles.

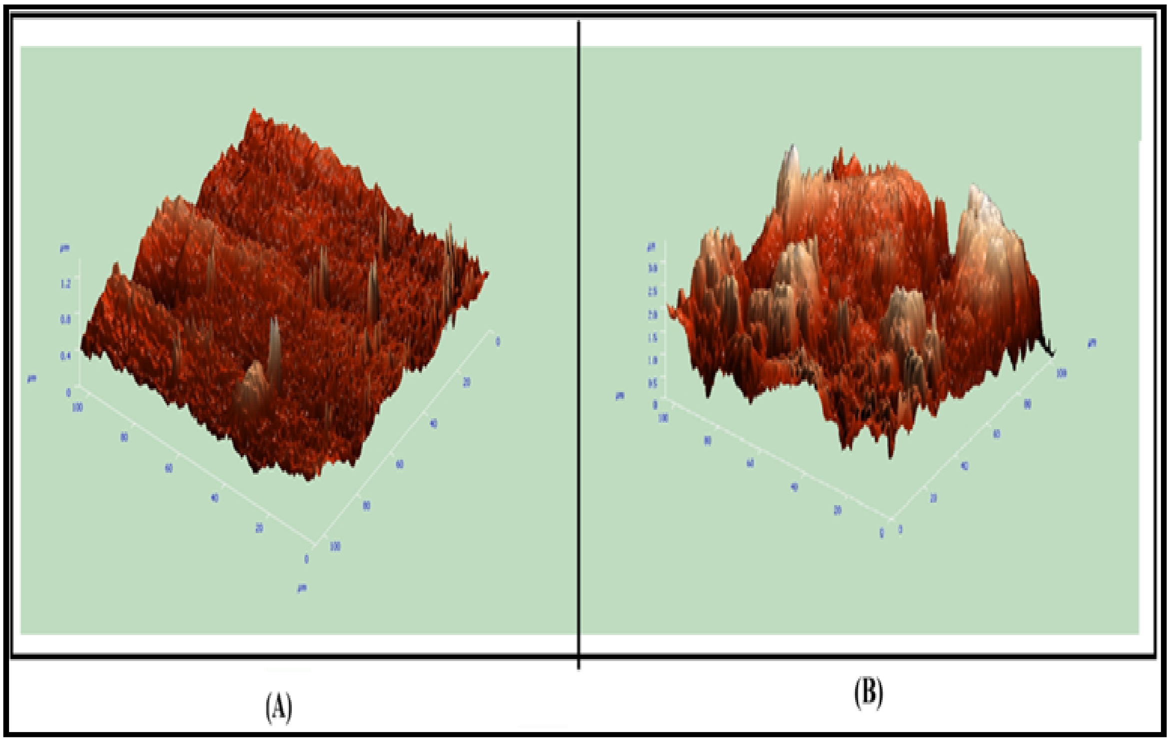
(A)
(B)

Fig. 4.6(A) and (B): The AFM images of Glox-X-Gel and Glox-X-Gel/PANI films.

4.2.4. X-ray diffraction(XRD) study

The diffractograms obtained are shows in Fig. 4.6. and 4.7.

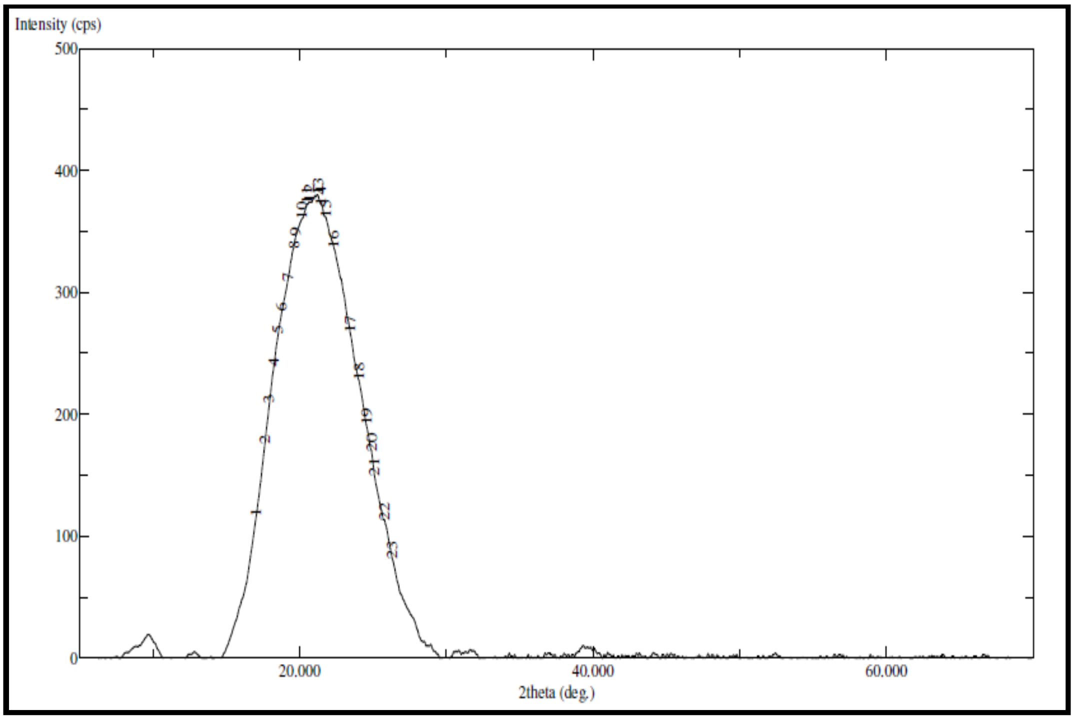

Fig. 4.7: X-ray diffractogram of Glox-X-Gel films.

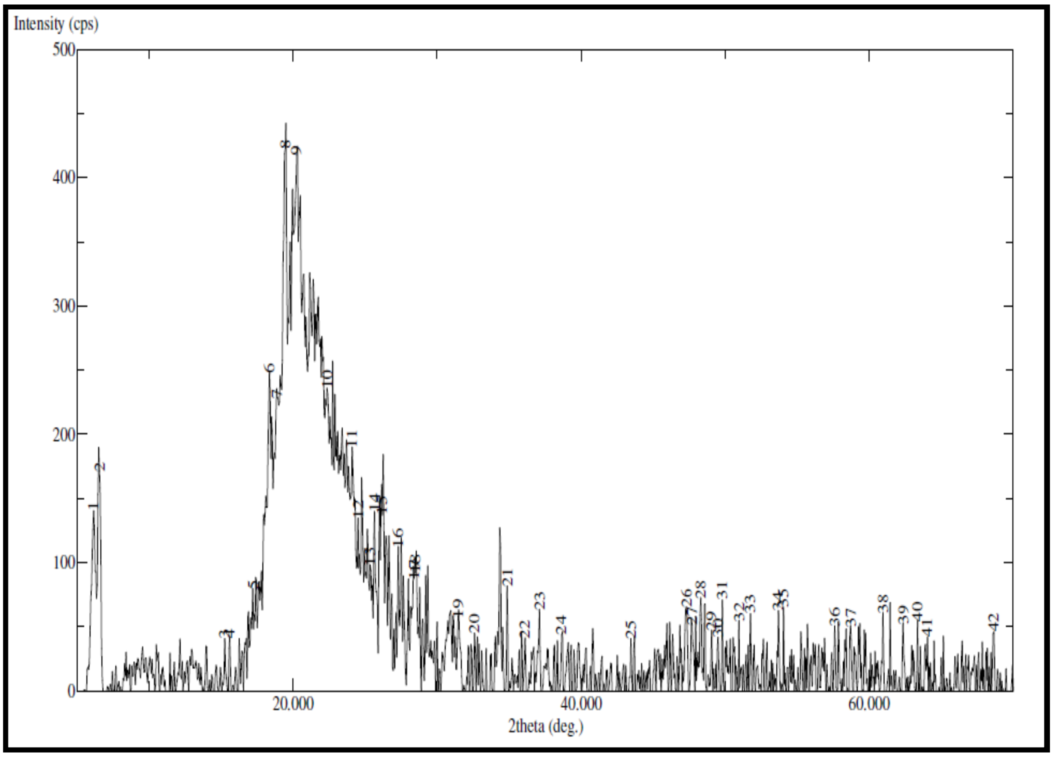

Fig. 4.8: The XRD patterns of Glox-X-Gel/PANI composite films.

The diffractogram obtained for the plain gelatin (gel) films were of features natural to a partially with crystalline the plain gel peaks at 2θ=7.8° (d101=11.08Å) and at

22.12° (d101=4.01Å), shown in Fig.4.7 and Fig.4.8. These typical peaks are usually related to the triple-helical crystalline structure in collagen and gelatin *(Gomes and Oliveira, 2012)*. On the other hand, *(Peña et al., 2010)*, have shown that the first diffraction peak at 8° which is sharp and intense, is directly dependent on the rate of the diameter and the triple helix, respectively*(Bigi et al., 2004)*. The XRD images of Glox-X-Gel/PANI composite film are depicted in Fig.4.7 and Fig.4.8. The diffractogram vertex expresses pure amorphous nature of constituent PANI with a wide peak at 23°which is a peak charactistics of PANI *(Chetouani et al., 2014)*. However, the diffraction peak of gelatin and PANI appears to be covered.

4.2.5. Water uptake behavior of hydrogel films

Many hydrogel film samples were investigated over the water uptake at 37°C buffer medium of pH 7.4. The results of rapid analysis for the samples A, B, C and D, witch included in 0, 3.4, 17.2, and 27.5 milimol of cross-linker Glox (see Table 4.1 and Fig.4.9.)

Table 4.1. SR value of various cross-linkers Glox-X-Gel samples A, B, C and D.

Time (min)	Swelling ratio			
	A	B	C	D
0	0	0	0	0
5	2.2051	1.414	1.1818	0.9494
10	3.064	1.78	1.505	1.1666
15	1.6923	1.975	1.5757	1.1888
20	1.5256	2.17	1.7777	1.3
25	0.5631	2.268	1.808	1.4111
30	0	2.39	1.9696	1.6
35		2.536	2.0505	1.6777
40		2.804	2.0808	1.7666
50		2.926	2.2424	1.8888
60		3.317	2.303	1.9666
70		3.536	2.3939	2.0444
80		3.756	2.4646	2.1

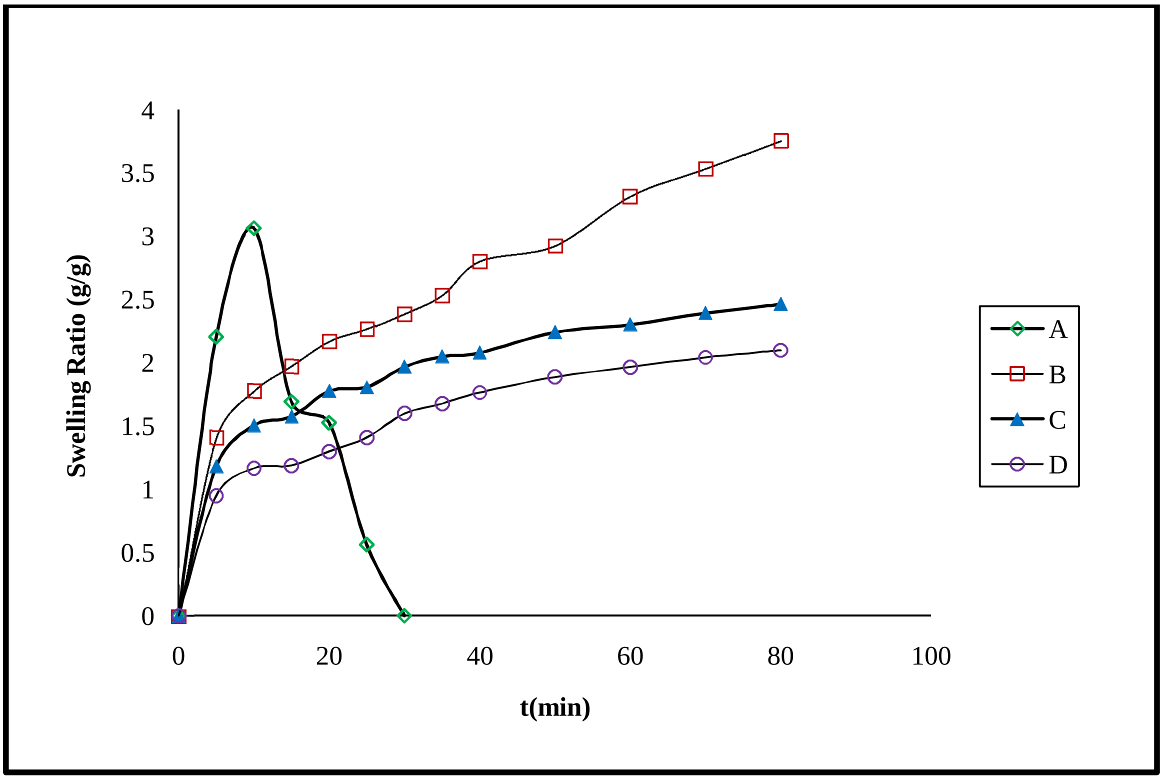

Fig. 4.9: Dynamic water uptake for the film samples A., B, C and D.

The results found that un-crosslinked sample 'A' achieves a maximum SR of 3.1g/g in 10 minute and then it begins to lose weight of 'A' and finally a total time duration 30 min. of dissolves. This is because gelatin chains aren't cross-linked & thus they have a strong tendency to dissolve in water. However, the samples, having larger quantity of crosslinker viz. B, C and D continue to swell by absorbing water and attain a max swelling ratio of 3.8, 2.6 and 2.1g/g respectively in an overall period of nearly 110min. are shows in Table 4.2 and Fig. 4.10. It is noteworthy that for a given time, SR decreases with the rise in the amount of Glox film. This is due to the fact that with the increase in the Glox contents in the film, the degree of crosslinking rises. This leads to the number of crosslinks between the two chains rises and this causes (i) reduction of the available free space for the somewhere to stay of invading water molecules, and (ii) The rigidity of the gelatin chains increases, which, in turn limits the chain relaxation process *(Subrahmanyama et al., 2012)*. As a result both factors described above, the SR decreases. Similar results are reported in a number of studies *(Farris S, et al., 2010)*.

The varying concentrations of the gel above the water uptake of film samples Ė, F and G, but the same ratio of gelatin for glycol material in every film is shows in table 4.2 and Fig.4.10.

Table 4.2.Data showing dynamic water uptake for the film samples E, F, and G.

Time (min)	Swelling Ratio		
	E	F	G
0	0	0	0
5	0.5692	0.3861	0.3189
10	1.1384	0.7326	0.6034
15	1.6846	1.4752	0.931
20	2.1307	1.8811	1.3577
25	2.4153	2.1386	1.362
30	2.7076	2.1584	1.5775
35	2.8461	2.396	1.6163
40	2.8615	2.4059	1.6896
50	2.9461	2.4455	1.8103
60	3.1153	2.4851	1.8146
70	3.1461	2.5148	2.0474
80	3.1841	2.7722	2.1982
90	3.4	2.8415	2.2198
100	3.5	2.8514	2.3534
110	3.5307	2.9009	2.3965
120	3.5461	3.1386	2.5775

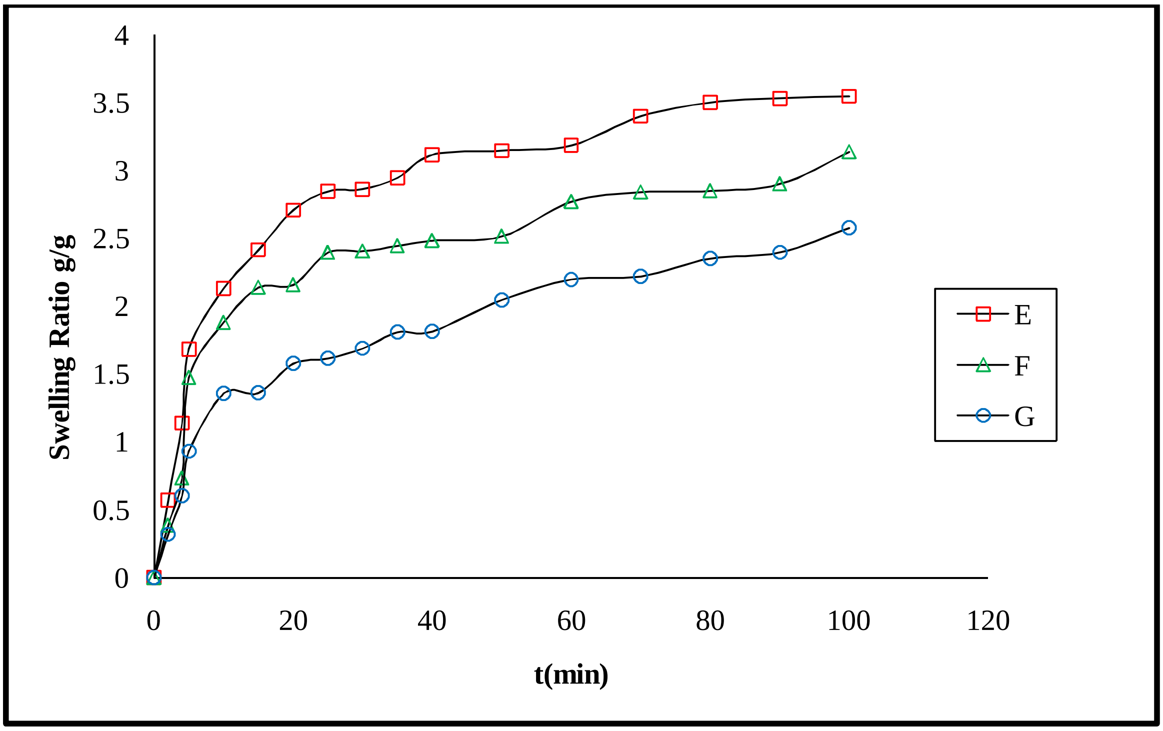

Fig. 4.10: Dynamic water uptake for the film samples E, F and G.

The results show that increases the amount of gelatin film in the matrix, the SR decreases. It is of concern that the rise in the gelatin (gel) content, the density of network crosslinked macromolecular chains increases rapidly. Therefore, false crosslinks are produced due to an increase in entanglement within the matrix, thus discouraging the entry of water into the film. The ESR, shown by the samples E, F and G was 3.5, 3.1 and 2.6g/g respectively.

4.2.6. Effect of PANI on the swelling of Glox-X-Gel films

PANI exhibits hydrophobic nature by reason of lack of polar groups like hydroxyls, carboxylic etc., and therefore PANI has been used extensively as a corrosion inhibitor *(Bardajee and Pourjavadi, 2010,Li and Ruckenstein, 2003)*.

Water absorption charactistics of samples Glox-X-Gel/PANI is synthesized by equilibrating sample, Glox-X-Gel/PANI$_{10}$, Glox-X-Gel/PANI$_{20}$, Glox-X-Gel/PANI$_{30}$ and Glox-X-Gel/PANI$_{40}$ where the number in subscript is the % (v/v) of aniline solution, pre-added with proper amounts of HCl and APS, and was investigated. The films may be designated as used. The water absorption of films in PF of pH 7.4 is shown in Table 4.3 and Fig.11.

Table 4.3. Data showing the SR values of the Glox-X-Gel/PANI films.

Aniline(ml)	Swelling Ratio
1	0.87
2	0.34
3	0.11
4	0.06

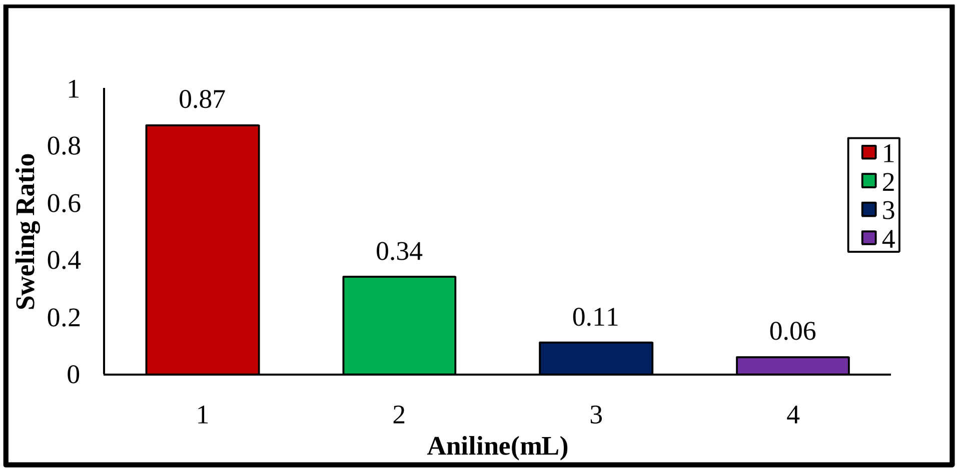

Fig. 4.11: Water uptake shows of the films Glox-X-Gel/PANI sample

It can be considered that as the amount of aniline increases, the result is that film ESR decreases. This is simply because of hydrophobic nature of PANI present in the films. However, it is necessary that ESR of pure crosslinked Glox-X-Gel (plain) sample 'C' is 2.55 since that of sample Glox-X-Gel/PANI$_{10}$ is 0.87. This means that the absorption of water in the film is approximately three times lower, due to the involvement of the PANI molecules within the Gel film matrix. It is possible that additional crosslinks may be produced between the PANI and gelatin chains. The H-bonding interactions between hydrogen atoms of PANI and oxygen of amino acids from gelatin molecules can be operative in determining the behavior of the swelling.

4.2.7 Modeling of water uptake data

4.2.7.1 Power function model

There are number of mathematical models available to describe the hydrogel swelling kinetics. These models falls under three categories: 'Fickian diffusion, collective diffusion and Non-Fickian diffusion models' *(Dhawan et al., 2015)*. Usually hydrogel swelling models are based on the diffusion of Fick's law. For many gels it should be also taken as a convection mechanism by means large transport of solvent/analyte molecules. Both the rate and amount of sorption of penetrant into the polymer are achieved by amount gradient-controlled and/or relaxation-controlled diffusion. The most frequently used models are the 'power function law' which expresses fractional water uptake as a time-dependent phenomenon *(Porter et al., 2007)*:

$$\frac{M_t}{M_\infty} = kt^n \qquad \text{… (4.1)}$$

Where, M_t and M_∞ refers the masses of the swelling hydrogel at time t and in the initial dry state, respectively and n refers the swelling exponent and k is the hydrogel characteristic constant respectively. In the logarithmic form the equation can be given as:

$$lnF(M_t/M_\infty) = lnk + nlnt \qquad \text{… (4.2)}$$

This equation can be applied only to the initial stages of swelling, i.e. to a 60% increase in the mass of hydrogel ($Mt/M\infty \leq 0.6$; $log\ (Mt/M\infty) \leq -0.22$). A plot between *lnt* and *lnF* yields straight line, whose slope and intercept may be employed to evaluate parameters '*n*' and '*k*'. Based on the relative rates of diffusion (R_{diff}) and polymer relaxation (R_{relax}) three classes of diffusion are easily distinguishable. With plane geometry, the value of *i*) $n = 0.5$ indicates a Fickian diffusion mechanism Case I in which the rate of diffusion is much lower than the rate of relaxation ($R_{diff} \ll R_{relax}$, system controlled by diffusion, *ii*) $n = 1.0$ indicates Case II, where the diffusion process is faster than the relaxation process ($R_{diff} \gg R_{relax}$, scheme controlled by relaxation, iii) 0.5 <n<1.0 indicates non-Fickian diffusion mechanism, which demonstrates those cases where the diffusion and relaxation rates are comparable ($R_{diff} \approx R_{relax}$) *(Peppas & Korsmeyer, 1987)*. Once the water penetration rate is very smaller than the polymeric chain relaxation rate, then it can note the lower values below 0.5 *(Lin et al., 2005)*.

The linear plots, obtained for the samples ‘B, C, D’ and ‘E, F, G’ as depicted in Table 4.4 and Fig.4.12, Table 4.5 and Fig. 4.13 respectively. The respective parameters ‘n’ and ‘*k*’ are given in Table. 4.6.

Table 4.4. Data showing the value of ‘n’ and ‘k’ for samples B, C and D.

lnt	**$\ln(M_t/M_\infty)$**		
	B	**C**	**D**
1.6094	-1.0155	-0.7691	-0.8081
2.3025	-0.785	-0.5274	-0.6036
2.708	-0.681	-0.4814	-0.5848
2.995	-0.5868	-0.3608	-0.4954
3.2188	-0.5426		
3.4011	-0.4902		

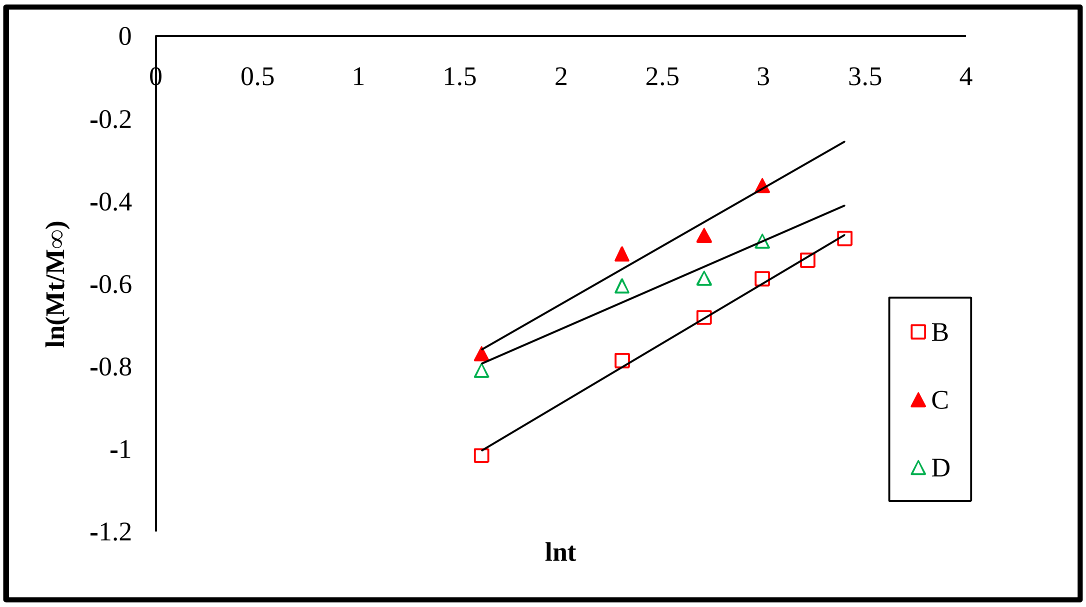

Fig.4.12. Evaluation of ‘n’ and ‘k’ for the film samples B, C and D.

Table 4.5. Data showing the value of ‘n’ and ‘k’ for the film samples E, F and G.

lnt	$\ln(M_t/M_\infty)$		
	E	F	G
0.6931	-2.1619	-2.4372	-2.4686
1.3862	-1.4662	-1.7963	-1.8303
1.6094	-1.0741	-1.0966	-1.3967
2.3025	-0.839	-1.0272	-1.0194
2.708	-0.7137	-0.725	-1.0163
2.9957	-0.5994	-0.716	-0.8694
3.2188	-0.5495	-0.6115	-0.8451
3.4011	-0.5442	-0.6073	-0.8007
3.5553	-0.515	-0.5909	-0.7318
3.6888	-0.4591	-0.575	-0.7293
3.912	-0.4494	-0.5629	-0.6086
4.0943	-0.4374	-0.4656	-0.5326
4.2484	-0.3717	-0.4409	-0.5278
4.382		-0.4374	-0.4693
4.4998			-0.4512
4.6051			-0.3784

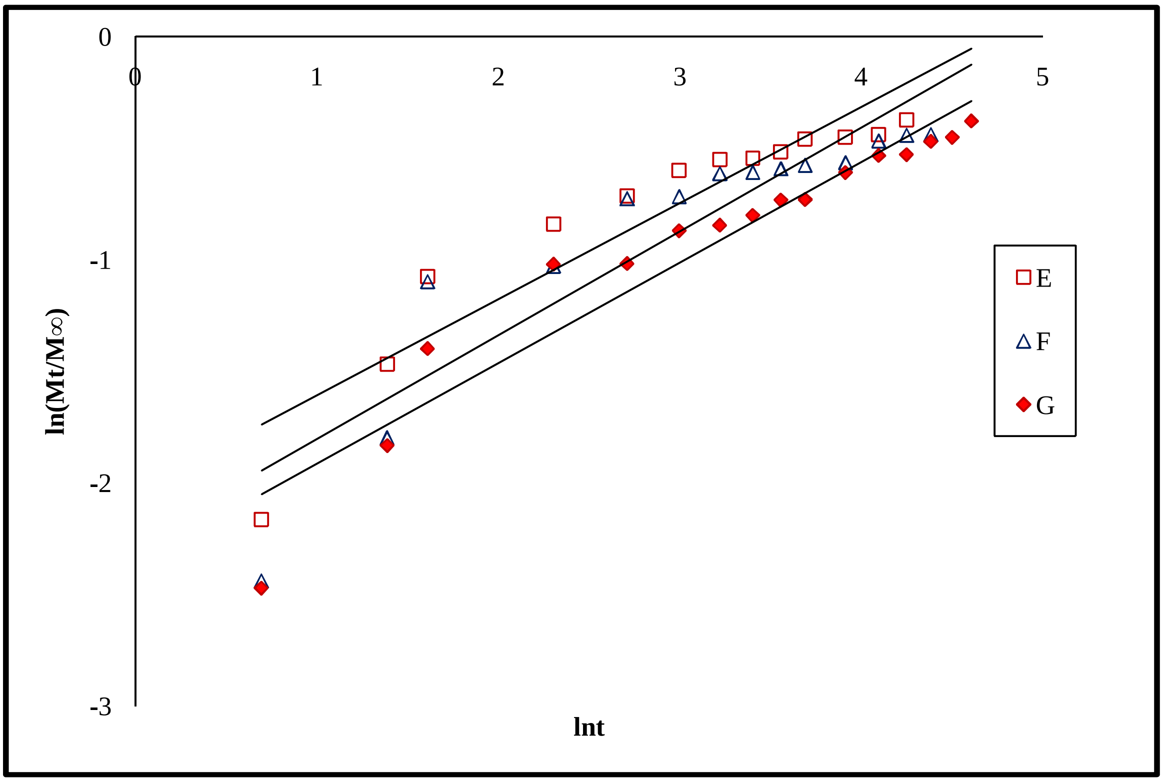

Fig. 4.13: Evaluation the value of ‘n’ and ‘k’ for the film samples E, F and G.

Table 4.6.Data showing the value of various parameters for power function model.

Sample Code	Power Function Model				
	n	**k**	$M_{\infty(Exp)}$	$M_{\infty(Theo)}$	R^2
B	0.28	$29.1\text{x}10^{-2}$	3.8	3.8	0.9716
C	0.29	$22.9\text{x}10^{-2}$	2.5	2.7	0.9961
D	0.21	$32.0\text{x}10^{-2}$	2.1	2.4	0.9496
E	0.43	$13\text{x}04\text{x}10^{-2}$	3.54	3.85	0.8692
F	0.46	$10.38\text{x}10^{-2}$	3.13	3.31	0.8382
G	0.45	$10.60\text{x}10^{-2}$	2.57	2.8	0.9918

On closer look the values of swelling exponent ‘n’ reveal some interesting information. It is most significant to notable that for all the film samples except B, ‘n’ lies quite below 0.5, showing that rate of water penetration is quite below in comparison to the relaxation rate of polymeric chains.

This is especially termed as ‘less-Fickian diffusion (Wang et al. 2008). It means, the swelling of these gelatin films is governed by compactly slower water diffusion processes. Swelling analysis was done in distilled water (DW), since, when the Glox-X-Gel) film is taken as 6.6, the swelling is immersed in the DW with the pH medium, slightly above isoelectric point, the gelatin that is pH = 4.9. It can therefore be assumed that adequate number of positive -NH^{+3} and negatively charged -COO- groups are within gelatin film matrix.

In other words, the water slowly spreads through film diffusion through the diffusional process. As far as sample ‘B’ is concerned, the swelling exponent n has a value of 0.5, thus shows Fickian diffusion system. It appears that the relatively less crosslinking than other samples, the process of relaxation can be a bit more contributing. Thus, swelling Fickian is controlled instead of 'less Fickian'.

4.2.7.2 Schott kinetic model

Schott model states that swelling rate is directly proportionate to the quadratics for swelling capacity before achieving the equilibrium state at any particular period of time *(Ganji et al. 2010; Schott, 1992)*:

$$\frac{dM_t}{dt} = k_2\,(M_\infty - M_t)^2 \qquad \ldots (4.3)$$

where, ‘k_2’ is the second order rate constant for swelling. Integration of above equation yields:

$$\frac{t}{M_t} = \frac{1}{k_2 M_\infty^2} + \frac{t}{M_\infty} \qquad \ldots (4.4)$$

Or

$$\frac{t}{M_t} = A + Bt \qquad \ldots (4.5)$$

Where, A’ and B are coefficients having following expression: At very long retention time $Bt \gg A$and therefore $B = 1/M_\infty$. In the relation, at too short time interval $Bt \ll A$ and so,

$$\lim_{t \to \infty} \frac{dM_t}{dt} = \frac{1}{A} \qquad \ldots (4.6)$$

Thus, the intercept ‘A’ is equal of initial swelling rate. Finally, the constant rate of Schott kinetic k_2 is calculated as:

$$k_2 = \frac{slope^2}{intercept} = \frac{B^2}{A} \qquad \ldots (4.7)$$

The outcomes of Schott model, applied on the water uptakes for the film samples, B, C, D and E, F, G are shown as linear plots obtained between t/M_t and t (see Fig.4.14 and fig. 4.15.

Table 4.7. Data showing the value of t/ M_t Vs t for the film samples A, B, C and D.

t(min)	t/Mt			
	A	**B**	**C**	**D**
5	2.2674	3.536	4.2308	5.2664
10	3.2637	5.6179	6.6445	8.5719
15	4.2984	7.5949	9.5295	12.6177
20		9.2165	11.2504	15.3841
25		11.0229	13.8274	17.7166
30		12.5523	15.2315	18.75
35		13.8012	17.069	20.8618
40		14.2653	19.2233	22.6423
50		17.2653	22.2975	26.4718
60		18.0886	26.0529	30.5095
70		19.7963	29.2409	34.2398
80		21.2992	32.4596	38.0952

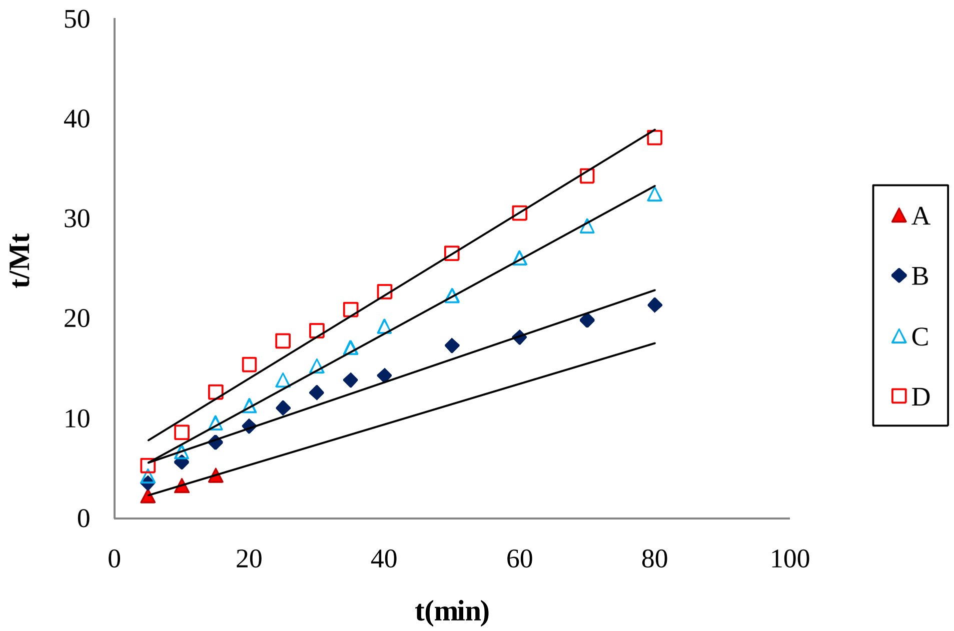

Fig. 4.14: t/M$_t$ versus t plots to assess of A, B, C and D.

Table.4.8. Data showing the value of t/M$_t$ versus t for the film samples E, F and F.

t(min)	t/Mt		
	E	F	G
2	3.5137	5.18	6.2715
4	3.5137	5.46	6.6291
5	2.968	3.3893	5.3705
10	4.6931	5.316	7.3653
15	6.2134	7.0139	11.0132
20	7.3866	9.2661	12.6782
25	8.7839	10.434	15.4674
30	10.484	12.4693	17.7556
35	11.8801	14.312	19.3338
40	12.8398	16.0959	22.0434
50	15.8926	19.8822	24.4212
60	18.8436	21.6434	27.295
70	20.5882	24.6348	31.5343
80	22.8571	28.0563	33.9933
90	25.4906	31.0248	37.5547
100	28.1999	31.8613	38.7972

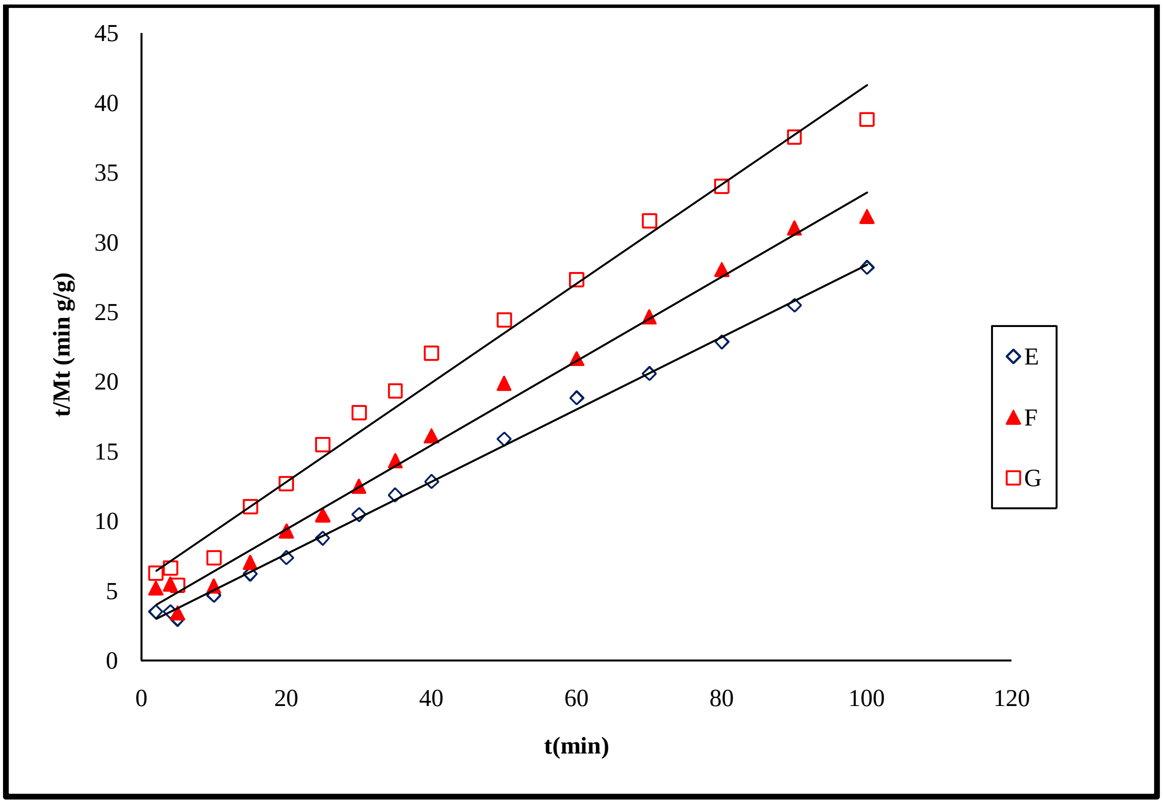

Fig. 4.15: t/M_t versus t plots to assess fitness for the film samples E, F and G.

Table 4.9.The value of various parameters for Schott model.

Sample Code	Schott Model			
	k_2	$M_{\infty(Exp)}$	$M_{\infty(Theo)}$	R^2
B	$70x10^{-2}$	3.8	3.8	0.996
C	$3.2x10^{-2}$	2.5	2.7	0.9942
D	$2.8x10^{-2}$	2.1	2.4	0.99
E	$2.76x10^{-2}$	3.54	3.85	0.9916
F	$2.70x10^{-2}$	3.13	3.31	0.991
G	$2.2x10^{-2}$	2.57	2.8	0.9874

It is clear that the plots are linear; therefore, on the dynamic water absorption data it indicates the suitability of this model. The various related parameters for Schott model are shows in Table 4.7, Table 4.8, and Table 4.9. A close examination of the obtained values has shown that regressions are fairly high for the Schott model and that this model is, therefore, suitable to water uptake data. In addition, it can be also noting that the theoretical ESR values are very close to the experimental data and also support this model's suitability.

4.2.8 Evaluation of diffusion coefficients

4.2.8.1 Diffusion coefficients

Most of the diffusion processes are best interpreted by the Fick's first and second laws of diffusion. The initial diffusion coefficient D_I gives a fine understanding of the penetration of water in the hydrogel matrix in the initial phase of the swelling. In order to obtain D_I, the following equation was employed *(Karadag et al., 2001)*:

$$F = M_t/M_\infty = 4(D_I\, t/I^2)^{1/2}/\pi^{1/2} \qquad \ldots (4.8)$$

Where F is fractional uptake and D_I is initial diffusion coefficient. We can re-arrange above equation as:

$$F = 4D_{I^{1/2}}/I^2\, t^{1/2} \qquad \ldots (4.9)$$

The slope of linear plot between F and $t^{½}$ was used to calculate D_i as:

$$D_I = slope^2 \times l^2\, \pi/16 \qquad \ldots (4.10)$$

With the help of initial 60% of the dynamic swelling data, linear plots between lnF and $t^{1/2}$ were drawn. The slope of these linear plots was used to calculate the initial diffusion coefficients $D_{I.}$

For calculating average diffusion coefficient D_{ave}, F=0.5 and t=$t_{1/2}$ were substituted in equation (4.11), presuming that 60% of the total swelling, achieved by the hydrogel film, can enable us to calculate D_{ave}. The above substitutions yielded following expression:

$$D_{ave} = 0.049\, I^2/t_{1/2} \qquad .. (4.11)$$

In order to evaluate coefficient of late time diffusion $D_{L,}$ used an interesting observation made by *(Shankar, 1979; Yoshizawa et al., 1997)*, who claimed that a plot between the *ln* ($1-M_t/M_\infty$) and 't' exhibits a linear plot but with a distinct break in the slope. This is observed experimentally also for both Fickian and non-Fickian diffusion. The break in the slope is related to the time when two advanced boundaries meet each other. The late time diffusion coefficient D_L was determined using the subsequent 60 % of the total equilibrium swelling data for different samples using dynamic swelling data; the *ln* ($1-M_t/M_\infty$) values were plotted against t for various samples. The plots observed were bi-phasic linear plots as shown in Fig.4.16 and Fig.4.17 for the samples B, C, D and E, F and G respectively.

The following expression calculates the D_L using the slopes set for the later part of swelling process *(Smith and Fisher, 1984)*:

$$D_L = -(slope \times I^2)/\pi^2 \qquad \ldots (4.12)$$

The diffusion coefficients for each sample discussed below are shown in Table 4.10.

Table 4.10. Data showing value of ln (1-F) versus t for film samples A, B, C and D.

t(min)	$\ln(1-M_t/M_\infty)$		
	10%	14%	18%
0	0	0	0
2	-0.1226	-0.0914	-0.0885
4	-0.2624	-0.1814	-0.1747
5	-0.4179	-0.4064	-0.2842
10	-0.5658	-0.4431	-0.4475
15	-0.6729	-0.6622	-0.4492
20	-0.7965	-0.6707	-0.5433
25	-0.8608	-0.7819	-0.5612
30	-0.8682	-0.787	-0.596
35	-0.91	-0.8069	-0.6558
40	-0.9991	-0.8271	-0.6581
50	-1.0161	-0.8428	-0.7854
60	-1.0376	-0.988	-0.8773
70	-1.1695	-1.0311	-0.5278
80	-1.2371	-1.3711	-0.9818
90	-1.2559	-1.0697	-1.0128
100	-1.2697	-1.2402	-1.1548

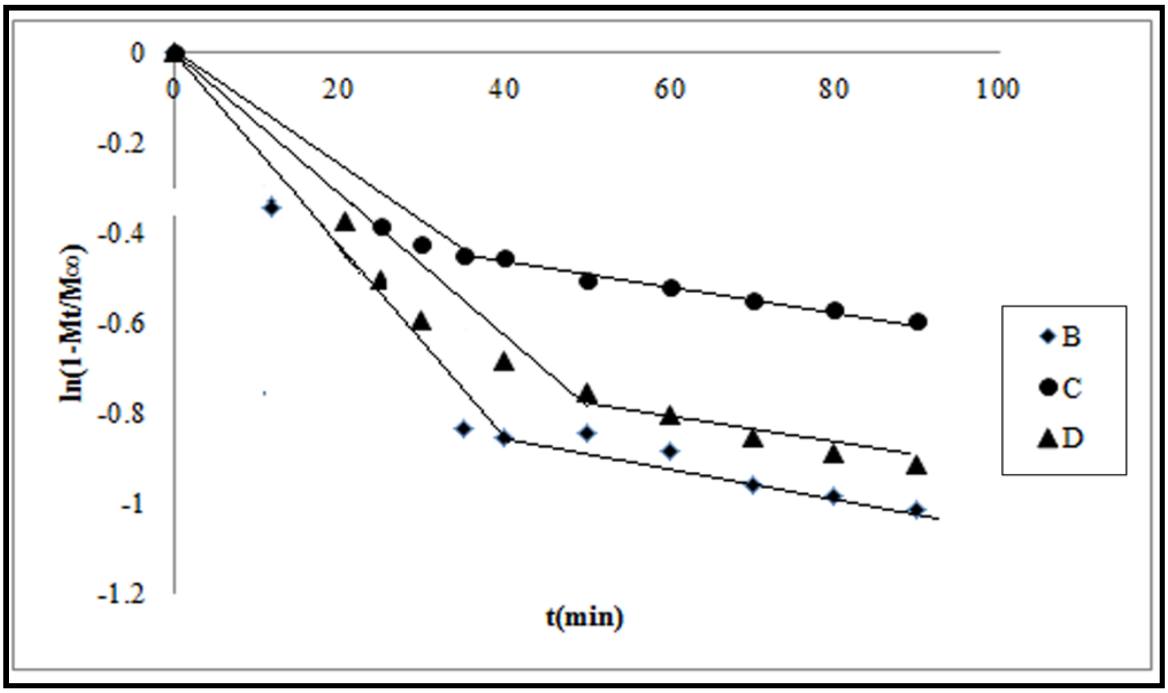

Fig. 4.16: The water uptake of ln (1-F) versus t plots for film samples A, B, C and D.

Table 4.11 Data showing value of ln (1-F) verses t for the film samples E, F and G

t(min)	ln(1-Mt/M∞)		
	E	F	G
0	0	0	0
2	-0.1226	-0.0914	-0.0885
4	-0.2624	-0.1814	-0.1747
5	-0.4582	-0.2015	-0.1789
10	-0.5632	-0.5895	-0.3584
15	-0.6729	-0.6622	-0.4492
20	-0.7965	-0.6707	-0.5433
25	-0.8608	-0.7819	-0.5612
30	-0.8682	-0.787	-0.596
35	-0.91	-0.8069	-0.6558
40	-0.9991	-0.8271	-0.6581
50	-1.0161	-0.8428	-0.7854
60	-1.0376	-0.988	-0.8773
70	-1.1695	-1.0311	-0.9278
80	-1.2371	-1.0711	-0.9818
90	-1.2559	-1.0697	-1.0128
100	-1.2697	-1.2402	-1.1548

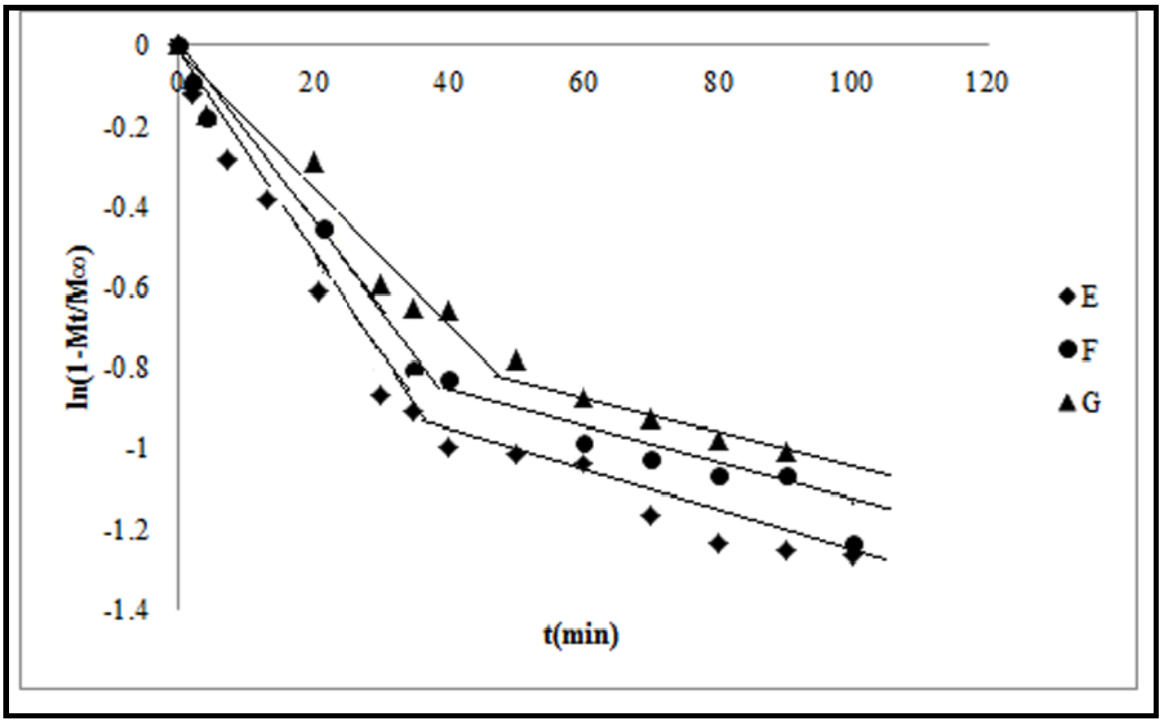

Fig. 4.17: ln (1-F) versus t plots for the water uptake of film samples.

Table 4.12. The value of the various types of diffusion coefficients the samples.

Sample	D_I	D_L	D_{ave}
B	141.05X10^{-6}	75.22 X10^{-6}	18.58 X10^{-6}
C	35.63X10^{-6}	62.58 X10^{-6}	19.45 X10^{-6}
D	35.29 X10^{-6}	82.53 X10^{-6}	23.7 X10^{-6}
E	102.67 X10^{-6}	109.29 X10^{-6}	13.28 X10^{-6}
F	115.64 X10^{-6}	182.2 X10^{-6}	26.93 X10^{-6}
G	124.39 X10^{-6}	231.73 X10^{-6}	45.44 X10^{-6}

A closer inspection on the displayed values shows that all diffusion coefficients are in the order of 10^{-6}, which is a commonly observed phenomenon in terms of polymer films. For example, *(AlešMráček, 2010)*, using the interferrometric method, reported the average diffusion coefficient for hyaluronan films and that it was in the magnitude of 10^{-6} cm^2 min^{-1}. Almost similar results were also reported for swelling of thin gelatin films *(Wu and Yen, 1994)*.

4.2.9 Moisture sorption behavior

The data for the moisture uptake data, obtained experimentally, for the film samples Glox-X-Gel and Glox-X-Gel/PANI at 30°C is shown in the Table 4.13 and Fig.4.18.

Table 4.13 The value of water activity (a_w) on moisture uptake (M_c) at 30^0C.

a_w	aniline	gelatin
0.0932	0.061	0.081
0.2311	0.076	0.095
0.4316	0.153	0.225
0.7547	0.205	0.311
0.8511	0.309	0.328
0.9759	0.969	2.035

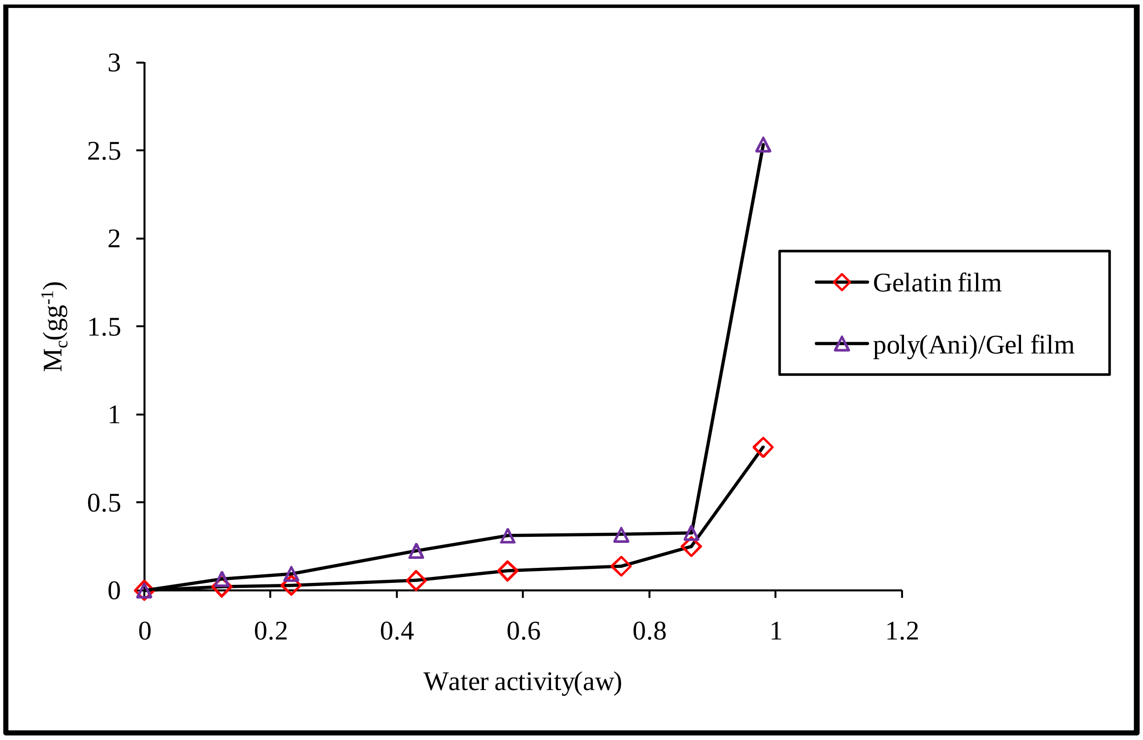

Fig. 4.18 Moisture sorption isotherms for Glox-X-Gel and Glox-X-Gel/PANI films.

. The above curves show that both are sigmoid, exhibiting characteristic type-II isotherms. Such curves are maximally natural of biopolymers such as soya protein *(Pornchai and Suryathem, 2012),* milk protein *(Khojare and Hembade, 2016),* polysaccharides. Gum harmony *(Haque et al., 2016),* cellulosic material *(Pournachie and Virongong, 2009),* chitosan *(Dang and Mong, 2012),* etc. It can be appreciated that Glox-X-Gel exhibits high moisture behavior in all water activities in associate with Glox-X-Gel/PANI films. The hydrophilic nature of gelatin is responsible for the number of polar groups with macromolecular chains. These polar groups interact with entering vapor molecules and fix them on their active polar sites, which results in excessive water uptake.

However, the Glox-X-Gel/PANI film has a PANI network as its constituent, which does not interact with water vapor due to its absent structural network due to non-existence of all polar sites. However, seen moisture uptake behavior may simply be because of existence of gelatin molecules. On the isotherms, three zones are obtained viz. zone–I (aw: 0.0 to 0.2), zone–II (aw: 0.2 to 0.7) and final zone–III (aw: 0.7 to 1.0). In the region I (termed as called monolayer sorption region).

The EMC increases with water activity because a very large number of polar groups prefer -NH2, -COOH owing to the presence of gelatin molecules. These groups provide strong binding places for entering water vapor molecules. The water vapor molecules where get bounded very strongly to these available active polar sites *(Falade and Aworh, 2004)*.

In Zone II, which is also called multilayer circulation area, moisture content increases significantly with water activity (aw) and increased rate significantly. In this area, although silt accumulates in less active places, but due to water sorption of the macromolecular chains are not disclosed.

This increases the exposure of new active sites to incoming vapor molecules, thus accelerating moisture. However, it is more noticeable for pure gelatin film. Finally, there is a sharp increase in EMC in Zone-II (commonly termed as the capillary condensation zone) that can be due to diffusion of voids in the gelatin film matrix and moisture into the capillaries. The water in this area is in Free State. This isotherm shows that the substrate adsorbed more water proportionately after reaching the later part of plot.

4.2.9.1 GAB isotherm model

According to the observation, the moisture behavior of the samples was studied by three parameters GAB (Guggenheim-Anderson-de Boer), and a theoretically derived isotherm model *(Frederic and Ahrne, 2004)* as given below:

$$M = \frac{M_o\, C\, K\, a_w}{(1-K\, a_w)(1-Ka_w+C\, K\, a_w)} \qquad \ldots (4.13)$$

Where, M_o is the unilayer moisture content, C is a constant which is related to the first layer heat of the sorption and the K is a factor dependent to the heat of sorption of the multilayer. In order to exterminate parameters of GAB isotherm model, GAB equation was rearranged into polynomial equation of second degree, as shown below:

$$\frac{a_w}{M} = \alpha a_w^2 + \beta a_w + \gamma \qquad \ldots (4.14)$$

where,

$$\alpha = \frac{K}{M_o}\left[\frac{1}{C-1}\right] \qquad \ldots (4.15)$$

$$\beta = \frac{1}{M_0}\left[1 - \frac{2}{C}\right] \qquad \ldots (4.16)$$

And

$$\gamma = \frac{1}{M_0 CK} \qquad \ldots (4.17)$$

Fig.4.19. the two polynomials show a fair degree of regressions. Thus the coefficients *a*, *b* and *g*were subtracted from this polynomial equation and replace each into the GAB constants. The evaluated parameters for GAB model are given in Table

4.14. A non-linear regression analysis of a_w/M_c as a_w resulted polynomial of second order as see in Fig. 4.19.

Table 4.14. The values of a_w and a_w/M_c of Glox-X-Gel and Glox-X-Gel/PANI film.

a_w	a_w/M_c(gg^{-1}d.b.)	
	aniline	gelatin
0.0932	1.52	1.15
0.2311	3.04	2.43
0.4316	3.82	2.91
0.7547	3.68	2.42
0.8511	2.75	2.29
0.9759	0.9	1.47

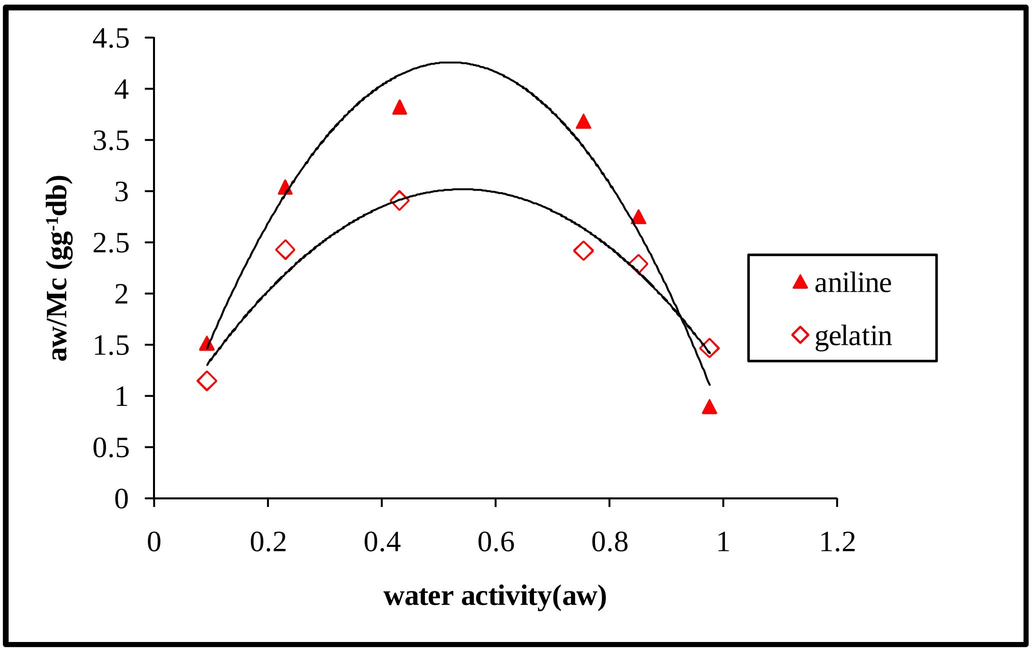

Fig. 4.19: Polynomial curve b/w a_w/M_c and a_w for Glox-X-Gel and Glox-X-Gel/PANI films.

GAB isotherm model has a sound theoretical basis and its parameters carry significant information regarding the conduct of substrate within the sight of moisture. M_0 is of point of interest because its value points to the amount of PANI which is greatly and strongly adsorbed at specific sites on the substrate surface and can be taken as the optimum value to assure stability of substrate material. Therefore, M_0 is identified as the content of moisture witnessing the longest period of time with minimum quality loss at a given temperature. Below it, the deteriorative reactions occur at minimum rate. Hence, at a particular temperature, the ensure water activity level is that which is associated to the value of M_0 or lower. The values of 'M_0', as given in Table 4.15, are 0.0260 and 0.0986g/g for, PANI/Gel and pure gelatin films respectively.

Table 4.15.Data showing the related parameters for GAB model.

GAB parameters	Gel/PANI film	Gel film
K	0.9491	0.4765
C	62.9687	11.1336
$M_0(gg^{-1}db)$	0.0620	0.0986
R^2	0.9659	0.9390

The higher value of M_0 for the pure gelatin film can be interpreted because of the presence of deferent polar groups in a gelatin matrix along the gelatin chains, thus making it the site of the attachment of water vapor molecules unlike Glox-X-Gel/PANI film which possess PANI as a component for it. The absence of polar groups in the PANI contributes towards reducing the absorption of moisture. The GAB constant C explains adsorbent–adsorbate interactions and it has been investigated that *(Blahovec and Vanniotis, 2008)* the parameter C must satisfy the following relations:

The GAB model for $C>2$ should result in a sigmoidal shape with point of inflection (Type II of Brunauers (1943): and the isotherm for $0<C<2$ is only of type–III (isotherm without infinity).

In this research, the C value for the film sample was greater than two for both film and the isotherm curves evaluated were also sigmoidal, which supports above predictions. Finally, the value of K gives us a measure to draw conclusions about the interactions between molecules in the multilayer with adsorption and shows the tilt between the energy values of the molecules under study and the liquid water in the monolayer. The specified range for K values is $0<K\leq1$. As can be seen, the values of K, obtained for both of the film samples fall within the prescribed range.

4.2.9.2 Effect of temperature on moisture uptake

Temperature of the moist environment shows a very important role in controlling the moisture uptake of the polymeric films. The sorption isotherms sample of Glox-X-Gel and Glox-X-Gel/PANI films at ‘283, 293 and ‘303’ *K* are shows in Fig. 4.20 and Fig. 4.21 respectively.

Table 4.16. The value of the temperature on moisture uptake Glox-X-Gel/PANI films.

Mc	**Glox-X-Gel films.**		
	0.283k	**0.293k**	**0.303k**
0.1234	0.02	0.061	0.02
0.2338	0.021	0.076	0.02
0.4338	0.017	0.153	0.033
0.5736	0.043	0.205	0.111
0.7567	0.052	0.245	0.138
0.8677	0.066	0.309	0.25
0.9818	1.094	0.969	0.815

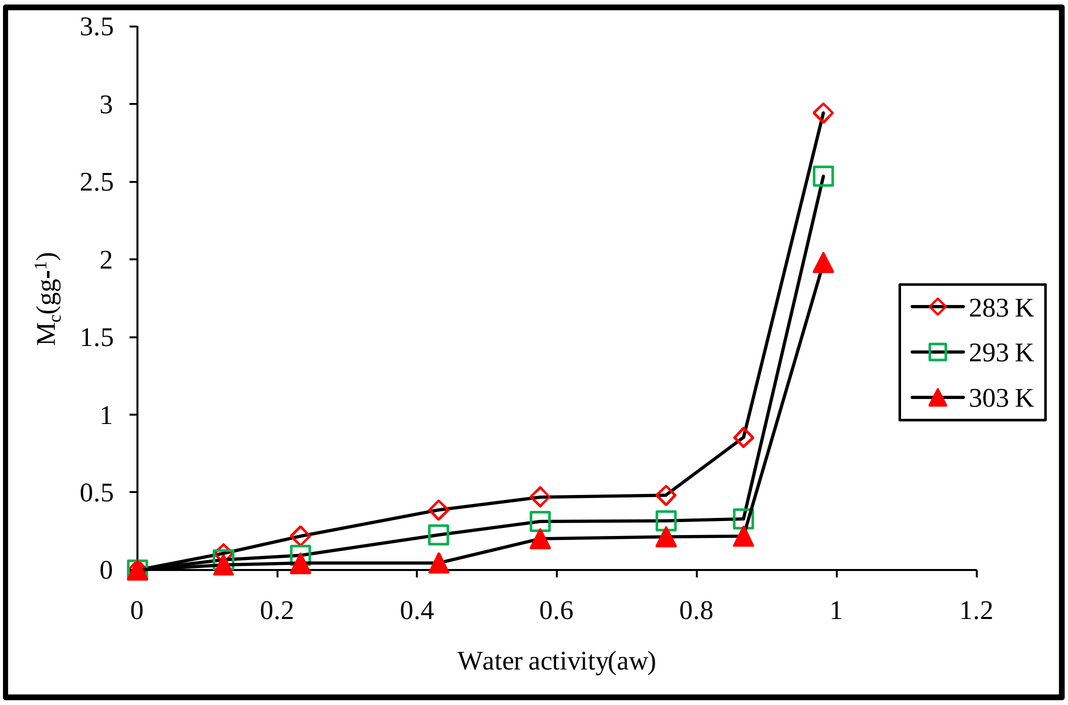

Fig. 4.20: Effect of temperature on moisture uptake of Glox-X-Gel films.

Table 4.17.The value of the temperature on moisture uptake of Glox-X-Gel/PANI films.

M_c	Glox-X-Gel/PANI Films		
	0.283k	**0.293k**	**0.303k**
0.1234	0.075	0.081	0.031
0.2338	0.174	0.095	0.043
0.4338	0.291	0.225	0.046
0.5736	0.461	0.311	0.2
0.7567	0.421	0.318	0.214
0.8677	0.853	0.328	0.216
0.9818	2.942	2.535	1.978

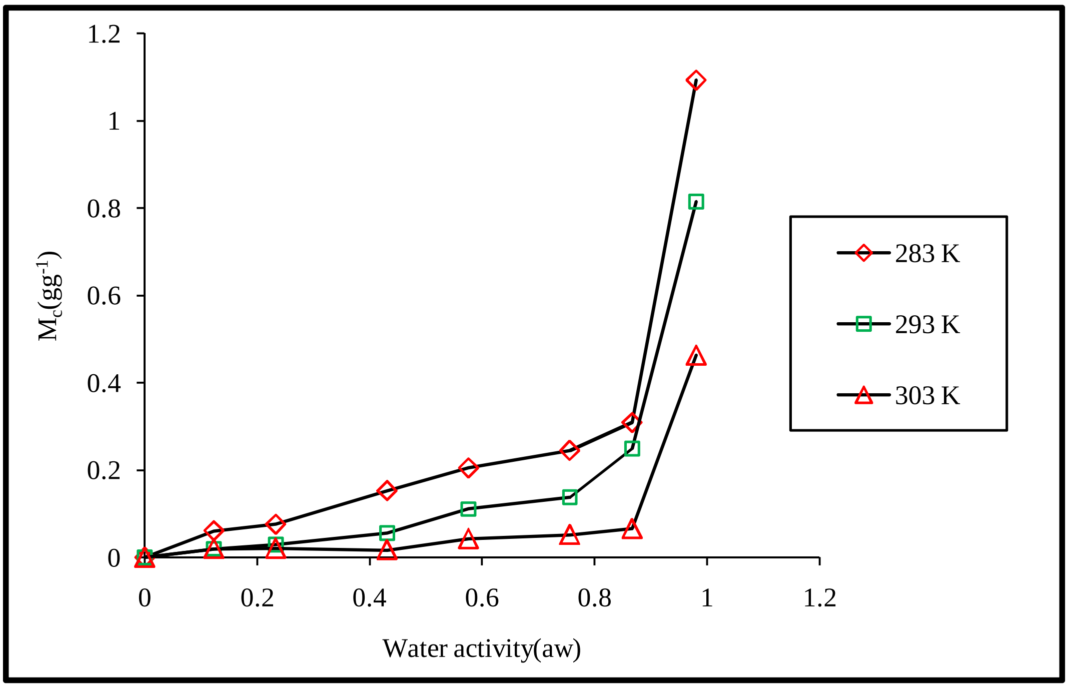

Fig. 4.21: Effect of temperature on moisture uptake of Glox-X-Gel/PANI films.

It can be seen that the films, namely Glox-X-Gel and Glox-X-Gel/PANI films, reflect sigmoidal type–II at all the temperatures under study. In addition, they obtain negative trends, that is, the moisture uptake the increase in temperature. The reason behind this can be described as follows: When the temperature is low, the inter molecular attractive forces between the active polar sites within the film matrix and the water vapor molecules are stronger as the less kinetic energy of vapor molecules decreases. However, with increase in temperature, the kinetic energy of entering water vapor molecules increases and therefore they are not so strongly bound for available sites, which results in a decrease in the equilibrium uptake.

4.2.9.3 Evaluation of thermodynamic parameters

The moisture sorption data, when applied on the various thermodynamic principals, provides useful information about the active sites of the film matrix and properties of water bound to physical phenomena based on the film surfaces and sorption kinetic parameters. These parameters are very effective, especially when the film is used for packaging of food ingredients or similar products.

Here, *(qst)* is defined as the total heat of water evaporation *(qst)* in the system temperature *(Torgul and Arslan, 2007)*. The pure isostric heat of sorration or differential sac is reflecting the need for energy to remove moisture from the food content (water-solids bond strength) and is a practical use in calculating and modeling of complete drying of energy *(Macmine and Maggi, 2003)* .

Apart from this, entropy changes also shows a most important role in the energy analysis of food processing systems and the differential entropy of sorption, S_d, can be calculated using Gibbs- Helmholtz equation *(Torgul and Arslan, 2007)*. For calculation of q_{st} and S_d, different values of moisture contents from '0.75 to 2.0' and '0.06 to 0.44' (gg^{-1} dry basis) respectively. For sample Golx-X-Gel and Golx-X-Gel/PANI films. Through these values, the relevant values of a_w were evaluated at different temperatures. By plotting $\ln a_w$ versus $1/T$, for a specific moisture content of polymeric film and then determining the slope ($-q_{st}/R$) and intercept (S_d/R), the finel isosteric heat (q_{st}) and differential entropy (S_d) of sorption were obtained using the following equation:

$$- \ln a_w \frac{q_{st}}{R}\frac{1}{T} - \frac{S_d}{R} \qquad \dots (4.18)$$

where, q_{st} is the final isosteric heat of sorption ($kJ\ mol^{-1}$), S_d is the differential entropy ($kJ\ mol^{-1}K^{-1}$), R the universal gas constant ($kJ\ mol^{-1}\ K^{-1}$), T is the absolute temperature, (K) and a_w is the activity of water. The respective plots between $\ln a_w$ and $1/T$ for Glox-X-Gel/ PANI films are showed in Fig. 4.22 and Fig 4.23 respectively.

Table 4.18. Data showing effect of 1/T and ln(a_w) for the film Glox-X-Gel.

1/T	ln(aw)				
	0.1	0.2	0.3	0.4	0.8
0.0035	-2.12026	-2.12026	-1.13943	-0.82098	-0.15082
0.0034	-1.42712	-1.48653	-0.73397	-0.15082	-0.12783
0.0033	-0.22098	-0.95882	-0.12783	-0.12783	-0.09431

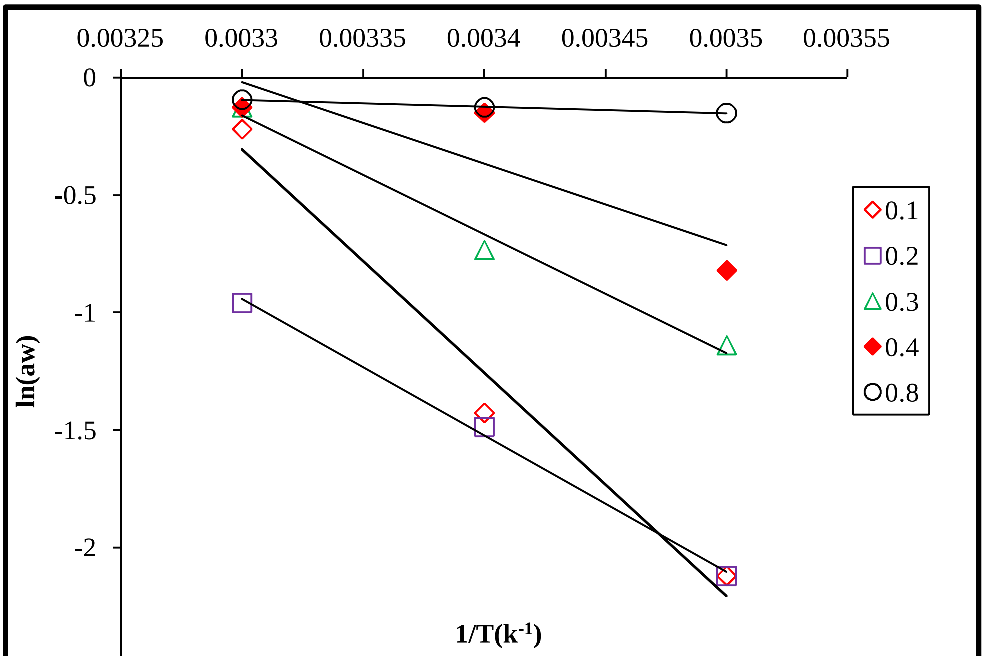

Fig. 4.22: Variation in M_c with 1/T for the Glox-X-Gel film.

Table 4.19. Data showing the effect of 1/T and ln(a_w) for the Glox-X-Gel/PANI film.

1/T	ln(aw)				
	0.04	**0.05**	**0.1**	**0.2**	**0.4**
0.0035	-2.81341	-2.12026	-1.20397	-0.57982	-0.12783
0.0034	-1.96611	-1.48653	-0.84473	-0.19845	-0.10536
0.0033	-1.60944	-0.95882	-0.65783	-0.10536	-0.04082

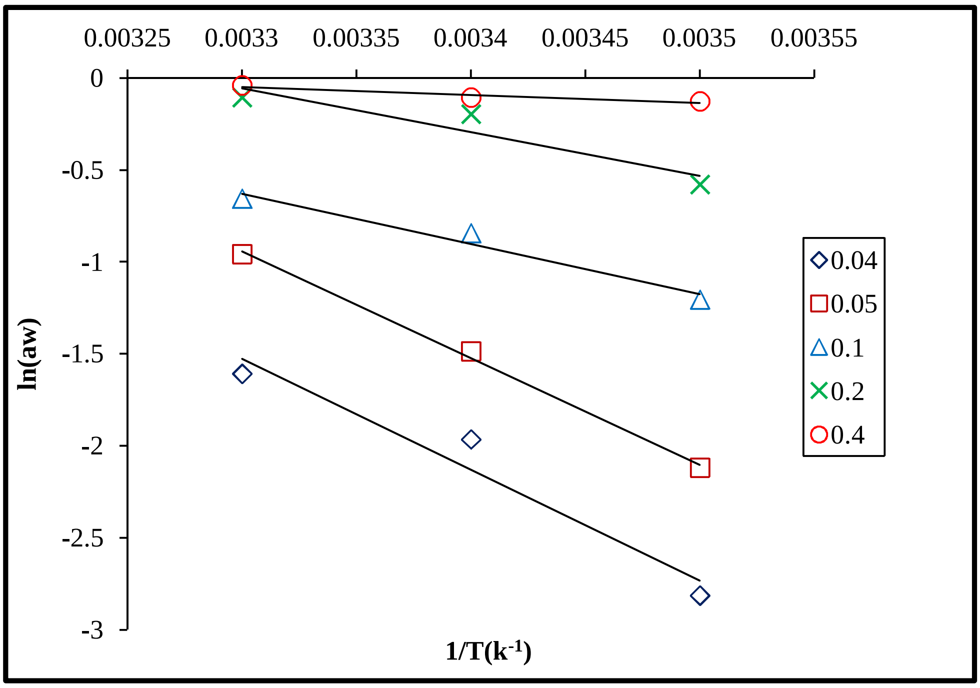

Fig. 4.23: Variation in M_c with $1/T$ for the Glox-X-Gel/PANI film.

Table 4.20.Data showingthe effect of q_{st} with M_c for the film Glox-X-Gel.

M_c (g/g-1)	q_{st}
0.2	78.9497
0.4	48.2794
0.6	42.0522
0.8	28.808
0.9	23.487

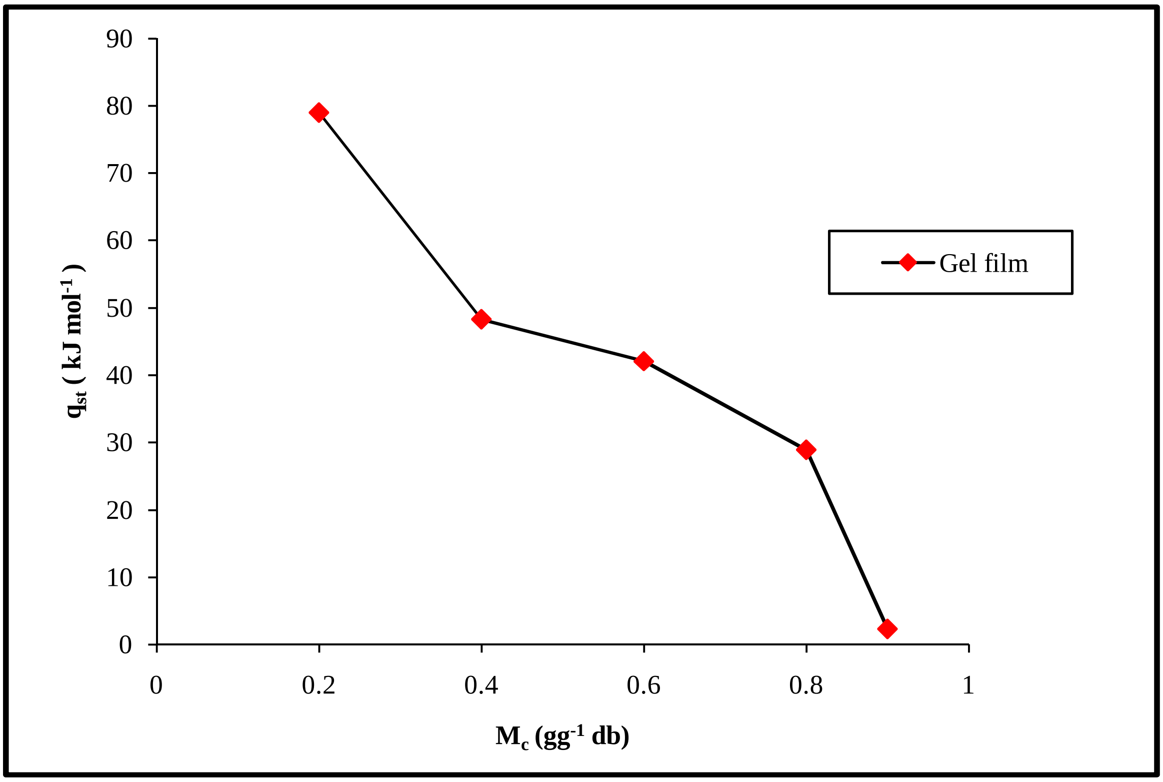

Fig. 4.24: Variation in q_{st} with M_c for the Glox-X-Gel film.

Table 4.21.Data showing the effect of q_{st} with M_c for the filmGlox-X-Gel/PANI.

M_c (gg-1)	q_{st}
0.04	48.9585
0.05	47.2341
0.1	22.2058
0.2	19.2938
0.4	3.53829

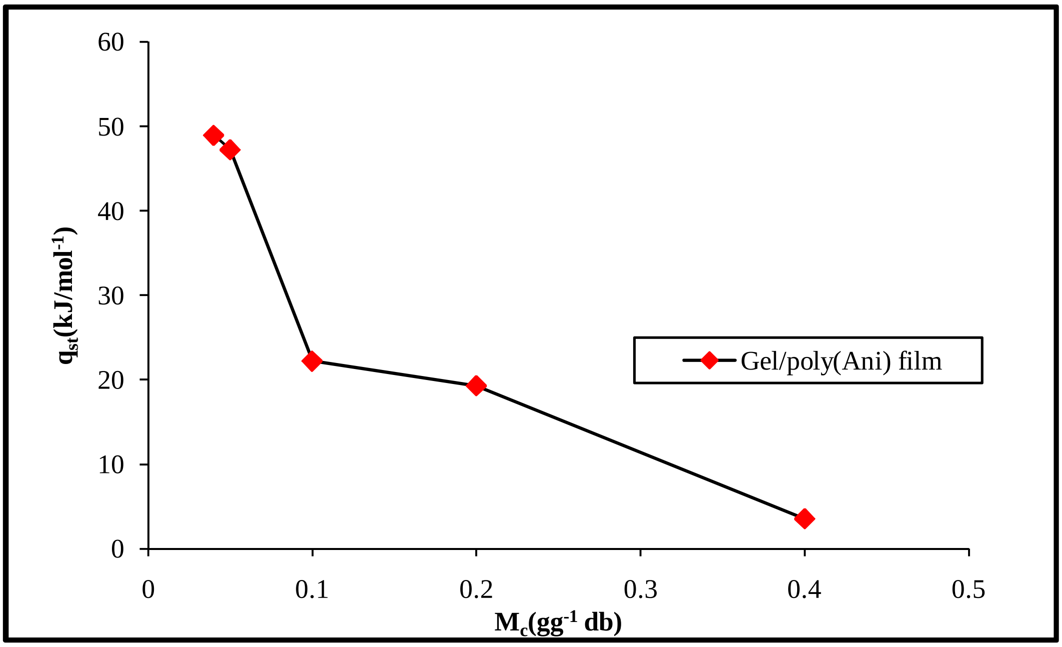

Fig. 4.25: Variation in q_{st} with M_c for the Glox-X-Gel/PANI films.

Using the intercepts and slopes of linear plots, displayed in Fig.4.20 and Fig 4.21 values of q_{st} and s_d were evaluated. The data obtained indicated that q_{st} decreased from 78.94 to 2.34 kJ/mol^{-1} with the increase in $M_c$from 0.2 to 0.9 *g/g db* for native Glox-X-Gel film while the decrease in q_{st} was from 48.95 to 3.53 kJ/mol^{-1} over the increase in M_c from 0.04 to 0.4 *g/g db* for Glox-X-Gel/PANI film respectively (see Fig.4.24 and Fig 4.25).

This decrease can be attributed to the fact that most active sites occur initially, thus giving rise to the largest interaction energy. As the increasing moisture the content, the sites available for water vapor sorption are reduced, resulting in reduced q_{st} values *(Tsami et al., 1990)*. In the amount of low moisture, higher q_{st} values may be due to strong interaction between starch molecules and water molecules in hydrophilic groups. Almost comparable results have been mentioned elsewhere q_{st} ($kJ\ mol^{-1}$) *(Muhtaseb et al., 2004)*. The variance entropy of isotherm sorption S_d between moisture content plot shown in Fig. 4.26 and Fig 4.27.

Table 4.22.Data showing the effect of M_c (g/g-1) and s_d for the Glox-X-Gel film.

M_c (g/g-1)	s_d
0.2	0.257
0.4	0.151
0.6	0.137
0.8	0.094
0.9	0.006

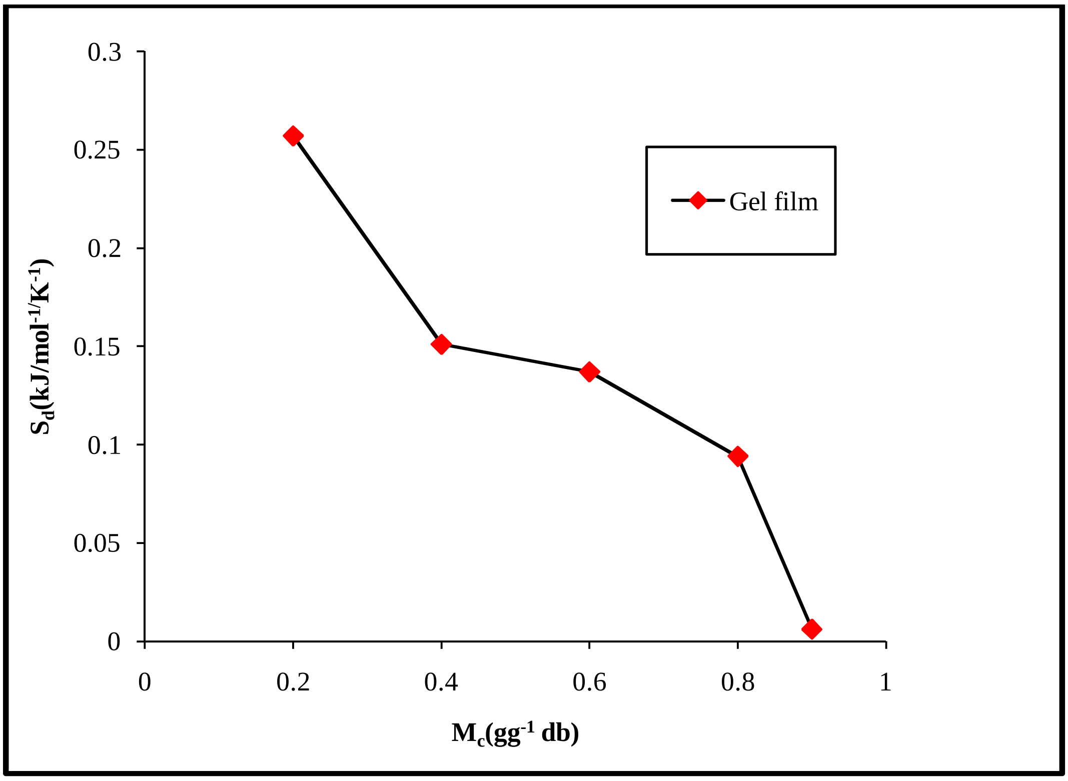

Fig. 4.26: Variation in s_d with M_c for the Glox-X-Gel film.

Table 4.23. Data showing the effect of Mc (gg-1) and s_d for the Glox-X-Gel/PANI films.

M_c (gg-1)	s_d
0.04	0.152
0.05	0.151
0.1	0.069
0.2	0.064
0.4	0.011

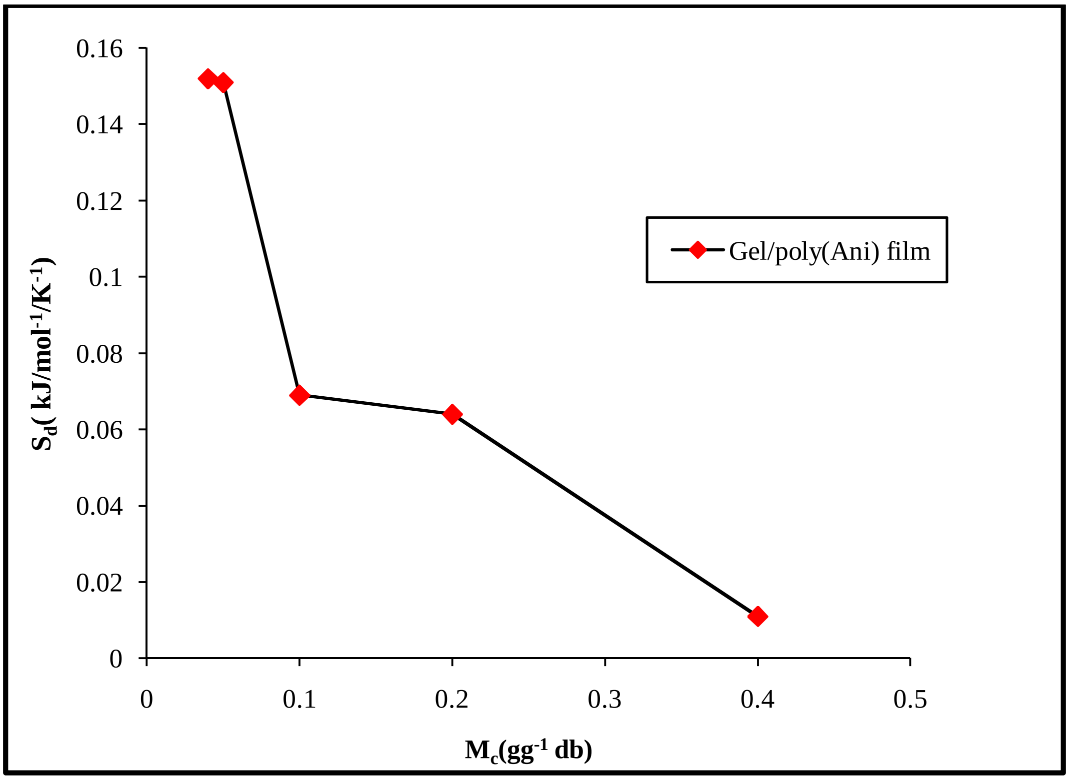

Fig. 4.27: Variation in s_d with M_c for the Glox-X-Gel/PANI films.

It is evident that the differential entropy decreases as the moisture content increases. The value of s_d decreased in M_c Gel Film from 0.257 to 0.006, from 0.2 to 0.9 $gg^{-1}db$. The addition, decrease in q_{st} from 0.152 to 0.011 kJ/mol^{-1} was observed for the related to increase in M_c from 0.04 to 0.4, for sample Glox-X-Gel/PANI film. These results show strong dependence of pure q_{st} and S_d on moisture content. Similar trends have also been studied by other researchers *(Muhtaseb et al., 2004B).*

4.2.9.4 Entropy-enthalpy compensation theory

According tocompensation theory, there exists a good coorelation ship between S_d and q_{st}*(Igathinathane et al., 2007)*. It is expressed mathematically:

$$Q_{st} = T_\beta S_d + \Delta G_\beta \qquad \text{… (4.19)}$$

Here, T_β is the isokinetic temperature and the free energy ΔG_β, provides a criterion to evaluate if water absorption is a spontaneous ($-\Delta G_\beta$) or non-spontaneous process ($+\Delta G_\beta$), placed at the same rate. This is the phenomena of the material surface *(Aguerre et al., 1986)*, and it represents slope of the enthalpy-entropy linear relationship. The linear carve between q_{st} and S_d for plain Glox-X-Gel and Glox-X-Gel/ PANI films are showed in Fig. 4.28 and Fig 4.29 respectively.

Table 4.24. Data showing the effect of s_d versus q_{st} for the Glox-X-Gel film.

s_d	q_{st}
0.257	78.949
0.151	48.298
0.137	42.052
0.094	28.808
0.006	23.487

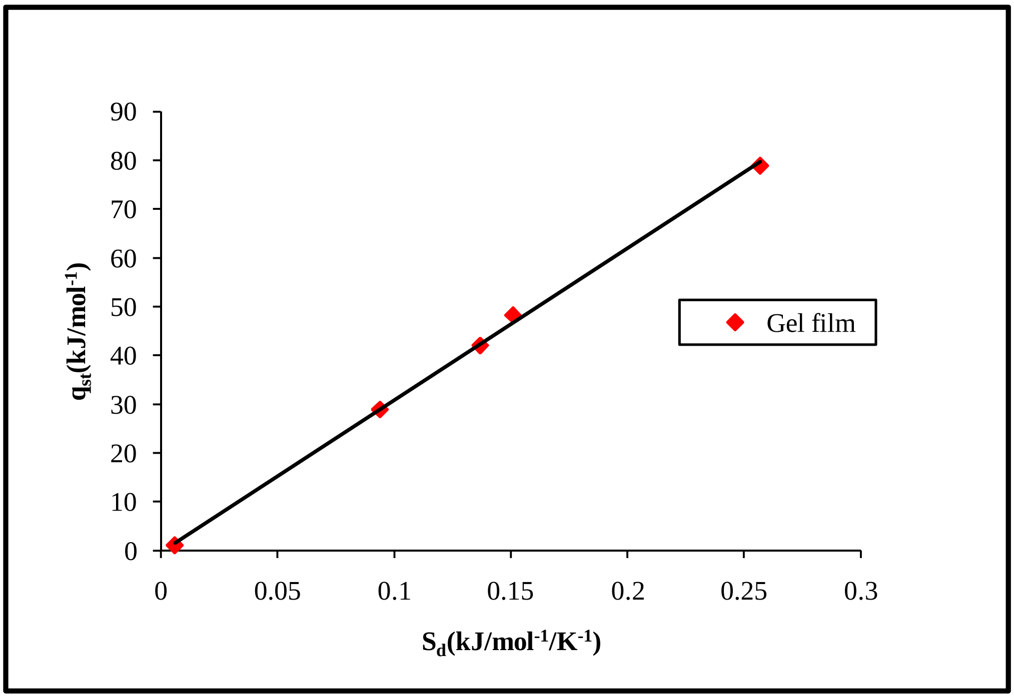

Fig. 4.28: S_d versus q_{st} plot for Glox-X-Gel film.

Table 4.25.Data showing s_d versus q_{st} for Glox-X-Gel /PANI film.

s_d	q_{st}
0.152	48.958
0.151	47.234
0.069	22.205
0.064	19.293
0.011	3.538

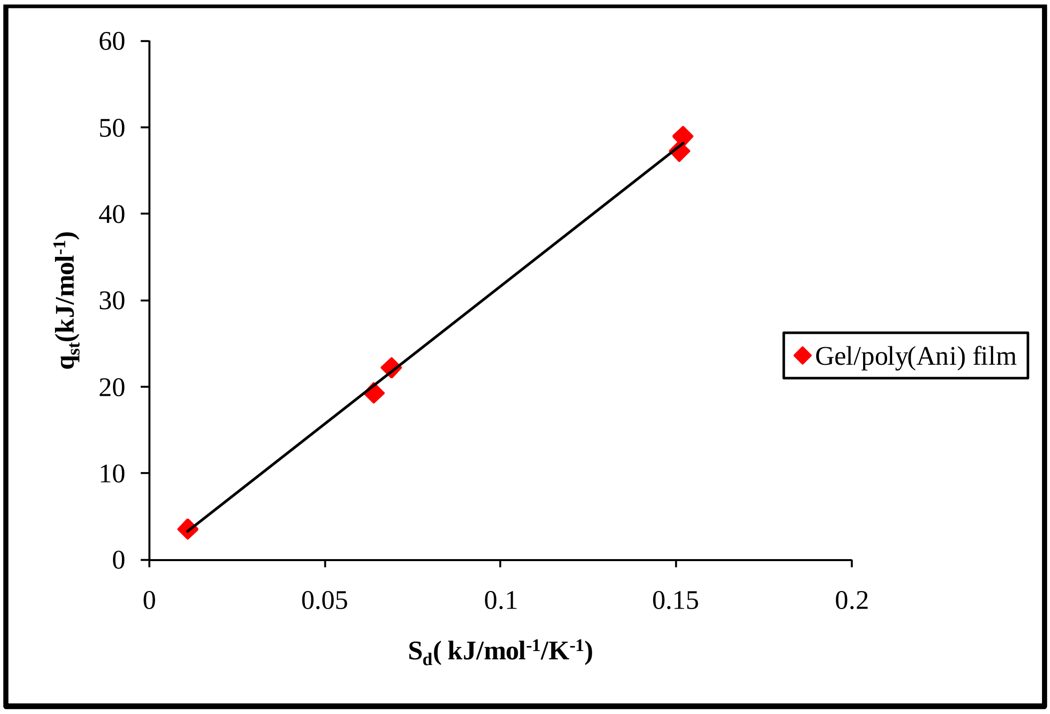

Fig. 4.29: S_d versus q_{st} plot for Glox-X-Gel/PANI film.

It may be noticed that there exists a fair correlation between qst and S_d as show by the higher values of R^2 for both of the films. In this work, values of T_β for the native Glox-X-Gel and Glox-X-Gel/PANI films were found 311.41 and 318.61K respectively. The values of ΔG_β were found to be -0.3278 and -0.2378*kJ/mol* respectively.

Negative value provides indication for the smooth moisture process for both films. This depends only on the fact that the presence of gelatin as the main component in both films causes the predominance of polar active sites within the film matrices and therefore water vapor molecules are spontaneously depicted on the films. In addition, the value of ΔG_β is more negative for the plain Glox-X-Gel film due to the presence of more active sites within the film matrix than the Glox-X-Gel / PANI film. The isokinetic temperature (T_β) is the temperature at which all the sorption reaction will take.

4.2.10 Blood compatibility

Two types of blood interactions, namely thrombogenicity and haemolytic potential, were investigated for the Glox-X-Gel and Glox-X-Gel/PANI films as per procedure reported *(Chu et al., 2006)*. All studies were done by triplicate and the data were given as mean±s.d. The saline solution used for this study was obtained by 0.9% NaCl, with adjust the final pH with pH = 7.4 *(Liu et al., 2010)*. Blood compatibility test is very essential for wound dressing application.

4.2.10.1 Thrombus formation test

An anti-thrombogenity activity of paraffin gauge, film samples Glox-X-Gel and Glox-X-Gel/PANI was investigation by measuring the weight of a dried blood clot. The weight of blood clots was 0.004± 0.0002, 0.004± 0.0004, and 0.005±0.0003 g respectively. In addition, the weight of the clot was 0.30 g on the glass film. Thus, it infers how low amounts of clot were formed on the films, thus confirming the biocompatibility and tremendous anti-thrombogenity of the films *(Kurhade et al., 2013)*.

4.2.10.2 Hemolysis test

The % Hemolysis for the commercial paraffin gauge, Glox-X-Gel and Glox-X-Gel/PANI films was determined to be 0.83±0.05, 1.35±0.09 and 1.07±0.08 respectively. As the values evaluated were less than 2%, the samples can be considered to be fairly non-hemolytic.

4.2.11 Mechanical properties of film

4.2.11.1 Tensile Testing

The plot of tensile strength of aniline concentrations in composite samples is shown in Fig.4.30.

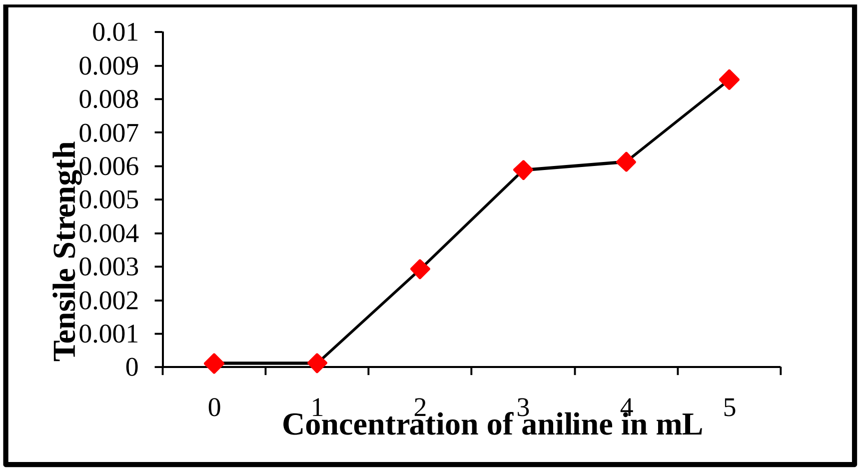

Fig. 4.30: Plot between tensile strength & aniline contents in the films.

The plot of concentration of aniline versus elongation in the samples, under study is shown in Fig.4.31. Again, there is variation in elongation with load for different samples with the different composition of aniline are depicted in Fig.4.32.

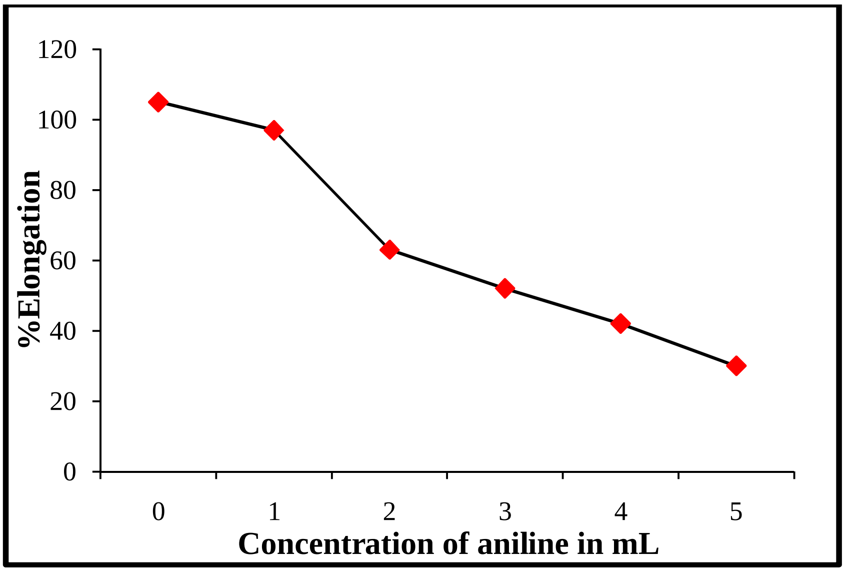

Fig. 4.31: Elongation (%) curves shown aniline contents in the composites.

It is clear (see Fig.4.30) that film sample Glox-X-Gel film , having no aniline, possesses minimum strength. It has been observed that the strength of composite increases as the amount of aniline in the film increases. It is observed that strength of the composite increases as the amount of aniline in the film increases. However, in the case of samples with aniline content of 1 mL, however, it is not to so. However, this growing trend continues for rest of the sample. The results, as shown in Fig. 4.32 reveal a typical nature of the elastic nature of hard material, however this graph clearly shows that yield strength increases with amount of aniline in the film samples.

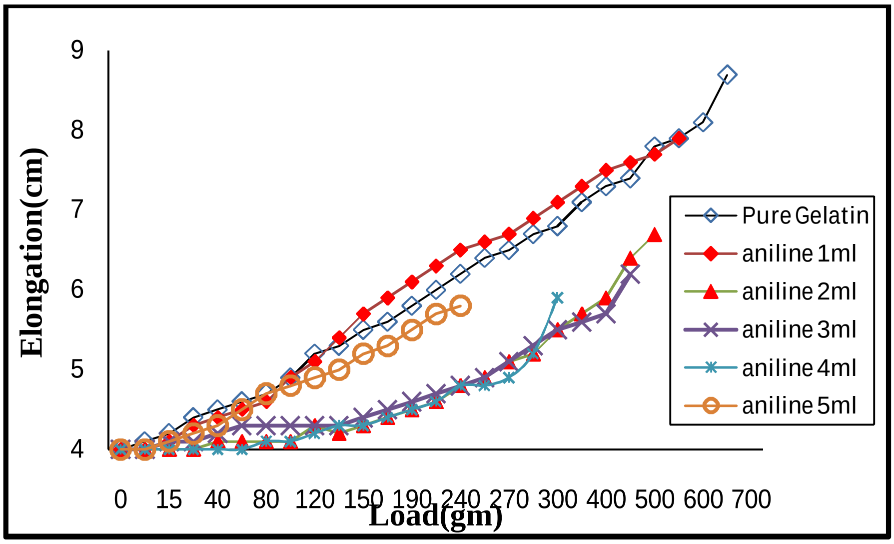

Fig. 4.32: Elongation verses load for different with varying composition of aniline.

Gelatin being semi-crystalline in nature, when allowed to react with glyoxal; the crosslinking will form in the matrix of gelatin due to ‘Schiff base’ reaction among the free amino groups of lysine residues of proteins and aldehyde groups of glyoxal. From Fig.4.32 it is clearly shows that crystallinity increases with the addition of amorphous aniline, while crosslinking with Glox increases thermal stability *(Wu and Yan, 1994)* as reported elsewhere.

Increase in elastic strength that is yield strength is attributed to increase in crystallinity which is due to introduction of Polyaniline in composite material, under inspection. PANI insertion in Glox-X-Gel film increases the elastic strength and crystallinity of the plasticizer.

4.2.12 Electrical properties of film

The plot of conductance, inductance, impedance, capacitance and phase angle with varying frequency of applied AC is shown respectively in Fig. 4.33, 4.34, 4.35, 4.36 and 4.37.

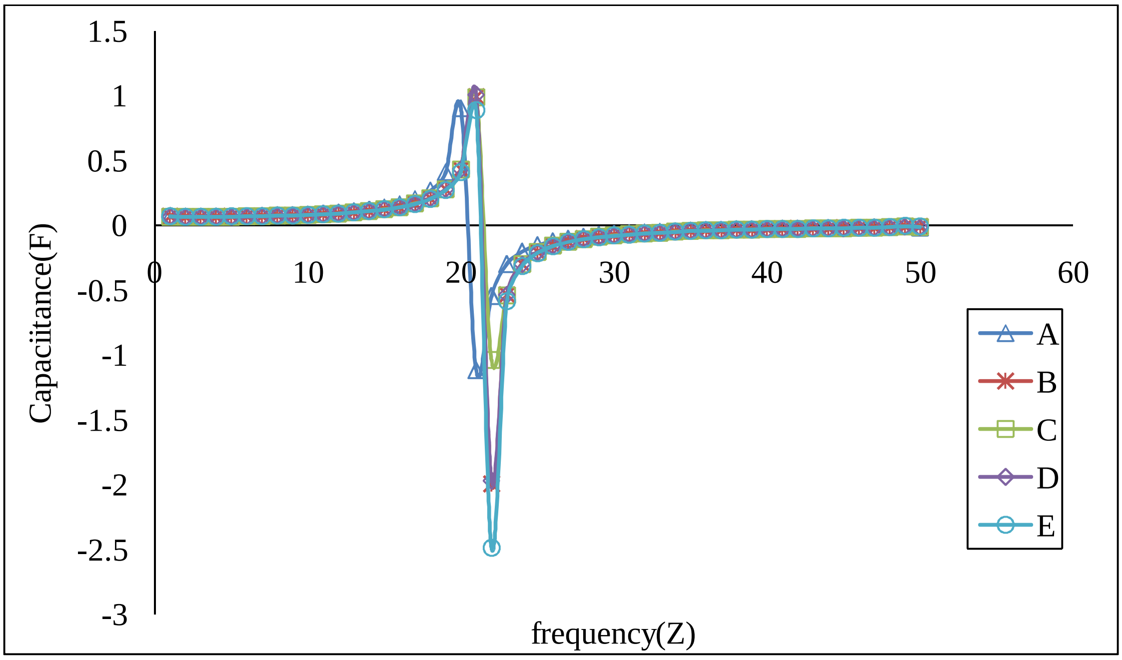

Fig. 4.33: The plot of capacitance of aniline doped Glox-X-Gel/PANI Films.

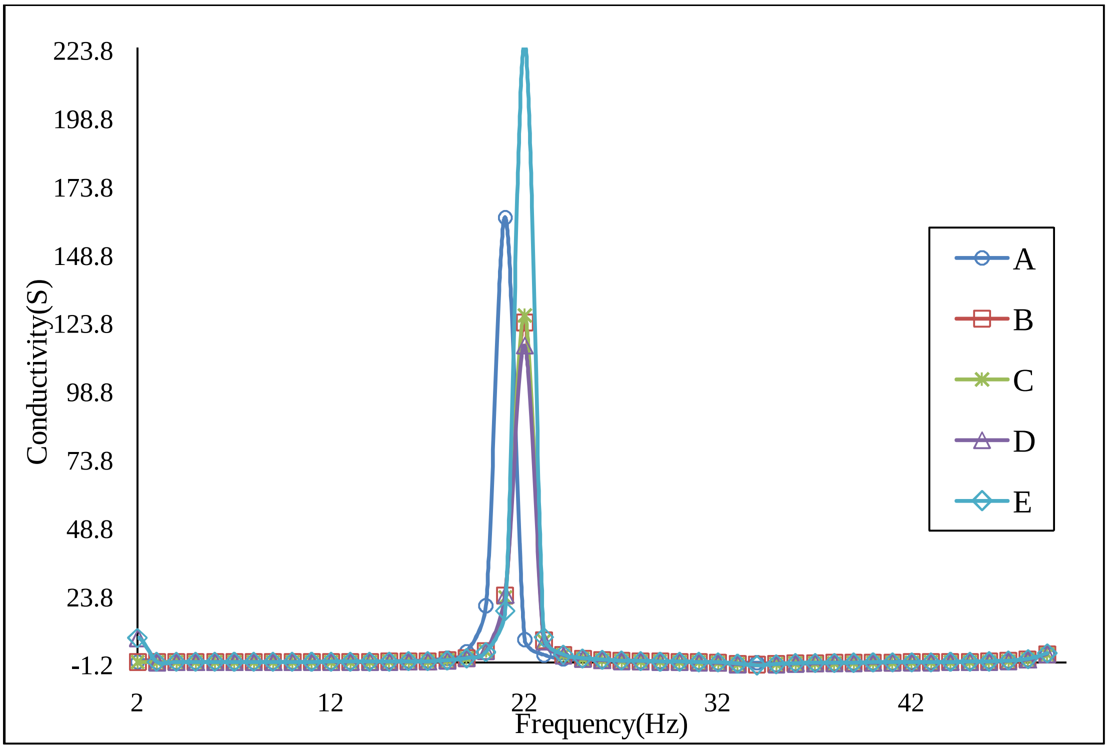

Fig. 4.34: The plot of conductivity of aniline doped Glox-X-Gel/PANI Films.

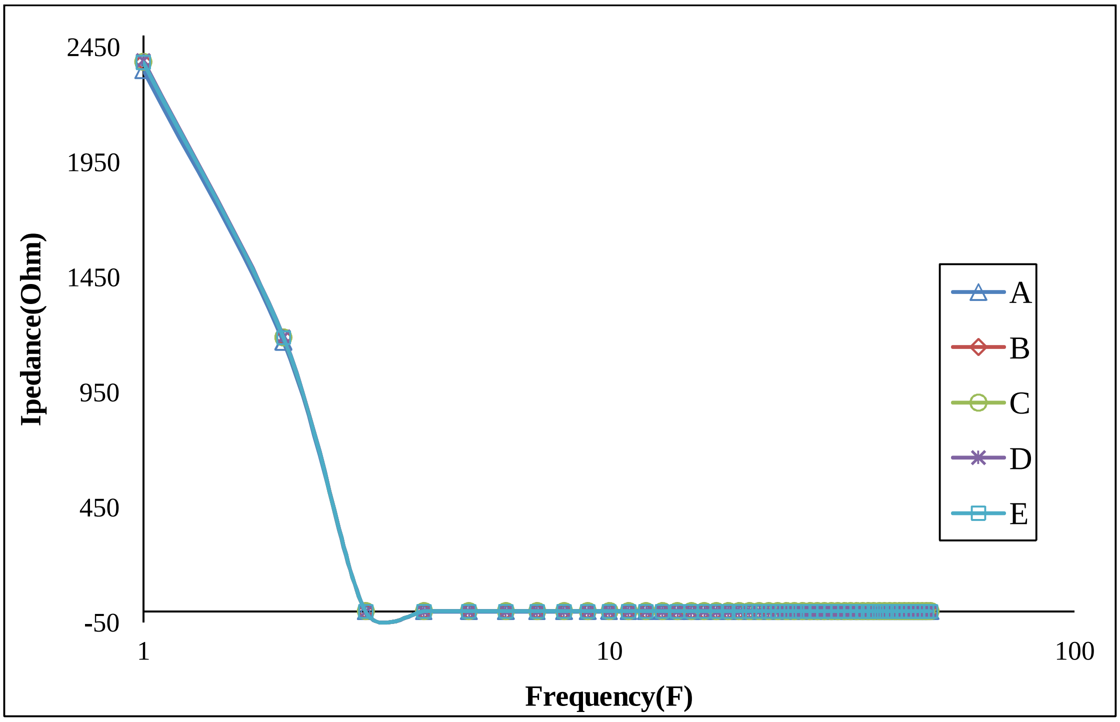

Fig. 4.35: The plot of Impedance of aniline doped Glox-X-Gel/PANI Films.

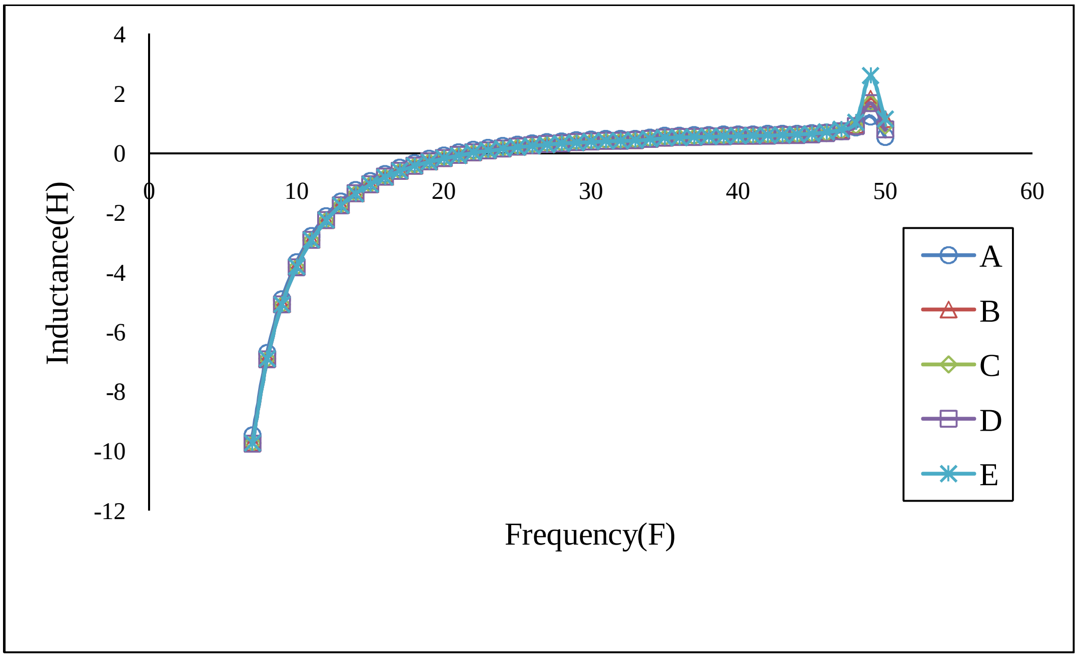

Fig. 4.36: The plot of inductance of aniline doped Glox-X-Gel/PANI Films.

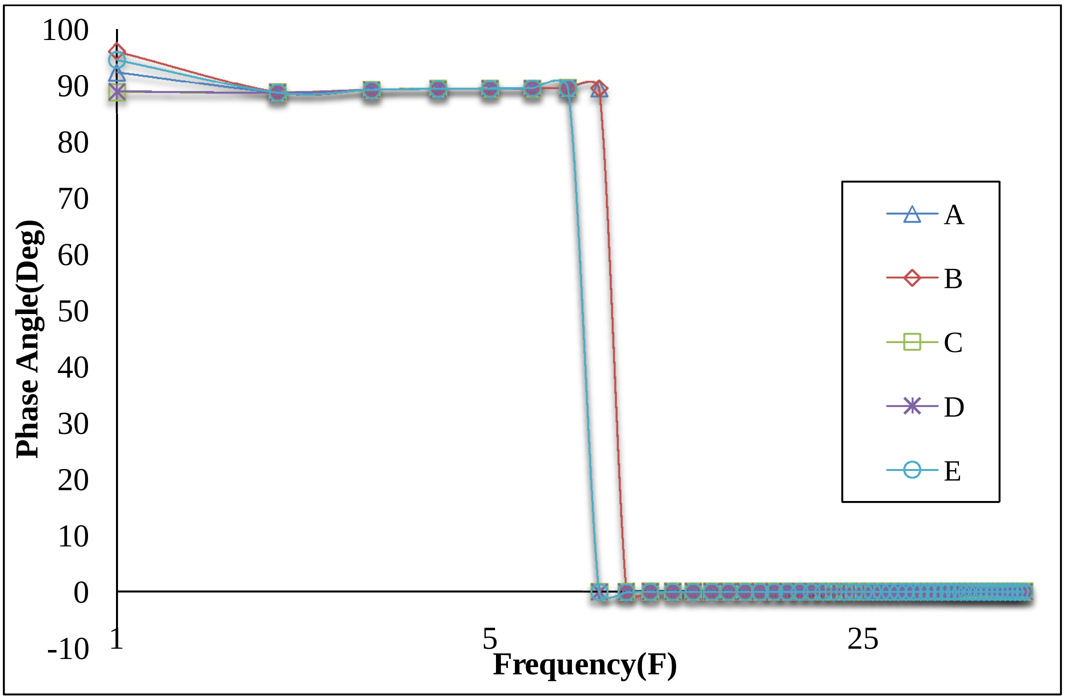

Fig. 4.37: Data showing Phase angle of aniline doped Glox-X-Gel/PANI Films.

It is evident that conductance of the samples increases with concentration of aniline. Appreciable conductivity of Glox-X-Gel/PANI composite has been reported which shows that on insertion of conducting PANI in otherwise non-conducting Glox-X-Gel makes the resulting composite conducting. All samples show rise in electrical conductivity with concentration of aniline.

The plot of AC conductance with frequency for the samples shows identical trend. The conductance first decreases with increasing frequency the samples. The film samples around 29MHz, conductance almost become zero and then show negative conductance (not following ohms law) upto 31MHz. The conductance than again increases in positive direction and approaches zero upto 41MHz for the samples. After 41MHz, conductance again increases and reaches maximum at 49MHz. The maximum conductance for all samples is around 22MHz.

The AC impedance for all testing samples decreases with frequency, having largest impedance value for the lowest frequency of band chosen for measurement. The decrease in impedance clearly show increase in AC conductivity with frequency. The impedance for the samples is capacitive in nature. All samples shows negative inductance, due to which phase difference between voltage and current for every sample is about 90°. The phase shift of -270° is compensated; therefore voltage leads current by 90°. The capacitive nature may be because of the bounding of crosslinked gelatin between the conducting PANI molecules thus forming a parallel plates capacitor like formation which are connected in parallel throughout the composite structures.

CHAPTER – 5

CONCLUSIONS AND FUTURE PROSPECTS

CHAPTER-5

CONCLUSIONS & FUTURE PROSPECTS

5.1. Conclusion

Polymer Science are the most promising branches of materials science, because of widespread applications of polymers and materials derived from them, worldwide almost every field such as construction, communication, medical science, textile, transport, space science etc. The researchers were interested in different classes of synthetic and natural polymers, for not only to understanding the relationship between chemical and physical structure of polymers but also for their wider applications. These materials may be tailored as a desired material as per needed.

It is customary to use “plastics”, a very common term for the polymer blending, obtained by mixing polymers with various agents to by altering the material and electrical nature of polymers in any way. The plastics which are composites can be a homogeneous or heterogeneous mixture. Composite plastics means those plastics which are obtained by bonding two or more homogeneous materials having different material properties, finally arriving at a product that has certain desired mixture and mechanical properties.

A material falls in a class of polymer composites, if it has a combinations or composition which comprises two or more materials in separate phases, at least one of which is a polymer. By mixing, chemically or physically a polymer with some, smartly chosen one more smartly chosen material, such as glass, carbon, or any another polymer, it is always possible to obtain desired unique combination of properties, suitable for particular application. Typical examples of artificial polymeric composites used everywhere, in every fields related to development of human civilization include polymer composites reinforced with fibers of glass, carbon or polymers, It is frequently valuable to consider those materials as composites, which are used in coatings and crystalline polymers (which are like crystallites in a polymer matrix). Examples of naturally occurring composites are wood and bone. The first goal of synthesis of polymer composites is to improve strength, firmness, or stiffness, or dimensional strength by set in particles or fibers into the polymer matrix which is nothing but binding phase. To expend a second goal again, it is economical, easily to use available fillers which is more expensive or its availability is limited; this goal is becoming increasingly important because petroleum supplies are expensive and less reliable.

The third goal is to modify electrical properties, thus they can be used in biomedical and for traditional electronics applications. Other noble applications of composites are using some filler such as glass spheres to improve the progress, incorporating dry-lubricanting particles such as molybdenum sulfide is the result of a self-lubricating effect, and reduced permeability to use filters.

Hydrogels, have crosslinked three-dimensional polymeric network structure of hydrophilic polymers, which can retain up appreciably large amount of water. They can swelling in water and can hold a large amount of water, while their structure remains intact and maintained due to their chemical or physical cross-linking of individual polymer chains. Because of their notable water content, hydrogels have much larger flexibility than natural tissue. The hydrophilicity of hydrogel network is due to the presence of hydrophilic groups like -COOH, -CONH-, $-NH_2$, -OH, $-CONH_2$, and $-SO_3H$. Hydrogels undergo a significant amount of phase transition or hydrogel phase transition solution upon application of certain physical and chemical stimuli. The physical stimulus like electric and magnetic fields, temperature, solvent light intensity, composition, and pressure, while the chemical or biochemical stimulus like pH, ions, and specific chemical structures can induce, phase transition. Controlled drug delivery systems, which are used to deliver drugs at given rates for initially fixed time periods, have been preferably used to overpower the limitations of regular drug formulations. The excellent and remarkable properties of hydrogels make them very useful in drug delivery applications. The hydrogel structures with high porosity can be achieved by controlling two factors: the degree of cross-linking in the polymer matrix and the attraction of hydrogel to the aqueous medium which results in swelling of hydrogels. Due to their porous structures, hydrogels are highly permeable to number of different drugs and these drugs can be loaded into the hydrogel and, can be released in proper conditions. The ability of hydrogels to release pharmaceuticals after prlonged (sustained release) is one of the most significant advantages obtained from them in drug delivery studies, resulting in high concentration of active pharmaceutical substance transported to a specific location over a long period of time. In last few decades uses of drug-delivery devices is boomed and nowadays, scientists are widely used and tested for use in various types of treatments around the world.

In this context, conducting polymer-based devices involves the advantages of conductivity and is researched to test how they are applied as drug-delivery devices, which are electrically controlled inside the body. One of the major challenges in this research is to derive a drug-delivery system which allows firm control on the on/off state of device. In addition, such equipment must be capable of transporting an essential drug at the required controlled doses that are necessary to achieve desirable therapeutic effects.

Among all the known conducting polymers, PANI is very important due to its several useful properties and related applications. Synthesis of PANI can be done through number of known chemical methods. Despite of having wonderful properties, PANI's utilization has been limited because synthesized PANI from these chemical processes has a difficultly to manipulate when subjected to normal melt processing techniques. Since PANI requires thin-driven films, for most applications like control of electromagnetic interference, sensor devices, electrodes, and the dissipation of electrostatic charge-more easily processable PANI-based materials are the current era. As we know that, the major drawback of PANI is its poor processability, and because of this reason, some of its potential applications have not been fully explored and used. By using easily and smoothly processable polymers for the core material and PANI for the shell material, one can improve processability of PANI, through synthesizing its core–shell composite. The PANI composites, prepared in this way have a good stability between electrical and mechanical properties. In the present study we are using a bio-polymer gelatin as a shell material for composite. Gelatin exhibits high brittleness in solid form. Since decades scientists were doing research to modify the charactistics of gelatin and tailoring it for specific applications. Crosslinked gelatin proved to be excellent hydrogel. We have synthesized gelatin film crosslinked with glyoxal (Glox). The gelatin (Gel) films, crosslinked with glyoxal (Glox) have been loaded through molecules of aniline then in-situ oxidative polymerization was done to obtain Glox-X-Gel/PANI composite films. The biopolymer gelatin (having excellent hydrogel properties) and conducting PANI as a shell proves to be very interesting composite investigated. The films, so synthesized, have been considered by FTIR, AFM, TGA, and XRD investigation. The extent of crosslinking with varying composition of crosslinker glyoxal was analyzed using ninhydrin method. With increasing composition of glyoxal, percentage of crosslinking first increases and the crosslinking reaches saturation level; further increasing glyoxal content does not produce any appreciable increase in level of crosslinking in Glox-X-Gel films. Using milimol of cross-linker Glox is almost sufficient to crosslink the film sample to a saturation level, after that using still higher Glox concentration, does not bring any change and percentage crosslinking of the sample remains almost unchanged. The FTIR spectrum of Glox-X-Gel sample, confirms crosslinking of gelatin (gel) film by glyoxal.

In the spectrum of Glox-X-Gel/PANI film, it is clearly confirmed that the formation of polymer composite of aniline and gelatin. The thermal strength of Glox-X-Gel/PANI film and Glox-gel film sample was studied by TGA. The TGA study confirms that addition of aniline imparts thermal stability to Glox-X-Gel/PANI film. TGA study also reveals that aniline reduces water holding capacity; the Glox-X-Gel film has more water holding capacity. The AFM images of Glox-X-Gel and Glox-X-Gel/PANI clearly shows uniform distribution of gelatin particles as well as PANI is also distributed throughout the shell material, which is gelatin. The XRD pattern of Glox-X-Gel/PANI sample clearly shows increase in crystallinity of sample of otherwise semi crystalline Glox-X-Gel sample. The study clearly confirms *in-situ* oxidative polymerization of the gelatin (gel) in aniline (Ani) matrix, to yield Glox-X-Gel/PANI composite films.

The absorption of films under investigation has been examined in the functional fluid having pH of 7.4 at 37°C. The swelling ratio decreases with rise in glyoxal concentration , the un-crosslinked sample has maximum swelling ratio. We can conclude that increase in glyoxal concentration increase crosslinking between chains of gelatin which in turn increases water holding capacity but decreases swelling ratio; while the un-crosslinked sample tends to dissolve in water.

The dynamic water uptake value has been investigated by various kinetic models like power function and Schott kinetic model. The different diffusion coefficients from different models have also been obtained. The parameters associated with power function model reveals that sample having minimum concentration of glyoxal, exhibits less Fickian diffusion. With rise in amount of glyoxal, crosslinking increases which makes diffusion in samples more of Fickian nature. A sample having higher percentage of crosslinking have water penetration rate that is rate of diffusion much higher than the polymer chain relaxation rate; this shows Fickian diffusion. The results of Schott kinetic model show that for the system under investigation, this model is suitable on water uptake data. In addition to this, theoretically equilibrium swelling ratio values are quite close to experimental values.

The time diffusion coefficients obtained for the samples both for initial phase of swelling and later stage of swelling. One can conclude by observing these values that all the diffusion coefficients are in the magnitude of 10^{-6}, which is a very common phenomenon for the polymer films. The cooperative diffusion coefficients were found in the magnitude of 10-6 cm^2 min^{-1} for all the samples. From water absorption studies of the samples, one can conclude that the glyoxal-crosslinked gelatin films have satisfactory water absorption properties and although the inclusion of PANI within the gelatin (gel) film sample leads to a rapid decrease in the water uptake behavior, but still the Glox-X-Gel/PANI have fair water absorption properties.

The moisture uptake behavior of the pure gelatin and Glox-X-Gel/PANI films has been studied at fixed temperature of 300°C under varying relative humidity (RH) environment and the moisture isotherms were studied. The experimental data obtained from this study as wre discussed in the context of GAB (Guggenheim-Anderson-de Boer) model. The thermodynamic factors such as qst and s_d have also been determined using ‘Clasius-Clapeyron’ equation. This study shows that gelatin based film exhibits a remarkable change in its water absorption properties due to inclusion of PANI network in the film matrix of gelatin. When PANI is loaded into the polymer matrix, the mono layer M_c, decreases since 0.0986 g/g to 0.0260. There is reduction in moisture uptake with rise in temperature for gelatin/crosslinked as well as for Glox-X-Gel/PANI. Temperature of the moisture environment affects the moisture uptake behavior of hydrogels. The net isosteric heat of sorption, q_{st} decreases from 78.94 to 2.34 kJ/mol-1 with the rise in M_c from 0.2 to 0.9 g/g db for native Gel films while the reduction in qst was from 48.95 to 3.5s3 kJ/ mol-1 with the rise in M_c from 0.04 to 0.4 g/g db for Glox-X-Gel/PANI film respectively. The addition of polyaniline in the gelatin matrix which is basically a hydrophilic polymer results in reduction in moisture uptake of composite samples. In spite of this the composite of gelatin and aniline has appreciable moisture uptake behavior. For studying blood compatibility, the gelatin as well as its composite sample with PANI was subjected to thrombus formation test and hemolysis test. The thrombus formation test reveals that very small amount of blood clots were formed for, films under investigation. The amount of blood clots is far less than that for glass film. The test confirms that composite material under investigation have bio-compatibility as well as have an excellent anti-thrombogenity behavior. For hemolysis test, the percentage of hemolysis was achieved to be very-very small than the value of 2% (a standard required for a sample to be non-hemolytic). The hemolysis test clearly confirms samples were non-hemolytic. The films have promising features which can find their uses in biomedical applications.

The mechanical and electrical behaviors of films so prepared have been studied through conductivity measurement and tensile testing. The variations in mechanical and electrical properties of Glox-X-Gel/PANI composite films having varying concentration of aniline have been thoroughly researched. It was appreciated that there is appreciable rise in electrical conductivity of the films, with the amount of aniline in the film. In addition, there is definite rise in tensile strength of the films with increasing amount of aniline. The % elongation decrease with rise in aniline content, which points to, increase in yield strength with concentration of aniline in materials.

As we know that the yield strength is a point on the stress-strain curve, which can be used safely without permanent deformation, so an increase in yield strength suggests that the aniline concentration increases with the increase of the composite. Mechanical power grows. Results and tensile tests from XRD were correlated. As revealed by XRD, the Glox-X-Gel/PANI composite films increased the crystallinity.

The increase in crystallinity results in material having greater hardness and mechanical strength. The TGA study reveals increased thermal stability for Glox-X-Gel/PANI composite films. A stronger and more thermally stable composite material being the additional benefit of conductivity is the result of this research work.

As we know that the electrical properties of composite films material depends upon preparation method, various oxidation states, doping level and the conformation of molecules in the final composite material. Here, variation in ac conductivity, impedance, and capacitance, inductance and phase angle with varying frequency of applied ac shows, interesting results. All the samples having varying concentration of aniline shows negative conductance around 29 MHz, this means that the polymer composite under investigation has potential to be used in microwave applications, however detailed research is required to further investigate this possibility. The frequency variation of ac impedance clearly shows that the with frequency, impedance decreases which is directly related to overall increase of conductivity for each the samples over entire frequency band above 29 MHz frequency. The impedance for the samples is more of capacitive nature which further leads to further exploration of this composite which is used as a dielectric for higher frequency applications or related application in electronics.

Taken from the overall conclusion, it is that polymer composite result synthesized by aniline's polymerization within the crosslinked gelatin film is a total change in the thermodynamic parameters of moisture absorption properties and films. However, the addition of PANI within the gelatin film does not affect the bioequivalence of the films.

Such synthesized films have the potential to be used for biomedical applications. Under this study, the improvement in mechanical properties has been reported with the increase in electrical properties for the overall composite. Crosslinked Glox-X-Gel/PANI overall show improves mechanical and electrical properties. Thus, we have a good water uptake behavior and are suitable for biomedical applications, further a composite having reasonable mechanical strength and interesting electrical properties.

Inclusively this study concludes following facts:

(i) The glyoxal-crosslinked gelatin films shows fair water absorption properties and aniline (Ani) can be produced *in-situ* to yield composite film.

(ii) The incorporation of aniline (Ani) within the gelatin film results in a sharp decrease in the water uptake behavior.

(iii) The improvement in mechanical properties with enhance in electrical properties have been reported. The crosslinked gelatin/aniline composite shows improved mechanical and electrical properties.

(iv) *in-situ* formation of aniline (Ani) within the gelatin film results in alteration of moisture absorption properties and thermodynamic parameters of the films. However, the biocompatibility of the films is not much influenced by addition of aniline (Ani) within the gelatin film.

5.2. Future Prospects

This work entitled "**A Study on Structural, Mechanical and Electrical Characterization of Poly(aniline)/gelatin composites and its water sorption behavior** " is a detailed and systematic study of electrical, mechanical and absorption properties of polymer composite of gelatin and aniline further the bio- medical application of the composite was also thoroughly investigated. The results obtained from this study have been keenly discussed and intermitted on the basis of the literature available in this topic. The overall conclusion drawn was in good agreement with the literature of such type of composited which were investigated in near past. The utilization of tensile testing for investigating mechanical properties and AC conductivity and impedance measurement for investigating electrical properties and then linking the results obtained from these techniques with XRD and TGA is unique approach which can be used and further developed by scientists working in this field. The selection of gelatin; a naturally found bio-polymer and conducting polymer polyaniline forms interesting candidates for synthesizing versatile composite which can be used in number of fields.

Polymer composite of gelatin with other conducting polymer like polypyrrole, would be a worth research for other scientists working in the field of composites of conducting polymer with some natural bio-polymer. The composite under study has a one member i.e. gelatin which is crystalline, hence crystallinity of the resultant composites (which possess semi crystalline behavior and therefore is far more complicated to be inferred from XRD alone) and its effect on mechanical and electrical properties must be further studied with Differential Scanning Calorimetry (DSC) or Differential Thermal Analysis (DTA), spectroscopic and magnetic resonance techniques.

There is further scope of studying mechanical properties of this composite by using non-destructive technique such as microhardness testing. As we have investigated bio-medical application of this composite, it is worthwhile to mention that since in such composite when in real use can face number of adverse environment such as radiation, it will be better to study the change in mechanical properties when the composite is irradiated through gamma radiation, X-rays and electron radiation. Since impedance variation revels important facts about composite under investigation, hence DC conductivity along with dielectric properties of the materials under studies needs further investigation. AFM study was conducted for the samples under study but this study can be extended further to study the variation in SEM of the investigated samples after passage of electric current both alternating and direct current. Also need of more detailed XRD analysis is needed to correlate the AC conductivity results with the variation in crystallinity of the samples.

In the study it is discussed bio-medical application of the composite under study, mainly for blood transfusion and storage but more deep study is needed to investigate its application as sensors or scaffold and other areas of medical science. The composite under investigation shows promising results which were beneficial academically as well as leads a way to further study its application in electronics and bio-medical applications. It is recommended to develop the proposed framework to improve these functions. Based on some possible changes that may occur in the future:

(i) There is further scope of studying mechanical properties of this composite by using non-destructive technique such as microhardness testing.

(ii) It is worthwhile to mention that since in such composite when in real use can face number of adverse environment such as radiation.

(iii) It will be better to study the change in mechanical properties when the composite is irradiated through gamma radiation, X-rays and electron radiation. Since impedance variation revels important facts about composite under investigation, hence DC conductivity along with dielectric properties of the materials under studies needs further investigation.

(iv) AFM study was conducted for the samples under study but this study can be extended further to study the variation in SEM of the investigated samples after passage of electric current both alternating and direct current.

(v) Also need of more detailed XRD analysis is needed to correlate the AC conductivity results with the variation in crystallinity of the samples.